UNIVERSITY OF CAPE TOWN
DEPARTMENT OF CIVIL ENGINEERING

CIV 500Z – THESIS

TORSIONAL BUCKLING and INSTABILITY OF STEEL STRUCTURAL MEMBERS

BY : QUINTEN CORNER

ST. NO. : CRNQUI001

FOR : DR ALVIN MASARIRA

DATE : AUGUST 2003

Dissertation submitted in partial fulfilment of the requirements for an MSc degree in Civil Engineering

i DECLARATION

I, Quinten Corner, declare that this is essentially my own work and has not been submitted in this form or any other form for a degree at the University of Cape Town.

Signature: . . . . . .

Date: __ __ / __ __ / __ __

DEDICATION

I would like to dedicate this thesis to my beautiful and sexy wife, Chorrine for her encouragement, support and patience.

ii ACKNOWLEDGEMENTS

The author owes a great deal to Dr. Alvin Masarira for many discussions, advice and supervision of this thesis.

I am particularly grateful to my wife, Chorrine for her patience and who has helped with the preparation of this thesis at all stages.

Special thanks are extended to my mother, Katrina for her support and encouragement.

Acknowledgement is made for the many authors of the publications cited in this thesis.

iii ABSTRACT

Instability of steel structures manifests it's origin from inadequate end-connections and member instability due to buckling and torsional effects. Torsional buckling studies arise from the need to accurately model the behaviour of steel members subjected to a load. The effect of end-conditions on torsional buckling of steel members is a relatively unexplored area. The onset of lateral-torsional buckling is characterised by a member's end-conditions, where spatially rotations and deflections are the serviceability limit state. The end-conditions, which are divided in "only" three categories theoretically (free, pinned and fixed), are refined to more categories, which include semi-fixed end-conditions with different stiffness. Finite element studies of the end-conditions are presented, which established that the end-conditions of the structural element determine the critical buckling load.

iv BACKGROUND

Steel structures and steel elements in buildings (including high rise buildings) are essential to increase the strength characteristics of a structure, which is all due to the phenomenal strength of steel. Even reinforced concrete can resist a fair amount of loading thanks to steel used in it. Immense amount of research was done thus far on steel, which includes strength, optimal geometric properties, instability of structures, buckling as well on **torsion** of steel structural elements. However, there are still areas that need to be investigated.

Euler was the first to come up with an analytical method for predicting the flexural buckling of columns in 1759, which provided an analytical method for predicting the extent of reduction of strength in slender columns (still in use today). Saint-Venant did some more research on torsion and produced the first reliable description on how members respond to torsion. Michell and Prandtl published the first publication on this topic, the treatment of narrow rectangular cross-sections subjected to flexural buckling in 1899 after extensive research. Timoshenko added the effects of warping torsion to this work later. Timoshenko, Gere, Goodier, Winter, Bleich, Vlasov and Chajes are all responsible for the formulation of a general theory for flexural-torsional buckling of single span beams, columns and beam-columns having fixed or simply supported end conditions. In 1960 the advent of computer programs alleviated the slow progress in research prior.

In 1970, Barsoum and Gallagher added growth considerably with the study of finite element analysis of flexural torsional buckling and made it possible to investigate almost all problems. Extensions to the theories of differential bending, torsion and energy equations of buckling, have led to many new general theories, which include one based on second-order relationships between deformations and strains that take place through bending and torsion. Timoshenko and Vlasov did most of the research. Timoshenko produced the first set of rules in 1924. Brown, Flint and Kerensky created the first modern treatment as a basis for the British Standard BS 153-1958.

Theoretical formulation and computer software for steel frame analysis considering local-buckling effects have been developed successfully. The advanced analysis needs to be extended to include the effects of lateral buckling. Considerable research has also been undertaken into various aspects of steel frame behaviour and design, which include:

- Material properties (Nethercot, 1992; Bradford, 1992),
- Residual stresses,
- Geometric imperfections (Trahair and Bradford, 1988),
- Loading history (Ings and Trahair, 1987),
- Second-order effects (Chen and Lui, 1987),
- Large deflections (Chen and Lui, 1987),
- Post-buckling strength and behaviour (Trahair and Bradford, 1988),
- Load eccentricities (Chen and Atsuta, 1976),

- Connections response, (Galambos, 1998)
- End restraint, (Nethercot, 1992)
- Erection procedures, and
- Interaction with foundations.

To qualify as an advanced analysis method, the analysis must be able to take into account all aspects mentioned above. It is envisaged that comprehensive assessment of the actual failure modes and maximum strengths of steel frame structures will be possible in practical design situations without resort to simplified methods of analysis and semi-empirical specification equations.

With this, it is intended to provide a basis for subsequent investigations into the development of an advanced analysis method that is capable of taking lateral-torsional buckling effects into account. The information used was obtained from a variety of sources as listed in the bibliography of this thesis.

v Terms of References

Dr Alvin Masarira of the Department of Engineering and Built Environment at the University of Cape Town suggested the research topic; Torsional and Stability problems of steel structures to me in partial fulfillment of the requirements for the Degree of MSc in Civil Engineering as course: CIV500Z.

Steel frame structures are widely used in industrial and commercial buildings in South Africa and right over the world. Practical advanced structural analysis methods can increase the accuracy and productivity in steel design and achieve greater economy and safe structures. The following issues have influenced the selection of this research topic.

- There are many incomplete design guidelines and disadvantages in the current steel design approach (e.g. SABS 0162-1: 1993).
  a. It is not practical to take interdependence of a member into account rigorously using SABS 0162, although the strength and stability of a structural system is an upperbound solution, and is not necessarily conservative.
  b. Using the approximate semi-empirical strength equations, the SABS 0162 approach cannot predict the failure modes of a structural system accurately.
  c. Elastic analysis to find the maximum loading effects and separate member capacity checks is an efficient design process.
- Steel frame structures may exhibit significant non-linear behaviour prior to achieving maximum load, hence a direct, non-linear analysis is the most rational means for assessment of overall system performance.
- Relatively slender I-section members are used to build most steel frame structures. Flexural torsional buckling often governs the limit strength design criteria of these structural entities. However, the prediction of global buckling is based on simplified elastic analysis and appropriate semi-empirical equations.
- The material non-linearity and the change in geometry of the structure must be taken into account in true stability analysis.
- Recent computer hardware and commercial finite element analysis (FEA) programs have enabled the development of detailed structural models in short time.

This research thesis includes the investigation into various aspects relating to the instability and "torsional buckling of steel structures", with particular emphasis on the effect of member's end-conditions on the buckling load. These aspects include:

- Conducting an extensive literature survey on the state of the art methods to design various types of steel structures subjected to torsional buckling. This involves a critical review on testing methods used for members or structures; new and improved calculation methods for torsional buckling; and computer simulations of structural behaviour.

- An investigation into the effects on the structural behaviour of members and/or structures as a result of torsional buckling. It will include analysis, using a FEM software packages; Abaqus and Prokon to evaluate the mode of failure due to instability and elaborate on the results found.

- The strength and stability of beams and beam/columns by which beams buckle by a combination of lateral bending and twisting with the most basic theoretical solution possible will be investigated.

- Also the elastic behaviour of geometrically imperfect beams and columns will be investigated as a prelude to the treatment of design procedures, which will include the effects of boundary conditions like support conditions e.g. end plates. Investigate the effect of hot rolling, flame cutting and welding and get basic (user-friendly) theoretical predictions for a range of beam supports and loading conditions.

vii LIST OF ILLUSTRATIONS

viii INTRODUCTION

Practicing engineers are often confronted with the design and analysis of steel buildings. The questions that always arise are whether the structure is over-designed with all the safety factors for uncertainties; how small (optimal design) can the structural elements be, and will this structure do what it is supposed to do, or will it fail? This can only be answered by thorough investigations numerically, analytically and practically (laboratory experiments). It is never enough, but one will be tempted to say that enough research was done on strength of steel under axial and bending effects. New and modern technology and theories ease the effort of the engineer to produce an easy, fast and economical solution to his problem.

Currently, if steel is evaluated for service subjected to axial, bending and torsion, almost no user-friendly formulations are available or even a computer program that can help, which makes it very tedious for engineers. The current design procedure for steel frame structures is a two-step process; including an elastic analysis to determine design action effects and a member capacity check using semi-empirical specification equations.

Torsion can effect many properties of steel and almost always result in instability of the member or structure. Failure due to lateral-torsional buckling is a three-dimensional distributed plasticity instability problem. Unlike in-plane buckling of beam-columns, the analytical solutions of ultimate strength for lateral-torsional buckling are not general for all elements. Colossal research was done on the instability of steel structures and modes of failure and formulated, but with lengthy calculations and some indecorous assumptions. For this reasons there is a need to do further research on the torsion and torsion combined with bending on steel. The fundamental aspect of lateral-torsional buckling is the end-conditions of the structural steel member in question.

The purpose of this research is not just in partial fulfillment of the requirements for a MSc degree in Civil Engineering, but to add to the technology and improve engineering solutions to problems. With this research it is intended to investigate modes of failure of steel members or structures and possibly add to formulae and methods to solve torsional problems in steel construction. The reason for this research is also to add to the outline of the general behaviour and methods of calculations for beams, columns and beam-column connections when they are subjected to transverse loading causing torsion. The modes of failure of the structural element that is of most interest are torsional buckling and flexural torsional buckling as well as local buckling. A beam subjected to an increasing uniform moment at a critical value of moment M_E (or compressive bending stress), it will collapse suddenly by buckling.

Deformations consist of a mixture of torsional and lateral flexure twisting and a sideways movement. This behaviour depends upon the following factors:

i. Beam sectional properties
ii. Boundary conditions (i.e. fixed, pinned, semi rigid, warping resistance etc.).
iii. Beam span.
iv. Imposed moment
v. Distance between lateral restraints on compression flanges.
vi. Direction of eccentricity of applied loads relative to the shear centre.

The relationship between the above factors is of great importance and proper relationships and/or effects on the structure need to be explored in action for design purposes. Strain is used to evaluate most of the deformations, and forces because they are easily measured experimentally.

The structure of this thesis is as follows. In chapter 1, a wide variety of available literature was surveyed, providing a comprehensive review on torsional buckling and instability of steel structures. Torsional effects on beams and columns are described in chapter 2. This is followed by a review of the structural fixity and member stability, as well as a brief on finite element analysis. The finite element studies of end-conditions and torsional buckling of structural steel members are presented and discussed in chapter 5. The thesis is concluded with some comments and suggestions for future development.

1 LITERATURE REVIEW

1.1 INTRODUCTION

In recent years, there has been increased and progressive interest in the need to correctly predict and assess the failure modes of steel members in order to make more realistic and economical predictions about the response of steel framed buildings. Research in the behaviour of steel member's failure mode spans approximately sixty years. Through that time steel member capacity calculations, has come in and out of the spotlight. This brief account highlights the major experimental work on torsional buckling and instability of steel structures.

A great deal of analyses on failure modes, especially on torsional buckling of steel members has been successfully performed for elastic behaviour. Some of these work has been done by Schafer[62] (1997), Yong Bai[5] (1995), Zeng Yuan[81] (2000), Nethercot[53] (2002), Kemp[38] (2002), and Masarira[47] (2002). However, the study of torsional buckling and instability of steel members is a relatively complex research area with many uncertainties still present. For example, Chou, Seah and Rhodes[18] (1996) summarized the state of the art prediction abilities of cold-formed steel design specifications and found limitations and discrepancies in all major design specifications. Also, Schafer[62] (1997) used finite strip and finite element analysis demonstrating that the torsional mode has greater imperfection sensitivity than local modes.

Similarly, experimental studies of torsional buckling and instability of steel structures are meager and incomplete due to huge costs of carrying out such experiments. Nethercot[54] (2002) highlighted the importance of combining experimental and numerical study in advancing structural engineering understanding by using evidence from research over varying periods of time. Della Corte[26] et al. (2001) developed a semi-empirical method for evaluating the connection hysteretic behaviour. Full-scale experiments are very expensive, however, appropriate 'hard' data greatly assists the research process with intuitive thinking.

1.2 TORSIONAL BUCKLING OF STEEL MEMBERS

After 50 years of progress, modern column research is still similar to Chilver's[16] (1951) work – elastic stability solutions for local plate buckling and 'effective width' for ultimate strength. Karren[36] (1965) showed significant variation in engineering properties around the cross-section, which was widely ignored at that time in the calculation of torsional buckling. Goldberg[29] et al. (1964) developed a folded plate method to predict the lateral and torsional buckling of thin-walled beams including sectional distortion. In the 1970's, research was focused on the interaction between local and overall buckling modes as evidenced by Dewolf (1974), Klöppel and Bilstien (1976), Rhodes and Harvey (1977), Peköz (1977), and Loughlan (1979)[54]. Barsoum and Gallagher[6] (1970) introduced the first derivative of the rotation about the axis of three-dimensional beam elements as the seventh degree of freedom at each note representing warping deformation. By using this, they analyzed elastic-torsional and torsional-flexural buckling of symmetric sections.

Hancock[33] (1985) extended and popularized Cheung's[15] (1976) finite strip analysis as a tool for understanding the buckling modes in thin-walled members.

Eurocode 3 Part 1.3[84] (1996) provide a method for predicting the distortional buckling of simple lipped sections such as channels accounting for the restraint provided by the web and the flange to the lip buckling as a strut. Research, conducted by research teams in Canada and Texas, examined Z-section columns in and provided experimental evidence of distortional failures and problems in the AISI specification[18]. Schafer[62] (1998) explicity showed that the AISC specification equations over-predict the torsional buckling stress, particularly as the ratio of the web height to flange width becomes large.

Zeng Yuan[81] (2000) claims that failure due to lateral-torsional buckling is a three-dimensional distributed plasticity instability problem, and unlike in-plane buckling of beam-columns, the analytical solutions of ultimate strength for lateral-torsional buckling are non-existent. The Euler formula theory is only

applicable at large slenderness ratios and real struts will fail by yielding at lower loads, due to eccentricity of loading, and initial curvature, etc. (Graham Slater[66] (2001)). Mazor and Rand[49] (2000) did a theoretical study of the importance of the in-plane deformation on the structural behaviour of thin-walled isotropic and composite beams, which are subjected to bending and torsional moments, where they have separated the effects of the out-of-plane- and the in-plane warping. Gotluru[30] et al. (2000) performed simple geometric analyses, finite element analyses and strip analyses and compared these with experimental results. The influence of typical support conditions were studied and found to produce partial warping restraint at the ends. Hypothetical springs (the magnitude of spring stiffness was assessed for commonly used connections) were introduced to account for this effect. However, they have accounted for only two end conditions namely, restrained and free.

Hiroaki Katori[37] (2001) used finite element method for the coupling problem of shearing and torsional deformation based on Saint Venant's theory to highlight the importance of the location of the shear center of a thin-walled cross-section. Furthermore, the stiffness matrix for space framework elements taking shear deformation into account was developed. Zha and Moan[82] (2001) used the finite element program, Abaqus to investigate the ultimate strength of aluminium plates with flatbar stiffeners with a torsional buckling or tripping failure mode. It was accounted (by both experimental and theoretical analysis) for the fact that unlike steel structures, the ultimate strength of aluminium structures is sensitive not only to residual stresses and initial deformation, but also to the deterioration of mechanical strength in heat affected zones. Kwak[43] et al. (2001) performed a geometric nonlinear analysis of three-dimensional beams with thin-walled open sections, and by using the total Lagrangian formulation, the displacement field is described, and the warping degree of freedom is taken into consideration to simulate the structural behaviour of slender or curved beams with arbitrary shape. In spite of having relatively stronger stiffness than concrete, the steel structures are predominantly affected by instability due to the buckling of structural members composed of very slender plates. An understanding of all stresses caused by

flexure and torsion is required, in order to use thin walled structures effectively.

Remarkable analytical and numerical approaches for analyzing the thin-walled open structures have been performed by several researches (Creaghan and Palazotto[22] (1994) and Rosen and Rand[59] (1986)) and many rigorous numerical models have been introduced. Moreover, a lot of research on thin-walled open sections has been conducted (Baba and Kajita[4] (1982), Borri and Hufendiek[8] (1985)) after the systematization of the general torsion theory for the thin-walled open sections by Vlasov[79] (1961) where the non-warping deformation effect is considered, but the transverse shear strain is neglected.

It has been shown by Daali and Korol[23] (1995) that given some specific values for flange slenderness, and a web slenderness, one can predict with an acceptable accuracy the rotation capacity at maximum moment, i.e. when local buckling is initiated. Abu-Sena[1] et al. (2000) were the first to use the energy method to find the critical stress for anti-symmetric lip buckling, for any given half-wave length, including the preferred half-wave length. The method describes the critical buckling interaction between the torsional-flexural and anti-symmetric lip modes, and its effect in reducing the critical buckling stress. The possible buckling modes and the corresponding buckling stresses must be known before strength equations, suitable for design, can be formulated (Chapman[12] et al. (2001)). Thus, initial imperfections with components sympathetic to the possible buckling modes must be introduced.

1.3 BOUNDARY CONDITIONS STUDIES

Experimental results (Rasmussen and Handcock[33] (1991)) showed the importance of different end fixity on the post buckling behaviour. Young[54] (1997) experimentally demonstrated that fixed ended columns do not suffer the same interaction problems as pin ended columns. Masika and Duna[48] (1994) did experimental (two full-scale frame corners) and analytical (combination of finite element and mechanical model) research on rafter-to-column joints of portal frames with bolted end-plate connections. With the experimental results, it was found that none of the results coincided with either

the rigid or pinned (theoretical results) but in the semi-rigid zone, and can be concluded that the connection designed for full strength capacity behave in a semi-rigid way. It has long been recognized that the two extremes of pin-joints and rigid-joints assumed in classical methods of member or frame analysis merely represent convenient simplifications (at either end of the range of possibilities of a more complex situation). Real steelwork connections between beams and columns posses varying degrees of moment capacity and rotational stiffness as evidenced from examining the many moment rotation curves obtained over the years from laboratory tests of different connection types (Nethercot[53] (2000)). Standard, commercially available computer packages often contain options to model joint behaviour using linear or non-linear springs resulted in numerous analysis variants and behavioural studies of semi-rigid joint action in frames being published.

Rather than merely assuming that connections may be modeled as springs, several researches (Masarira[47] (2002), Mofid[52] et al. (2001), Al-Shawi[3] (1998), Krenk and Damkilde[42] (1992)) have sought a more comprehensive representation of the different structural phenomena that collectively, produce the key connection characteristics of true strength and stiffness. Member/s are divided into simple and continuous structures, with the former being analyzed on the basis of pin joints, whilst the latter assumes full rotational continuity between members. More recently, Mofid[52] et al. (2001) and others studied the so-called 'semi-rigid-joint action', which led to the definition of a third class of 'semi-continuous' frames.

Krenk and Damkilde[42] (1992) studied the warping of joints in I-beam assemblages where it was tried to produce suitable models for thin-walled beam joints (four types of joints were treated). The type of joint is of importance for the torsional stiffness, and thereby the buckling load of thin-walled beam assemblages. Al-Shawi[3] (2000) went further by developing a mathematical model, based on the elastic behaviour of a structurally elastically supported at its ends and restraint at a point located along its length by an elastic restraint, by designing restraints considering strength as well as stiffness. The results obtained showed that, for a given induced restraint force,

the restraint stiffness requirement decreases with the increase of rotational stiffness at the ends of the struts. According to the investigation on real behaviour of connections, any structural beam-to column joint can be called semi-rigid, which means that even the most rigid connections have a relative flexibility, which should properly be taken into account.

The effect of joints on the stability behaviour of steel frame beams was investigated by Masarira[47] (2002) through finite element modeling of portal frames and, established that a consistent relationship exists between the critical load for lateral torsional buckling of the frame beams and the joint design. The analyses of eight different joints concluded simple coefficients that can be used in approximating the joint effect on the lateral torsional buckling load of steel frames. From Masarira's[47] (2002) research, it is evident that the warping stiffness values of the joint are mainly a function of the joint design and joint parameters.

1.4 STABILITY OF STEEL FRAME STUDIES

The lateral stability of coupled simply supported beams were analyzed (Tomka[76] (2001)) with the concentration force acting on the upper flange, where it was proved that the performance of coupled beams is considerably higher than that of stand-alone ones. Despite the occasional appearance of ingenious alternatives from time to time, virtually all modern forms of frame analysis are variants of the matrix stiffness approach (Nethercot[54] (2000)). From the earliest limitations of linear elastic behaviour, either pinned or rigid joints and consideration of only 2-dimensional in-plane effects, the method has progressively developed, which cover linear elastic-, rigid plastic-, elastoplastic- and temperature and time dependent material; as well as pinned-, rigid-, semi-rigid-, and partial strength joints. For frames, the design is often based on the formation of a plastic collapse mechanism. However, certain safeguards are necessary, especially relating to the occurrence of premature failure through some form of instability (local-, member failure or frame failure).

A nonlinear analysis of three-dimensional steel frames was developed by Kim[38] et al. (2001), which accounts for material and geometric non-linearties. The two advantages of their proposed analysis is; time and memory saving in computation since only one element per member is necessary to analyze, and to overcome the drawback of the geometric stiffness matrix overestimating the strength of the member subjected to large axial force. The effect of plane bending moment, applied to semi-rigid connection, causes relative rotation of beam and column and has a significant destabilizing influence on the frame stability, since additional drift will occur as a result of the decrease in effective stiffness of the members to which the connections are attached. An increase in the frame drift will intensify the load-deflection effect and hence, the overall stability of the frame will be affected.

A mixed-flexibility method of analysis was used by Kemp[38] (2002) to simplify elastic and inelastic structural analysis of frames in which the unknowns are element end moments and independent modes of sway deflection. The method is shown to provide an efficient and accurate solution to general non-linear analysis of steel frames, which can incorporate yielding and strain hardening of the elements and non-linear behaviour of semi-rigid joints.

Numerous researchers (Al Mashary (1991), King et al. (1992), and White (1993)) [53] have described perceived shortcomings in the plastic-zone approach, including uncertainty over the number of elements required for accurate modeling of both behaviour and inelastic material properties. Teh[73] (2001) on the other hand, has evaluated the reasons for these inaccurate perceptions of the plastic-zone method, as well as the benefits of this method. He has indicated the small number of elements actually required, and the importance of simplifying the analysis by pre-programming both the location of the nodes and discretisation of the cross-section using cubic elements.
To avoid perceived modeling effort and uncertainty in the number of elements required in the plastic-zone methods, Al Mashary and Chen (1991), King et al. (1992), and White (1993) [52], developed beam-column stiffness elements in which, in an incremental analysis, the relevant stiffness terms reduce from

their elastic values to zero between first yield and development of the plastic hinge.

Attalla[3] et al. (1994) have also developed a 'quasi-plastic hinge' approach which accounts for gradual plastification under combined bending and axial force by fitting non-linear equations to the moment-axial force curvature relationship, which are integrated over the length of the element.

1.5 CODE OF PRACTICE FOR STEEL DESIGN

All professions have laws and regulations. Standards and literature of other established countries and input from South African professionals were combined to produced the SABS 0162-1[60] code. There exist many methods of analysis for all type of members, which include a wide range of computer software packages. However, they all have to comply with the code of practice.

The codes of practice is not always straightforward and user friendly, which might result in over- or under-estimated capacities of members/structures. Today it is still not clear how to design comprehensively, steel members subjected to torsional effects.

1.5.1 SABS 0162-1:1993[60] – The structural use of steel Part 1: Limit-states design of hot-rolled steelwork

The SABS 0162[60] is a limit-state design steel code based on the Canadian Standards CAN/CSA-S16.1-M89, with a great deal of British influences.

The effects of loads on a structure can be; axial stresses, bending force, shear force, deflection, and torsion, which in most cases occur simultaneously.

1.5.1.1 Stability effects

The SABS 0162-1[60] provides guidance on how to calculate the additional moments and forces generated by the vertical forces acting through the deflected shape of the structure, which results in limit-states being exceeded.

In the SABS 0162-1[60], the effective length of a member is a major design consideration as it has a large influence on the member's resistance to buckling. The effective length is given by KL of the equation given in clause 13.6, where L is the unbraced length of the member and K is the effective length factor. For general cases the effective length factor K is given in annexure B of SABS 0162-1[60] and depends on the degree of restraint offered at the end of the member. In that table (refer to table 1.1 on page 15 of this thesis), the end conditions are theoretical, which represent either a perfectly hinged or perfectly restrained conditions, neither of which is practically obtainable.

An unrestrained beam according to SABS 0162-1[60], will deflect in the vertical plane due to bending, but as the moment increases, it reaches a critical value M_{cr}, less than the full cross-sectional resistance, where it buckles sideways, twists and collapses (lateral torsional buckling).

The critical elastic moment doubly symmetric sections in SABS 0162-1[60] is given by:

$$M_{cr} = \frac{\omega_2 \pi}{KL}\sqrt{EI_y GJ + \left(\pi E / KL\right)^2 I_y C_w} \qquad (1.1)$$

K = effective length factor for the length of segment L

$G = 77 \times 10^3$

$J = \sum\left[b\, t^3 (0.33 - 0.21\ t/b)\right]$ where b and t is the respective length and width of each rectangular element

$C_w = \dfrac{I_y (h - t_f)^2}{4}$

$E = 200 \times 10^3$

$\omega_2 = 1.75 + 1.05\kappa + 0.3\kappa^2 \leq 2.5$

Whereby, the St Venant torsion constant J, the shear modulus G and the warping torsional constant C_w are the factors relating to lateral torsional buckling resistance.

The effect of moment gradient for non-uniform moment along the member length is accounted for by the factor ω_2. The SABS 0162-1 account for the end fixities with both the factors K and ω_2.

No guidance is given in SABS 0162-1[60] for cantilever beams, except in the commentary to the code, base on Nethercot's[53] work. Refer to sections "3.6.2 and 3.6.3".

1.5.2 EUROCODE 3 (1993) – Design of steel structures. Part 1.1[84]

The Eurocode 3 (EC3) [84] and SABS 0162[60] code allow for perfectly hinged and perfectly restrained conditions. EC3, however, allows for a further definition, which are semi-rigid connections. For this type of end conditions, a predictable degree of interaction between members based on the design moment-rotation characteristics of the connections must be provided.

The EC3[84] also design for shear buckling resistance at member ends around a group of boltholes (see Clause 5.4.6-7 of EC3).

The elastic critical moment M_{cr} of a beam of uniform symmetrical cross-section with equal flanges, under standard conditions of restraint at each end, loaded through its shear-centre and subject to uniform moment, is given in EC3 (Appendix F) as:

$$M_{cr} = \frac{\pi^2 EI_z}{L^2}\sqrt{\frac{I_w}{I_z}+\frac{L^2 GI_t}{\pi^2 EI}} \qquad (1.2)$$

I_t = torsional constant

I_w = warping constant

I_z = second moment of area about the minor axis

L = length of beam between points which have lateral restraints

The standard end conditions referred to in the EC3[84] are; restraint against lateral movement, restraint against rotation about the longitudinal axis, and free to rotate in plan.

It is also stipulates that where the non-dimensional slenderness $\lambda_{LT} \leq 0.4$, no allowance for lateral torsional buckling is necessary. Slenderness λ_{LT} is given by EC3, Clause F.2.2-I as:

$$\lambda_{LT} = \frac{L\left[\frac{W_{pl.y}^2}{I_z I_w}\right]}{(C_1)^{0.5}\left[1+\frac{L^2 G I_t}{\pi^2 E I_w}\right]^{0.25}} \qquad (1.3)$$

where C_1 is a factor depending on the loading and end - restraint conditions and is tabulated in tables F.1.1 and F.1.2 and

W_{pl} is the plastic section modulus of steel - section.

I_w is the warping torsional constant

I_t is St. Venant torsion constant

I_z is the moment of inertia about weak axis

A beam with full restraint does not need to be checked for lateral-torsional buckling.

1.5.3 Method of BS 5950: Part 1: 1990[11]

1.5.3.1 Web bearing and buckling

Section 4.5: BS5950: Part I covers all aspects of web bearing, web buckling, and stiffener design of beams, which is usually most critical at the position of a support or concentrated load (problem of web buckling).

The critical point for web buckling will be at the centre of the web, where the maximum buckling moment will occur.

Section 4.5.2.1: BS5950: Part I gives the buckling resistance force, which should be more than the reaction or concentrated load at that point.

Section 4.5.3: BS5950: Part I shows how the bearing resistance is calculated at the flange/web connection and is essentially a much simpler check, which

ensures that the stress at the critical point on the flange/web connection does not exceed the strength of the steel.

If it is found that the web fails in buckling or bearing, it is not necessary to select another section; larger supports can be designed, or load-carrying stiffeners can be locally welded between the flanges and the web. Section 4.5: BS5950: Part I gives guidance on the design of such stiffeners.

1.5.3.2 **Lateral torsional buckling**

Lateral torsional buckling is covered by Section 4.3: BS5950: Part I. The more restraint provided at the beam supports, the higher the load required to make the beam twist sideways.

Checking of lateral torsional buckling for rolled universal beam sections can be carried out in two different ways. Firstly there is a slightly conservative, but quite simple check in Section 4.3.7.7: BS5950: Part I, which only applies to equal flanged rolled sections.

The approach involves the calculation of an equivalent slenderness, which depends on the loading and bending moment diagram, r_y the radius of gyration about the y-y axis.

Then the buckling strength is read from Table 19: BS5950: Part I, knowing þ and x (=D/T), a torsional index which can be obtained from steel tables.

Finally the buckling moment $M_b = P_b.S_x$
where S_x is the plastic modulus about the x-x axis.

The more rigorous approach to calculation of M_b is covered by Sections 4.3.7.1 to 4.3.7.6: BS5950: Part I. There are two approaches depending on the loading conditions.

If the section of beam is loaded between adjacent lateral restraints, the equivalent slenderness approach is used; the factor m = 1 and factor n is read from Table 15 or 16: BS5950.
However n = 1 for destabilizing loads, and for cantilevers.

If the section of beam is not loaded between adjacent lateral restraints, the equivalent uniform moment approach is used; factor m is read from Table 18 : BS5950 and factor n = 1;

The equivalent uniform moment M = m.MA, where MA is the maximum moment on the section of member under consideration.
However m = 1 for destabilizing loads, and for cantilevers. This is summarized in Table 13: BS5950.

Then, for both methods from Section 4.3.7.5: BS5950: Part I,

$\eta_{LT} = nuv\eta$

where η_{LT} is the equivalent slenderness,
n is a slenderness correction factor from Table 15 or 16: BS5950: Part I
u is a buckling parameter from steel tables
v is a slenderness factor from Table 14: BS5950

pb can then be determined from Table 11 or 12: BS5950 knowing η_{LT} and py.

Finally, as before

$M_b = p_b . S_x$, which must be greater than M.

1.5.4 Comparison of theoretical and recommended K values

For a beam supported at its ends only, with no intermediate lateral restraint, and standard restraint conditions at supports, the effective length is equal to the actual length between supports. When a greater degree of lateral and torsional restraint is provided at supports, the effective length is less than the actual length, and vice-versa. The effective length appropriate to different end restraint conditions is specified in Table OA and OB of SABS 0162-1[60]: 1993 and Table 9 of BS5950[11]: Part I. The table gives different values of effective length depending on whether the load is normal or destabilising. Determining the effective length for real beams, when it is difficult to define the actual conditions of restraint, and whether the load is normal or destabilizing, is perhaps one of the greatest problems in the design of steelwork. It is an aspect that has been amended in the 1990 edition of BS5950 in order to relate more to practical circumstances, but the fundamental problems still remain. There is no simple but accurate model to simulate the end-conditions of a structural element.

A load applied to the top of the beam will cause it to twist further, thus worsening the situation. If the load is applied below the centroid of the section however, it has a slightly restorative effect, and is conservatively assumed to be normal.

By following the procedure in section 3.5.2 of this thesis, K values for various support conditions can be derived. Some of the results are listed in Table 1.1 and compared to different codes of practice.

The criteria for estimating effective lengths of columns in continuous frames are given in Annex C of SABS 0162[69]. From the figures in the table above, the trend is very consistent, but in some cases vary by as must as 20%, if compared to other standards.

Table 1.1 Theoretical and Recommended K values for columns

Dashed lines represent column buckled shape						
Theoretical K value	0.5	0.7	1.0	1.0	2.0	2.0
Recommended in SABS 0162	0.65	0.80	1.0	1.2	2.0	2.0
Recommended in AS4100	0.7	0.85	1.0	1.2	2.2	2.2
Recommended in AISC (US)	0.65	0.80	1.0	1.2	2.1	2.0

End Condition code		
	Rotation fixed	Translation fixed
	Rotation free	Translation fixed
	Rotation fixed	Translation free
	Rotation free	Translation free

1.6 DIMENSIONAL TOLERANCES OF HOT-ROLLED SECTIONS

Hot-rolled sections are manufactured in accordance with standards, which allow tolerances on its mass and dimensions. Tolerances on the mass and dimensions of these sections are as shown in the following tables. Tolerances on batch mass of hot-rolled sections are given in table 1.2.

Table 1.2[68] Tolerances on batch mass

Sections or bar	Permissible variation under	Permissible variation over
I-sections H-sections	4%	4%
Channels	2,5%	2,5%
Angles $t \leq 4,0$ mm	6%	6%
$t > 4,0$ mm	4%	4%

When a section is manufactured, the relevant standards specify dimensional tolerances to work with. Indicative dimensional tolerances on hot-rolled sections are summarized in table 1.3.

Table 1.3[68]: Indicative dimensional tolerances on hot-rolled sections.

SECTION	DIMENSIONS (mm)	PERMISSIBLE VARIATION (mm)
I- and H- sections (all) 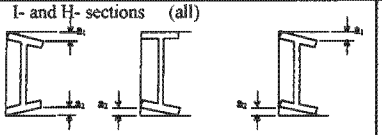	$a_1 + a_2$ (max):	
	$b \leq 64$	2,0
	$64 < b \leq 100$	3,0% of b
	$100 < b \leq 203$	3,2
	$203 < b \leq 305$	4,8
	$b > 305$	6,4
Channels (metric) 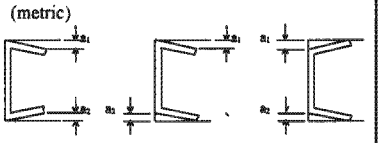	Depth h:	
	$80 < h \leq 200$	- 2,0 to + 2,0
	$h > 200$	- 3,0 to + 3,0
	Width b:	
	$b \leq 75$	- 1,5 to + 1,5
	$b > 75$	- 2,0 to + 2,0
	$a_1 + a_2$ (max):	
	$b \leq 100$	2,0
Channels (Imperial	Depth h:	
	$h \leq 305$	- 0,8 to + 3,2
	$305 < h \leq 200$	- 1,6 to + 4,0
Angles	Leg length h:	
	$h \leq 50$	- 1,0 to + 1,0
	$50 < h \leq 100$	- 1,5 to + 1,5
	$100 < h \leq 150$	- 3,0 to + 3,0
	$150 < h \leq 200$	- 3,0 to + 3,0

These dimensional and mass tolerances can result in an initial defect (not straight, not symmetrical etc.), which will reduce the critical buckling load calculated theoretically. These tolerances were not taken into account in this work.

2 TORSIONAL EFFECTS ON STEEL MEMBERS

2.1 INTRODUCTION

Attention is confined to the different modes of failures with particular emphasis on torsion of steel beams, as well as longitudinal stresses and bimoment. These items are coupled with boundary conditions, which are the most fundamental influences that should be considered.

All structural materials are to a certain extent elastic in nature. This means that if external forces, producing deformation of a structure, are applied, but do not exceed a certain limit, the deformation disappears with the removal of the forces. For this reason it is very important to find out where, or at what force this limit is.

The ductile behaviour is highly desirable when the structure is called upon to absorb energy. After the maximum load is reached, the material continues to withstand the load, undergoing large deformations without fracture. This capacity (critical buckling load), by virtue of which the material can sustain the load without undergoing fracture, is attributed to steel's ductile nature.

2.2 TORSION

When an external moment acts about the length axis of a structural member, it causes torsion rather than bending. The deformation takes the form of twisting or warping. The forces, deformations and stresses caused are tangential to the cross-section of the cut member. The result is that torsion is always associated with shear deformation due to shear stresses.

Despite the apparent differences in the loading, there are similarities between bending and torsion in the linear distribution of strains and stresses. Exact solutions exist only for special types of cross-sections, but we examine some approximations that apply to other cases.

The angle of twist in a member of any cross section subject to torsion and free to warp at its ends (i.e. pure or St. Venant torsion) is given by the formula:

$$\theta = \frac{T\ell}{JG} \qquad (2.1)$$

where, ℓ = length
θ = rotational displacement
T = torques
J = torsion constant
G = shear modulus

2.2.1 Torsion of prismatical bars.

When starting with torsional problems it is easier to introduce it with a circular shaft. The exact solution of the torsional problem for a circular shaft can be obtained if one assumes that the cross sections of the bar remain plane and rotate without any distortion during twist. Coulomb developed this theory, and Navier applied it later to prismatical bars of non-circular cross sections[7,8]. Navier then concluded that for a given torque, the angle of twist of the bars is inversely proportional to the centroidal polar moment of inertia of the cross section, and that the maximum shearing stress occurs at the points most remote from the centroid of the cross-section.

Figure 2.1: Twisting of rectangular bar[8].

A simple experiment was later done on a rectangular bar, which showed that the cross-section of the bar does not remain plane during torsion, and that the distortions of rectangular elements on the surface of the bar are greatest at the middle of the sides of the bar, i.e. at the points which are nearest to the axis of the bar (see fig. 2.1).

The most correct solution of the problem of torsion of prismatical bars by couples applied at the end was given by Saint-Venant[8,3], who used a so-called semi-inverse method. If one consider a prismatical bar of any cross-section twisted by couples applied at the ends, (see fig 2.2). Saint-Venant assumed that the deformation of the twisted shaft consists of *rotations of* cross-section of the shaft as the case of a circular shaft and *warping* of the cross sections, which is the same for all cross sections. It was found that the displacement corresponding to rotation of cross section is

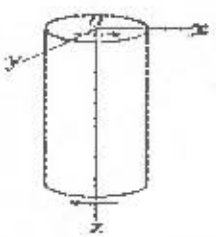

Figure 2.2: Twisting of round bar[7].

$$u = -\theta zy, \qquad v = \theta zx \tag{2.2}$$

where θz is the angle of rotation of the cross section at a distance z from the origin.

The warping of cross sections is defined by the function

$$w = \theta\psi(x,y) \tag{2.3}$$

With Eq's 2.2 and 2.3 it can be seen regarding the deformation that there will be no normal stress acting between the longitudinal fibres of the shaft or in the longitudinal direction of those fibres. Also no distortion in the planes of cross section will occur, since $\varepsilon_x, \varepsilon_y, \gamma_{xy}$, vanishes.

Consider a circular bar of elastic homogeneous material.

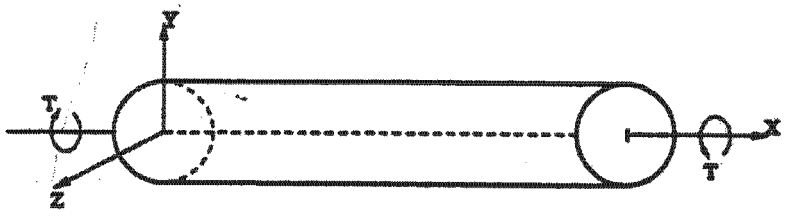

Figure 2.3 Torsion of round bar

The strain distribution will be linear for theoretical purposes.

With **strain distribution**, the following assumptions are made:

1. Plane cross-sections remain plane. No warping, wrinkling or distortion occurs.
2. Plane cross-sections rotate relative to each other about the X-axis.
3. Any radius on any cross-section remains straight. Graphically we assume

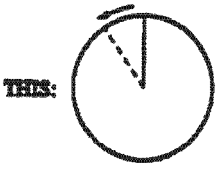

Figure 2.4

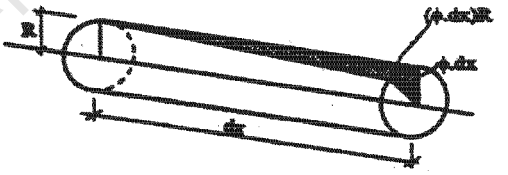

Figure 2.5

For circular bars in torsion let the twist per unit length be ϕ (rad/m)

Consider a small piece of circular bar with length dx (see fig. 2.5):

Consider the two radii, which have the same center-point before deformation and observe the shaded element in the diagram on the left, and the resultant position after torsion is applied (see fig. 2.6).

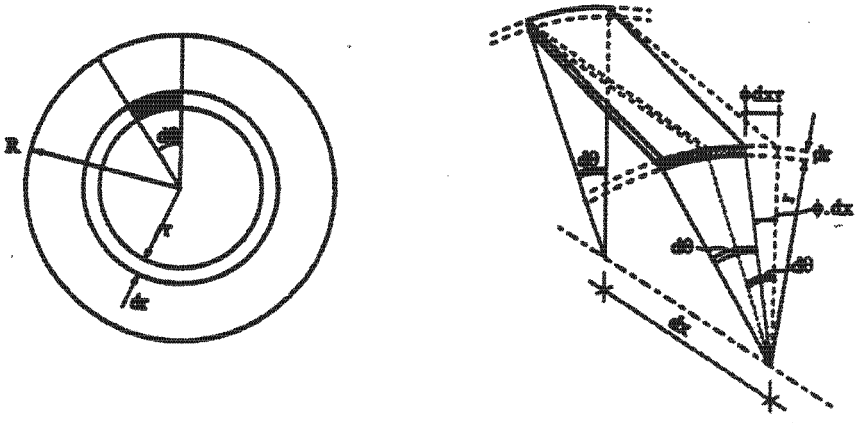

Figure 2.6: Schematic of rotational displacement[83]

Take the element from the annular shell of radius r, thickness dr and length dx, and draw a plan-view of the element and observe the deformation in figure 2.7.

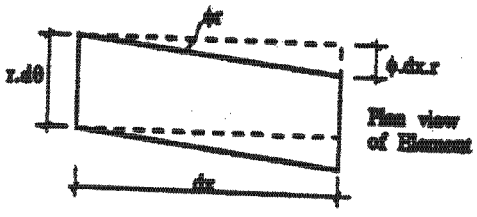

Figure 2.7: Pure shear deformation

The rectangular element deforms into a parallelogram. This deformation demonstrates **pure shear deformation**, and shear strain can thus be quantify as:

$$\gamma = \frac{(\phi dx)r}{dx} = \phi r \qquad (2.4)$$

The shear strain varies linearly with r; thus it is zero at the shaft centre and maximum at the shaft surface.

By using the elastic relationship, the **stress distribution** is given by:

$$\tau = G\gamma = G\phi r \qquad (2.5)$$

hence the shear stress τ also varies linearly with r.

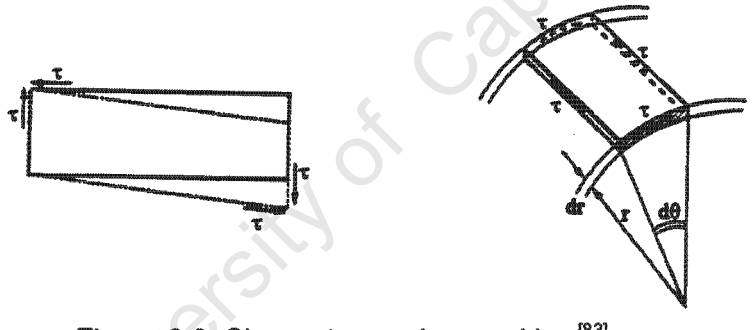

Figure 2.8: Shear stress τ in round bar[83]

Tangential force on the face of the element = τ (rdθ) (dr) (stress x area)

But the assumptions made for circular bars do not apply for non-circular bars:
Plane sections do not remain plane, warping occurs.
Shear strain distribution is not linear with respect to distance from the centre of twist.

2.2.2 Occurrence of twisting/torsion

Bending may take place without twisting in a loaded beam or girder, or while bending it can also twist at the same time. The difference in behaviour depends on the resultant of the load passing through a particular point called the torsion centre or shear centre on the cross section of the beam or girder. If the load is eccentric about that point, torsion or twisting can occur. The torsion/shear centre is located by calculating the shearing forces in different parts of the section and by determining the position of their resultant.

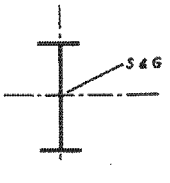

Figure 2.9: I-section

Evaluating resultant for shears in two directions at right angles, the shear centre is found to be the point of intersection. If the section is symmetrical in both x and y directions, the shear centre, S, coincides with the centre of gravity (e.g. an I-section in figure 2.9).

For a channel, there is symmetry only about the x-x axis with asymmetry about the y-y axis in the channel-section. Therefore the shear centre, S, is on the x-x axis and is outside the y-y axis and it is actually outside the section (see fig. 2.10).

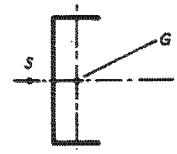

Figure 2.10: Channel-section

The position of the shear centre is eccentric to the axes x-x and y-y for totally asymmetrical sections (see fig. 2.11). For calculating the position of the shear centre in box or "closed" sections the above principles are also used.

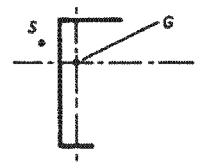

Figure 2.11: Asymmetrical-section

The loading on elements may be exerted in any direction and can be resolved into two forces P and L in two directions, x-x and y-y, at right angles.

The total torque, T, is: $T = Pe_x \pm Le_y$ (2.6)

2.2.3 **Resistance to torsion**

Because of the difference in behaviour of sections in resisting torsion they are split into two types. The two types are either "open" or " closed sections" (or closed-box). In figure 2.12(a), the "open" types are illustrated and they are those such as rolled sections, plate girders, etc. Illustrated in figure 2.12(b) are the "closed-box" type and examples of these are rectangular hollow sections, box plate girders, etc.

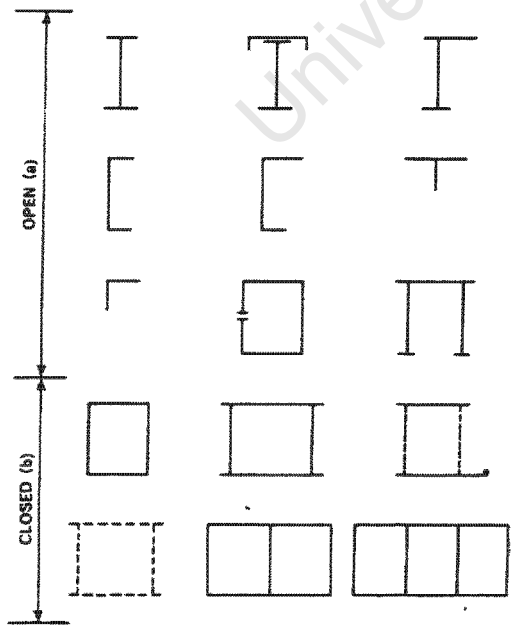

Figure 2.12: Sections

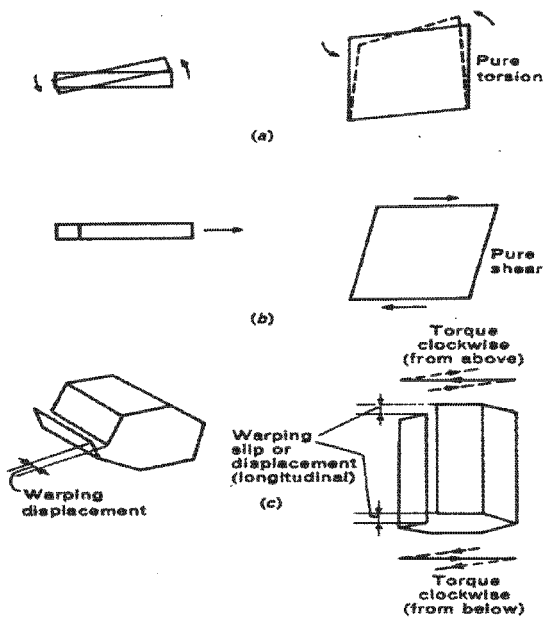

Figure 2.13: Warping of elements

When a section is twisted three modes of distortion can occur. The first mode of distortion is the pure torsion of the section. As shown in figure 2.13(a), the plates themselves tend to twist if the section is comprised of a series of connected plates. This can be seen in "open" sections. The second type of distortion that can be seen is that the plates tend to distort under shear as shown in figure 2.13(b). The exertion of the above effect can be seen in the "closed-box" sections. The third mode can be seen in figure 2.13(c), where the section when open tends to twist causing longitudinal displacements in opposite directions. The above are called warping. Under transverse loading the warping effect can be restrained, it can also be restrained by fixing ends, then transverse shears and longitudinal strains are set up causing a mode of resistance to torsion which can be seen in flanged beams or girders. The above can be seen in beams bending of flanges in opposite directions assist in resisting the torsion on the section. The three above effects that were mentioned will now be discussed in detail and their formulae will also be looked at and assessed.

2.2.4 **Pure torsion of " open" cross sections**

It can be seen in figure 2.14 that "open" cross section under pure torsion acts as if it is made out of a number of elementary narrow rectangles, each of length *m*, and thickness *t*, with the equation below to calculate the torsion constant, K (the measure of resistance torsion) where:

$$K = \frac{mt^3}{3} \qquad (2.7)$$

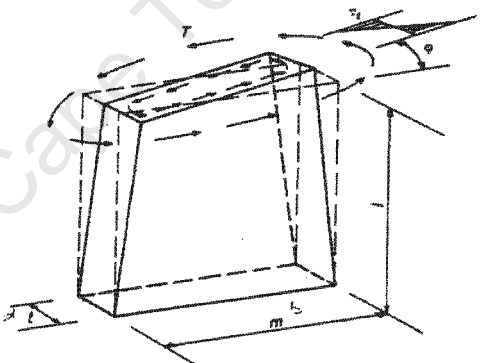

Figure 2.14[2]: Warping of cube

The magnitude of the torsion constant, K, for the total cross section is approximately 1/3 mt^3. Rolled steel sections have fillets between the web and the flanges and chamfers on the flanges. The British Constructional Steelwork Association Ltd took this into account and modified formulae for rolled steel sections, which are slightly more complicated formulae than EL Darwish and Johnson [83].

A section is subjected to pure torsional shearing, τ_t, stresses, if there is no transverse load on the section and the ends are twisted so that the flanges are not restrained and the ends are free to warp. The torsional shearing stresses vary linearly across thickness of the element of cross section. It also acts parallel to the centre line of the element and the sign on each side is equal and opposite of it, (see figure 2.14 and figure 2.15).

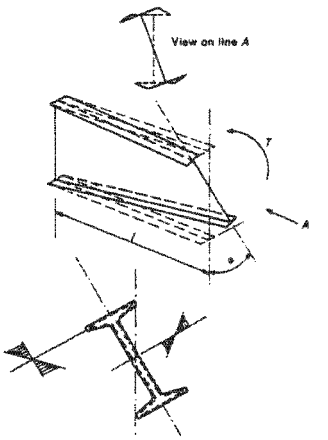

Figure 2.15[83]: Warping of I-beam

The rate of twist per unit of beam, $\frac{d\varphi}{dz}$ is constant, in

pure torsion, and is $\frac{\varphi}{l}$ where φ is the total angle of twist.

$$\text{The total torque, T} = GK\frac{d\varphi}{dz} = GK\frac{\varphi}{l} \quad (2.8)$$

$$\text{The maximum shearing stress at any section} = \frac{Tt}{K} = Gt\frac{d\varphi}{dz} = Gt\frac{\varphi}{l} \quad (2.9)$$

where G = modulus of rigidity

2.2.5 **Warping of "open" section under pure torsion**

Twisting of longitudinal fibres of a thin walled section of "open" section around the z-z axis into helices can be seen in pure torsion, (an example is the edges of the flanges of a joist). In figure 2.16, it can be seen how the flanges of a joist twist in their own planes in opposite directions, while the section remains normal to the longitudinal fibres. Take the total angle of twist as φ on a length *l*, the angle of twist per unit length = $\frac{d\varphi}{dz} = \frac{\varphi}{l}$.

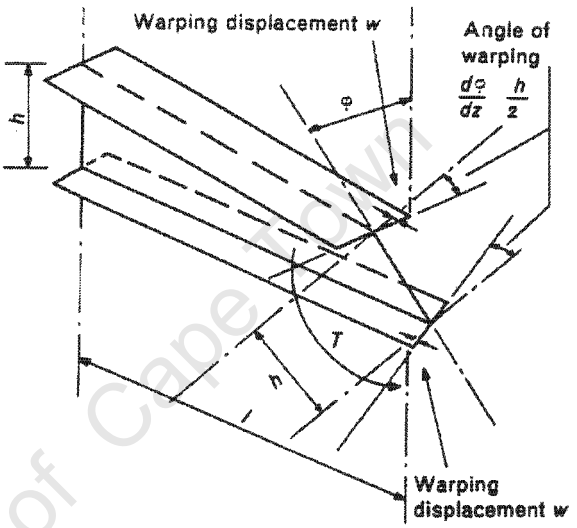

Figure 2.16[21]: Warping displacement of I-beam

The warping of the section is at an angle of $\frac{d\varphi}{dz}\frac{h}{2}$

where h is the distance between the centres of the flanges. The definition of the warping displacement, ω, of any point on the cross section, is the displacement from the corresponding point on the average or unstrained cross section of that point in the z or longitudinal direction.

A particular case of warping of any member "open" cross section is the warping of the I-section, which gives an expression with the value of ω for any "open" cross-section that has been evaluated. This expression can be applied to all types of sections such as joists, channels, or to composite sections.

In the calculations for pure torsion there is no need for the calculation of the value of ω at any point in a cross-section, but when warping is prevented or partially restrained, the value of ω is proportional to normal fibre stresses in the section the value of ω needs to be calculated because all sections under torsional loading are subjected at certain sections of their length to restrained warping.

Open cross-sections such as I-beams are particularly susceptible to lateral torsional buckling due to lack of torsional rigidity. There are type of torsional

rigidity that might exist in a member with a thin plate cross-section namely; uniform torsion and non-uniform torsion (also known as warping restraint torsion) restraints.

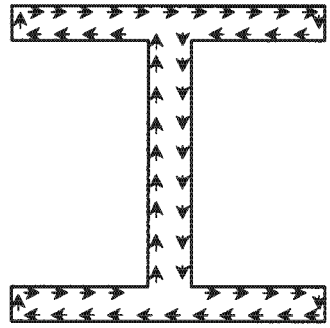

Figure 2.17: Stress distribution in I-section

Uniform torsion is a unique case of loading when the structural member has no warping resistance and subjected to equal and opposite torques[27]. In this type of torsion, the warping deformation in the beam is the same for all cross-sections without inducing any axial strain on the longitudinal fibres. This means that the applied torque is resisted solely by shear stresses developed in the cross-section. It is usually assumed that the shear stresses at any point acts parallel to the tangent to the axis of the cross-section (see figure 2.17) for open cross-sections. The magnitude of these shear stresses will be proportional to the distance from the axis of the component plate.

As a result, uniform torsion (T_{sv}) can be express in the following formula:

$$T_{sv} = GJ\frac{d\gamma}{dz} \qquad (2.10)$$

where: $d\gamma / dz$ = the rate of twist

G = shear modulus

J = torsional constant of the cross – section

For thin plate section, the torsional constant can be taken as :

$$J = \sum_{i=1}^{n} \frac{1}{3} b_i t_i^3 \qquad (2.11)$$

However, if the cross-section of the member's end is fixed in the longitudinal direction, in addition to uniform torsion rigidity, there exists another type of torsion called warping restraint torsion. When the cross-section is restraint to warping, axial strain and stresses will be induced in the member in addition to the shear stresses as in figure 2.18. For an I-section, these axial stresses in the two flanges create a pair of equal and opposite moments M_f. With the usual beam moment-curvature relationship, the magnitude of these moments can be expressed as:

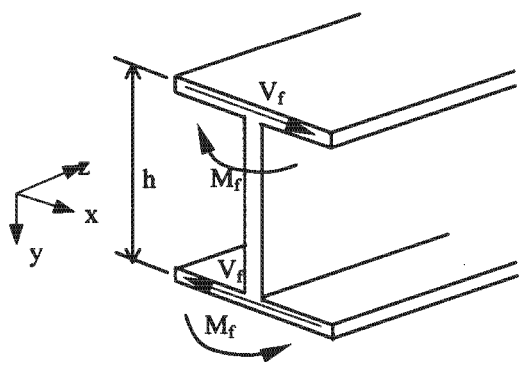

Figure 2.18: Moment and shear development due to warping

$$M_f = EI_f \frac{d^2 u_f}{dz^2} \qquad (2.12)$$

I_f = the moment of inertia of one flange about the minor axis

u_f = the lateral displacement of the flange

The pair of shear forces that is associated with the moment M_f provides the warping restraint torsion (T_w).

$$V_f = -\frac{dM_f}{dz} = -EI_f \frac{d^3u_f}{dz^3} = -EI_f \frac{hd^3\gamma}{2dz^3} \tag{2.13}$$

$$T_w = V_f h = -EI_f \frac{hd^3\gamma}{2dz^3} = -EI_w \frac{d^3\gamma}{dz^3} \tag{2.14}$$

h = the distance between the lines of action of the shear forces

$$I_w = \frac{I_f h^2}{2} = \text{warping constant of I-section}$$

The warping restraint torsion is dependent on end restraints. Moving away from the member's end, the magnitude of the torsion is decreasing, and thus it is called non-uniform torsion.

In summary, when a member is subjected to twisting, the internal twisting moment (T) equals to:

$$T = T_{sv} + T_w$$

When a member is subjected to twisting and rotates, the uniform torsion is always present. In contrast, warping torsion resistance will develop when a cross-section is prevented from warping. However, not all cross-sections will have warping resistance torsion. Some cross-sections have no warping constant, such as an angle-iron and T-sections. Other such as axisymmetric sections simply have no warping.

2.2.6 **Resistance of a section to torsion under transverse loading**

Illustrated in figure 2.19,an "open" girder bends and twists under a transverse eccentric load. The resistance to torsion is affected by two effects at any section along the length of the girder. These effects are its resistance in pure torsion and the tendency to resist warping. An example of this is when a girder is symmetrically loaded about mid-span and the ends prevented from twisting, but it is not build-in (to fix the flanges), then the torsional resistance at mid-span section is wholly by restraint of the flanges to warping; and the resistance is wholly by pure torsional strains at the supports. The flanges are not restrained to support the above-mentioned statement, the resistance is partly by pure torsion at all other intermediate sections along the girder and partly to warping.

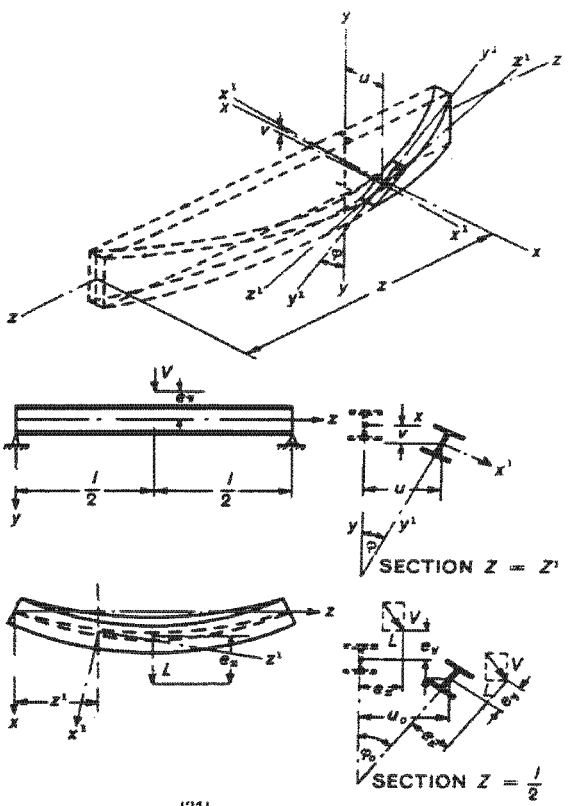

Figure 2.19[21]: Twisting of I-beam

Depending on compatibility between the loading and the degree of fixing at the end, the proportion of the resistance to torsion by pure torsion and by warping can be seen at any section of the girder.

2.2.7 Partial resistance by pure torsion of beam under transverse load

The proportion of the resistance by pure torsion is dependent on the rate of change of the angle of twist φ, which is $d\varphi/dz$ or φ'', this can occur at any section of the element. The values of φ and hence φ' vary along the beam or girder. If the girder is under transverse load, the magnitude of proportion of the torque resisted in pure torsion is T_1, then it can be said that at any point along the beam or girder, which has twisted through an angle φ,

$$T_1 = GK\varphi' \qquad (2.15)$$

and the corresponding pure torsional stresses τ_t are:

$$\tau_t = \frac{T_1 t}{K} \qquad = ct\varphi' \qquad (2.16)$$

2.2.8 Partial resistance by warping restraint of beam under transverse load

This is illustrated in figures 2.19 and 2.20 where the section bends and twists, at mid-span, the flanges are not free to warp. The above condition can be said to be the same as that of the fixed end of a cantilever, when the member is twisted and loaded at the free end, as can be seen in figure 2.21(a). Partial restraint to warping can be seen at various sections along the span, where pure torsion takes up the balance in each case. Because of the variation in warping restraint that occurs along the spans, longitudinal strains can occur and normal fibre stresses can also be created at any cross-section.

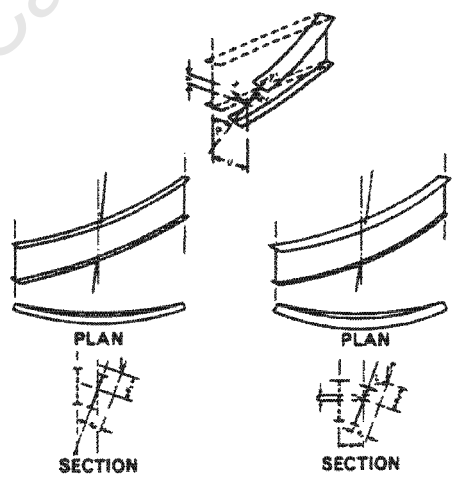

Figure 2.20[12]: Torsion of I-beam

It can be seen in figure 2.21(b) that in the general case of cross-section, the section flexes in opposite directions and in figure 2.21(c) in the I-section beam, although the whole section is stresses the flanges are mostly affected, by acting as beams in their own planes and stresses in different directions. Figure 2.21(d) gives a combined look at the variation from the general case as seen in figure 2.21(b), which approximates to the I-beam as seen in figure 2.21(c).

φ_{ws} are the normal fibre stresses due to non-uniform torsion of warping restraint where:

$$\sigma_{ws} = E\varphi'' W_{ns} \qquad (2.17)$$

W_{ns} is a factor calculated from dimensions of the cross-sections and for various types of cross-section values for W_{ns} was found and put into tables by the British Constructional Steelwork Association Ltd[11].

The flexing of the section creates normal fibre, and it is accompanied by shearing stresses across the section, and as illustrated by figure 2.22 the shearing forces across the flanges are in opposite directions, in the case of the I-beam. The above shearing forces give a couple, T_2, which is the balance of the total torque, T, on the section.

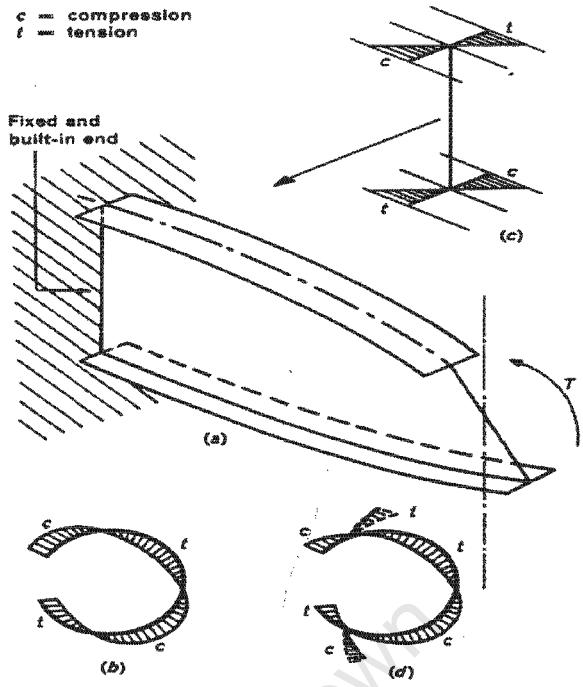

Figure 2.21[77]: I-beam partially restraint to warping

At any point on the section, the shearing stresses, τ_{ws}, can be:

$$\tau_{ws} = -\frac{ES_{ws}\varphi'''}{t} \qquad (2.18)$$

Calculated from the dimensions of cross-section and various types of cross-section value, you get S_{ws}. The torque, T2 contributed by shearing strains is a summation along the middle line of the section of the moments of shearing forces about the shear centre. The shear in the web is so small that it can be taken as zero in the case of the I-beam and the shearing forces in the flanges exert major torsional effects. The magnitude of the torque is given by:

$$T_2 = -EI_w\varphi''' \qquad (2.19)$$

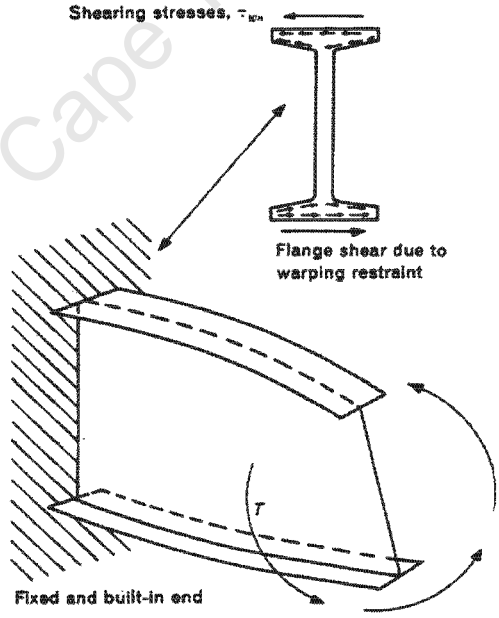

Figure 2.22[77]: Shearing stresses due to partially restraint to warping

Calculated from the dimensions of the cross-section and rolled values are the warping constant, I_w of a sector.

2.2.9 **Total resistance to torsion under transverse load**

The total resistance of a section to torsion at any section of a beam, of "open" cross-section, is the sum of the two effects, namely:

(a) Pure Torsion T_1
(b) Warping Restraint T_2

Hence,

$$T = T_1 + T_2 \qquad = GK\varphi' - EI_w\varphi'''$$

$$or \quad \frac{T}{GK} = \varphi' - a^2\varphi''' \tag{2.20}$$

Where,

$$a^2 = \frac{EI_w}{GK} \qquad \therefore \quad a = \sqrt{\frac{EI_w}{GK}} \tag{2.21}$$

The products of these equations for particular loading and end-conditions are φ and its derivatives.

2.2.10 **Constrained torsion equation**

During twisting, the cross-section of the core undergoes distortion, with different points on the cross-section suffering different displacements along the longitudinal axis of the core. If this distortion or warping as it is called is not free to take place, longitudinal stresses directed along the z-axis develop in the cross-section. The foundation for a high-rise core is usually stiff and can be considered to restrain almost completely the vertical movement of the relatively light walls. The resulting axial stresses in general are not restricted to the vicinity of the foundation as assumed in St. Venant torsion theory.
In Vlasov[79] theory two fundamental assumptions are made:

1. The cross section is completely rigid in the transverse direction.
2. The shear strain of the middle surface is negligible.

Consider an open tube shown in *figure 2.23*. An orthogonal system of coordinates *z,s* is chosen, consisting of a generator and the middle line of the profile (*figure 2.23a*). The origin for the coordinate *z* is taken at the base, and any generator is taken as the origin for the curvilinear coordinate *s*. Let θ_z be the angle of rotation of the profile at the distance *z* from the base. This rotation is in the *xy* plane and is measured with respect to any arbitrary center of rotation *R*.

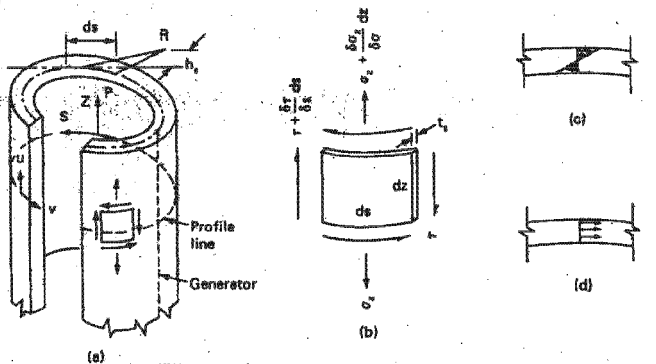

Figure 2.23[21]: Open tube. (a) Coordinate system; (b) Equilibrium of elements dz ds on the middle surface; (c) St. Venant torsion shear stresses; (d) Constrained torsion shear stresses.

Consider the displacements of any point *p* on the middle surface of the tube. The transverse displacement *v* in the direction of the tangent to the profile line is given by

$$v_{z,s} = \theta_z h_s \tag{2.22}$$

where h_s is perpendicular from the tangent at p to the center of rotation R (*figure 2.23*). If $u_{z,s}$ is the longitudinal displacement along the generator, the considering at p, of an dx ds (*figure 2.23b*), lying on the middle surface, the condition of zero shear strain is given by the relation

$$\gamma = \frac{\partial u}{\partial s} + \frac{\partial \upsilon}{\partial z} = 0$$

$$\frac{\partial u}{\partial s} + h_s \frac{d\theta}{dz} = 0 \qquad (2.23)$$

Integrating,

$$u_{z,s} = -\int^s h_s ds \frac{d\theta}{dz} \qquad (2.24)$$

The integrals is taken along the profile from an arbitrary point to point p for which the longitudinal displacement is required. The product h_s ds is equal to twice the area of the elementary triangle whose base and height are equal to ds and h_s ,respectively, and is usually given the symbol dω.

$$u_{z,s} = -\int^s \frac{d\theta}{dz} \qquad (2.25)$$

$$= -\frac{d\theta}{dz}\omega_s \qquad (2.26)$$

Since the displacement $u_{z,s}$ changes along the distance z, the strain ε_z is given by

$$\varepsilon_z = \frac{\partial u}{\partial z} = -\frac{d^2\theta}{dz^2}\omega_s$$

Hence, corresponding stress $\sigma_{z,s}$ is

$$\sigma_{z,s} = \frac{E}{1-\mu^2}\varepsilon_z$$

$$= \frac{E}{1-\mu^2}\frac{d^2\theta}{dz^2}\omega_s \qquad (2.27)$$

The origin of the coordinate s can now be found from the condition that there is no applied vertical load on the tube, i.e.,

$$\int_0^s \sigma_{z,s} t_s ds = 0 \qquad (2.28)$$

where t_s is the thickness of the tube.

The longitudinal stresses $\sigma_{z,s}$ are accompanied by shear stresses and are found from the consideration of equilibrium of an element t.ds.dz in the z direction (*figure 2.23b*)

$$t_s \frac{\partial \sigma}{\partial z} + \frac{\partial t_s \tau}{\partial s} = 0 \qquad (2.29)$$

$$\tau = \frac{E}{1-\mu^2} \frac{d^3\theta}{dz^3} \int_0^s \omega_s ds \qquad (2.30)$$

Using now the condition of zero external shear forces, it may be deducted that the origin of arbitrary center of rotation R is at the shear center. This determines completely the total stress distribution in terms of derivatives of θ. The torque M_1 carried by the membrane shear stresses (*figure 2.23d*), which accompanied the longitudinal stresses, is given by

$$M_1 = \int_0^s \tau t_s h_s ds = -\frac{E}{1-\mu^2} \frac{d^3\theta}{dz^3} \int_0^s \omega_s{}^2 t_s ds \qquad (2.31)$$

The quantity

$$\int_0^s \omega_s t_s ds$$

is a structural constant, the so-called warping moment of inertia, and is usually denoted by I_ω.

Hence $$M_1 = \frac{E}{1-\mu^2} I_\omega \frac{d^3\theta}{dz^3} \qquad (2.32)$$

The torque M_2 carried by St. Venant shear stresses (*figure 2.23c*) is given by

$$M_2 = GJ \frac{d\theta}{dz}$$

where GJ is the St. Venant torsional rigity of section.

The total torque $M=M_1+M_2$ is then given by

$$M = \frac{-EI_\omega}{1-\mu^2} \frac{d^3\theta}{dz^3} + GJ \frac{d\theta}{dz} \qquad (2.33)$$

Differentiating with respect to z, equation 2.33 becomes

$$\frac{EI_\omega}{1-\mu^2}\frac{d^4\theta}{dz^4} - GJ\frac{d^2\theta}{dz^2} = m_z \qquad (2.34)$$

Using notation

$$k = l\sqrt{\frac{(1-\mu^2)GJ}{EI_\omega}}$$

Equation 2.34 can be written

$$\frac{d^4\theta}{dz^4} - \frac{k^2}{l^2}\frac{d^2\theta}{dz^2} = m_z \qquad (2.35)$$

Equation 2.35 is the differential equation of constrained torsion and its solution yields the complete stress distribution.

2.2.1 Longitudinal stresses and bimoment

Consider the relation between the longitudinal stresses and warping,

$$\sigma_{z,s} = \frac{E}{1-\mu^2}\frac{d^2\theta}{dz^2}\omega_z$$

Multiplying both sides of this equation by $\omega_s t_s$ and integrating over the whole profile gives

$$\int \sigma_{z,s}\omega_s t_s ds = -\frac{E}{1-\mu^2}\frac{d^2\theta}{dz^2}\int w_s^2 t_s ds$$

and since

$$\int w_s^2 t_s ds = I_\omega$$

$$\int \sigma_{z,s}\omega_s t_s ds = -\frac{E}{1-\mu^2}\frac{d^2\theta}{dz^2} I_\omega \qquad (2.36)$$

The quantity

$$\int \sigma_{z,s}\omega_s t_s ds$$

is a generalized force called the bimoment and is represented by B_z.

Thus

$$B_z = -\frac{EI_\omega}{1-\mu^2}\frac{d^2\theta}{dz^2}$$

From equation 2.27

$$\frac{E}{1-\mu^2}\frac{d^2\theta}{dz^2} = \frac{\sigma_{z,s}}{\omega_s}$$

$$\therefore \quad \sigma_{z,s} = \frac{B_z\omega_s}{I_\omega} \qquad (2.37)$$

Hence the magnitude of bimoment at z and distribution of the sectorial area over the profile complete the longitudinal stresses.

2.2.12 Solution of differential equation

Using the notation $f_{(z)} = m(1-\mu^2)/EI_\omega$, equation 2.37 can be written as:

$$\frac{d^4\theta}{dz^4} - \frac{k^2}{l^2}\frac{d^2\theta}{dz^2} - f_{(z)} = 0 \qquad (2.38)$$

The solution is of the form,

$$\theta_{(z)} = C_1 + C_2 z + C_3 \sinh\frac{k}{l}z + C_4 \cosh\frac{k}{l}z + \overline{\theta_z} \qquad (2.39)$$

Differentiating equation 2.39 and using equations 2.27 and 2.36, equations for the displacements θ_z and θ_z and the two forces B_z and M_z can be written thus,

$$\theta_z = C_1 + C_2 z + C_3 \sinh\frac{k}{l}z + C_4 \cosh\frac{k}{l}z + \overline{\theta_z} \qquad (a)$$

$$\theta_z' = C_2 + C_3\frac{k}{l}\cosh\frac{k}{l}z + C_4 \sinh\frac{k}{l}z + \overline{\theta_z'} \qquad (b) \qquad (2.40)$$

$$B_z = GJ\left[C_3 \sinh\frac{k}{l}z + C_4 \cosh\frac{k}{l}z + \frac{l^2}{k^2}\overline{\theta_z''}\right] \qquad (c)$$

$$M_z = GJ\left[C_2 + \overline{\theta_z'} - \frac{l^2}{k^2}\overline{\theta_z'''}\right] \qquad (d)$$

The constants C_1, C_2, C_3 and C_4 can be determined from two boundary conditions at each end. However, calculations are greatly simplified if instead of the arbitrary C_1,C_2, C_3 and C_4, displacement and force boundary conditions, in terms of θ , θ', B and M, are used in equation 2.40. If θ_0, θ_0', B_0 and M_0 are two sets of displacements and forces at the section z=0, and id there are no applied forces, the constants C_1, C_2, C_3 and C_4 from equation 2.40 are given by

$$C_1 = \theta_0 + \frac{1}{GJ} B_0$$

$$C_2 = \frac{1}{GJ} M_0$$

$$C_3 = \frac{l}{k}\theta_0' - \frac{l}{k}\frac{1}{GJ} M_0 \qquad (2.41)$$

$$C_4 = \frac{-1}{GJ} B_0$$

Substituting these in equation 2.40 and writing in matrix form the general equations for the four quantities,

θ , θ', B and M will be of the form

$$\begin{bmatrix} \theta_z \\ \theta_z' \\ \frac{B_z}{GJ} \\ \frac{M_z}{GJ} \end{bmatrix} = \begin{bmatrix} 1 & \frac{l}{k}\sinh\frac{k}{l}z & 1-\cosh\frac{k}{l}z & z-\frac{l}{k}\sinh\frac{k}{l}z \\ 0 & \cosh\frac{k}{l}z & \frac{-k}{l}\sinh\frac{k}{l}z & 1-\cosh\frac{k}{l}z \\ 0 & \frac{-l}{k}\sinh\frac{k}{l}z & \cosh\frac{k}{l}z & \frac{l}{k}\sinh\frac{k}{l}z \\ 0 & 0 & 0 & 1 \end{bmatrix} \begin{bmatrix} \theta_0 \\ \theta_0' \\ \frac{B_0}{GJ} \\ \frac{M_0}{GJ} \end{bmatrix} \qquad (2.42)$$

or in matrix notation, $Z_z=G_0Z_0$, where Z_z is the action matrix, G_0 the distribution matrix, and Z_0 the initial boundary restraint matrix. If, in addition to the boundary restraints, concentrated forces and displacements are applied at any section z=t then, using the principle of superposition, the expressions for the actions at any z($t \leq z \leq d$) will be of the form

$$Z_{(z)} = G_{0(z)}Z_0 + G_{(z-t)}Z_t \qquad (2.43)$$

Where $G_{(z-t)}$ is of the same form as $G_{0(z)}$, except that the argument (z – t) replaces z, and z_t refers to the restraint matrix at z = t. The solution represented by equation 2.43 can easily be extended to other loading cases, such as several loads applied at various sections and distributed loads, by simple supersition and integration, respectively.

2.3 BUCKLING: MODES OF FAILURE

The simplest type of buckling is that of an initially straight strut compressed by equal and opposite axial forces introduced by Euler, as shown in the figure 2.24. The undeflected state of the member becomes unstable as the applied loads are increased in magnitude and the member prefers to adopt a deformed curved/buckled shape.

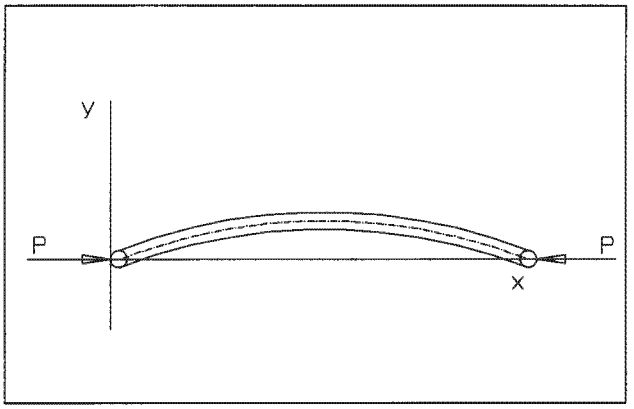

Figure 2.24: Buckling of a strut (Euler)

The members buckling resistance will increase with the bending stiffness of the member as well as the adjacent members, and hence with the thickness or depth of its section measured in the plane of buckling deformation. The buckling resistance decreases as the member's length increases. Thus buckling resistance is low if a member is slender and high if it is stocky.

Steel members tend to be slender in form, and likely to fail through buckling. However, it is not only slenderness of a member as a whole that leads to buckling. The thin plates in steel members, for both hot rolled and cold-formed elements may individually experience localized buckling effects when subjected to compressive stress. Some members of thin, open cross-section have a low torsional stiffness and experience buckling phenomena involving torsional as well as bending deformation.
A steel beam can fail in many different ways, and it is useful at this point to look at the most important of these ways.

(a) **Bending** - As a result of the bending moment in a beam, longitudinal stresses are set up in the beam. These stresses are tensile in one half of the beam and compressive in the other. As the bending moment increases yield is eventually reached. Failure takes place when steel yields in tension and/or compression across the entire cross section of the beam. When all of the beam cross-section has become plastic in this way the beam fails by formation of a plastic hinge at the point of maximum imposed moment. figure 2.25 reviews this process. Later it will be summarized how classical beam theory is derived from these considerations.

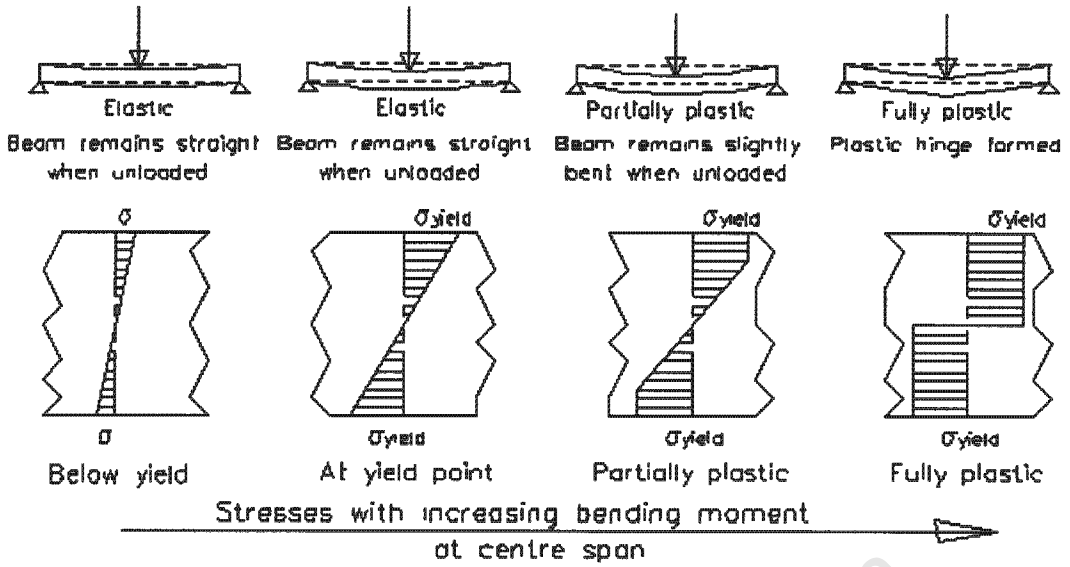

Figure 2.25[81] - Bending failure of a beam

(b) **Local buckling** - During the bending process outlined above, if the compression flange, or the part of the web subject to compression, is too thin the plate may actually fail by buckling, or rippling, as shown in figure 2.26, before the full plastic moment is reached.

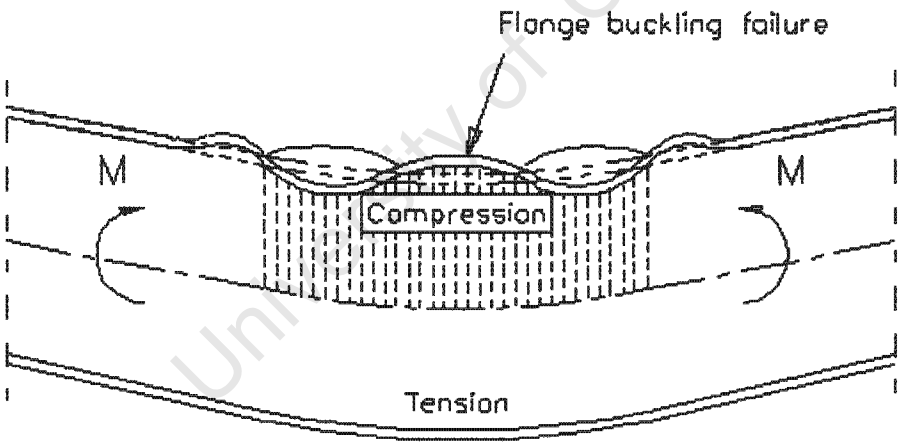

Figure 2.26[81] - Local flange buckling failure

(c) **Shear** - Due to excessive shear forces, usually adjacent to supports, the beam may fail in shear. The beam web, which resists shear forces, may fail as shown in figure 2.27(a), as steel yields in tension and compression in the shaded zones. The formation of plastic hinges in the flanges accompanies this process.

(d) **Shear buckling** - During the shearing process described above, if the web is too thin it will fail by buckling or rippling in the shear zone, as shown in figure 2.27(b).

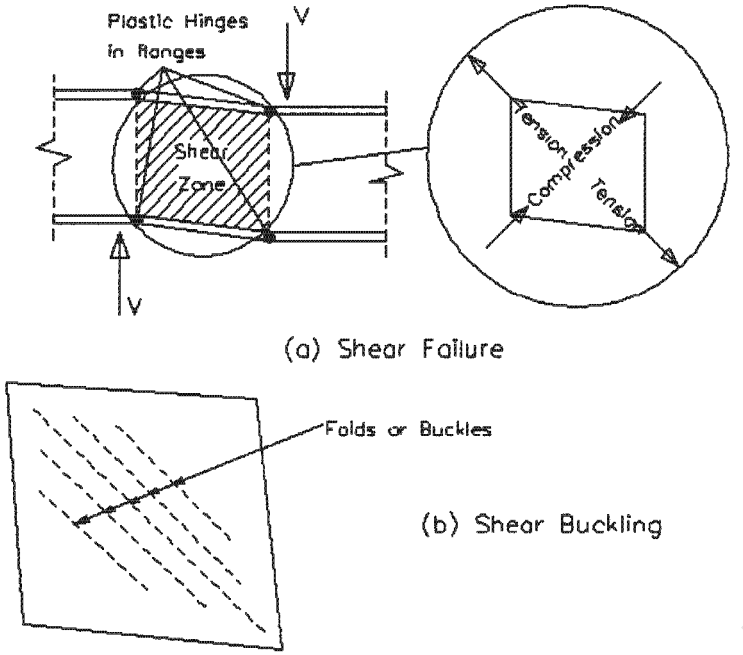

Figure 2.27[81] - Shear and shear buckling failures

(e) **Web bearing and buckling** - Due to high vertical stresses directly over a support or under a concentrated load, the beam web may actually crush, or buckle as a result of these stresses, as illustrated in figure 2.5.

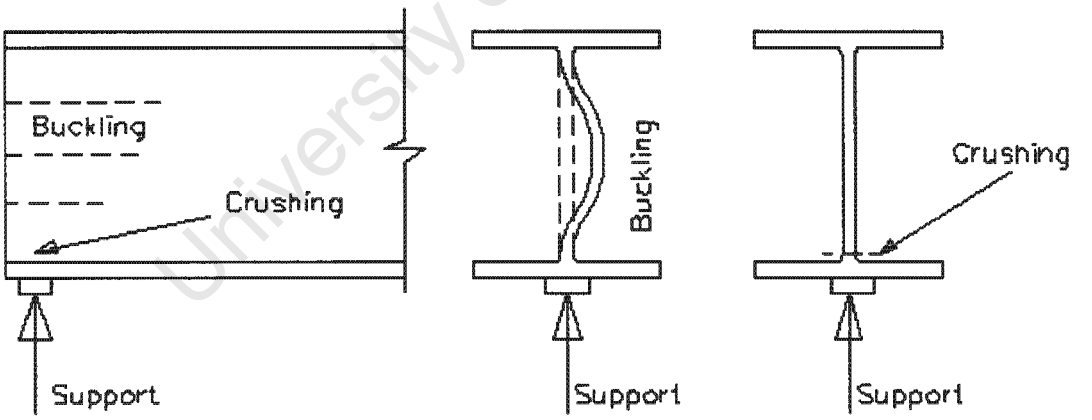

Figure 2.28[81] - Web buckling and web bearing failures

(f) **Lateral torsional buckling** - When the beam has a higher bending stiffness in the vertical plane compared to the horizontal plane, the beam can twist sideways under the load. This is perhaps best visualized by loading a scale rule on its edge, as it is held as a cantilever - it will tend to twist and deflect sideways. Where a beam is not prevented from moving sideways, by a floor, for instance, it is necessary to check that it is laterally stable under load. This is illustrated in figure 2.29.

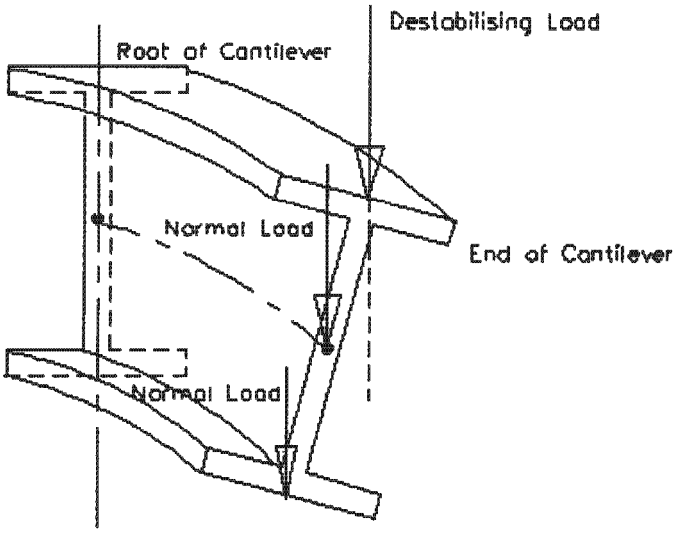

Figure 2.29[81] - Lateral torsional buckling of cantilever

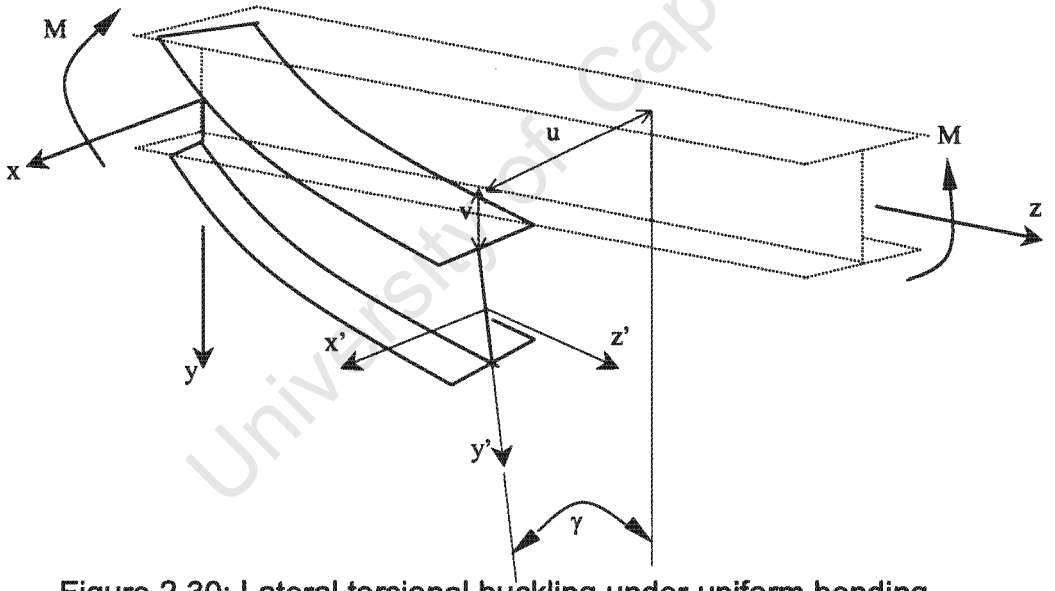

Figure 2.30: Lateral torsional buckling under uniform bending

Similar to columns, the critical load of a beam under various loading can be worked out using bifurcation analysis. An example of a simply supported I-beam subjected to uniform bending moment is illustrated in figure 2.29 and figure 2.30.

Two sets of co-ordinates are used to simplify the derivation of internal and external forces relationship. The x'-y'-z' axes are local co-ordinate axes that are fixed with the cross-section and move with the deflected position of the structural element. These two sets of co-ordinates have the following relationship as illustrated in figure 2.31.
It follows that the external moment at any cross-section equals to:

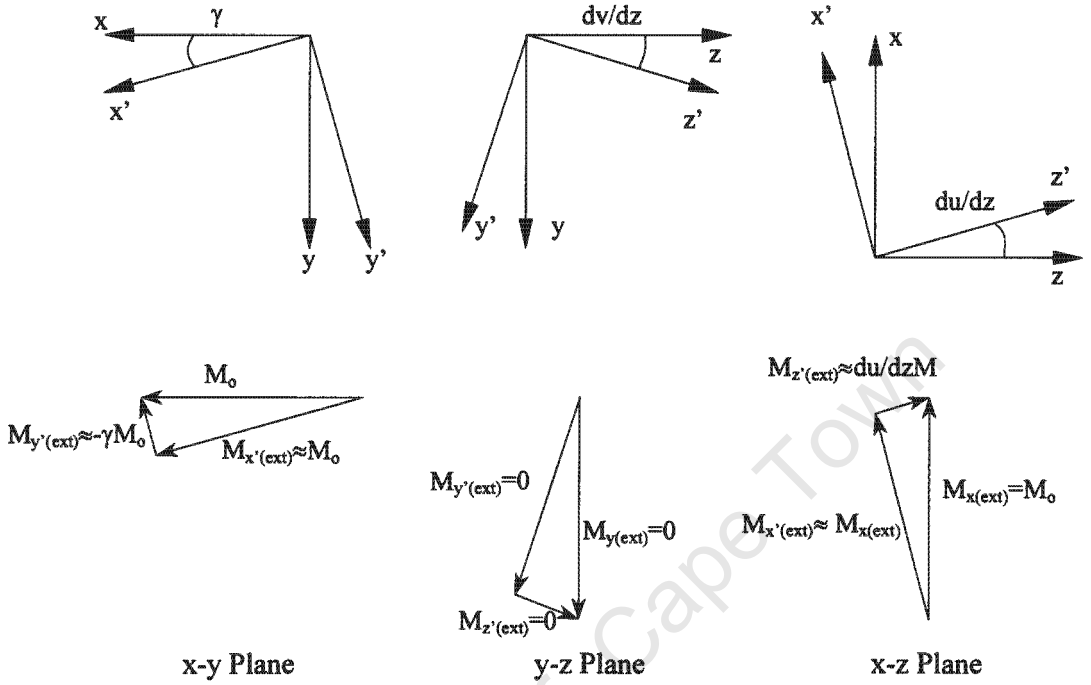

Figure 2.31: Components of moments

$$M_{x'(\text{int})} = -EI_x \frac{d^2v}{dz^2} \qquad (a)$$

$$M_{y'(\text{int})} = -EI_y \frac{d^2u}{dz^2} \qquad (b)$$

$$M_{z'(\text{int})} = GJ\frac{d\gamma}{dz} - EI_w \frac{d\gamma^3}{dz^3} \qquad (c) \qquad (2.44)$$

And the corresponding internal resisting moments equals to:

$$M_{x'(ext)} \approx M_{x(ext)} = M_o \qquad (a)$$

$$M_{y'(ext)} \approx -\gamma M_{x(ext)} = -\gamma M_o \qquad (b)$$

$$M_{z'(ext)} \approx M_{x(ext)} du/dz = M_o du/dz \qquad (c) \qquad (2.45)$$

And the governing differential equations for an I-beam subjected to pure bending equals to:

$$EI_x \frac{d^2v}{dz^2} + M_o = 0 \qquad (a)$$

$$EI_y \frac{d^2u}{dz^2} + \gamma M_o = 0 \qquad (b)$$

$$GJ\frac{d\gamma}{dz} - EI_w \frac{d^3\gamma}{dz^3} - \frac{du}{dz}M_o = 0 \qquad (c) \qquad (2.46)$$

The first equation (2.46a) is independent of the other two equations, which means that it describes the in-plane behaviour of the beam before lateral buckling. By combining the last two equations, the lateral torsional buckling behaviour can be obtained (see equation 2.47).

$$EI_w \frac{d^4\gamma}{dz^4} - GJ\frac{d^2\gamma}{dz^2} - \gamma\frac{M_0^2}{EI_y} = 0 \qquad (2.47)$$

By solving equation 2.48 with simply supported conditions, the critical moment can be obtained:

$$M_{ocr} = \frac{\pi}{L}\sqrt{EI_y GJ}\sqrt{\left(1 + \frac{\pi^2 EI_w}{L^2 GJ}\right)} \qquad (2.48)$$

With the above equation it is assumed that the in-plane deflection has no effect on the lateral torsional buckling behaviour of the beam. If the major axis rigidity is much greater than the one of the minor axis, the assumption will be justified. However, if both rigidities are of more or less of the same order or magnitude, the solution will become more complicated. Kirby and Nethercot[54] derived an approximate solution to the problem given as:

$$M_{ocr} = \frac{\pi}{L}\sqrt{\frac{EI_y GJ}{1-(I_y/I_x)}}\sqrt{\left(1 + \frac{\pi^2 EI_w}{L^2 GJ}\right)} \qquad (2.49)$$

This formula predicts that lateral torsional buckling will never occur when the acting load is in the plane of strong axis.

(g) **Deflection** - Although a beam cannot fail, as a result of excessive deflection alone, it is necessary to ensure that deflections are not excessive under unfactored imposed loading.
Excessive deflections are those resulting in severe cracking in finishes, which would render the building unserviceable.

It is perhaps most often the case in the design of skeletal building structures, that bending is the critical mode of failure, and so beam-bending theory can be used to make an initial selection of section.

If a beam is not effectively laterally restrained, it is possible for the beam to twist sideways under a load less than that which would cause the beam to fail in bending, shear or deflection. The latter scenario is called lateral torsional buckling.

2.3.1 **Concepts of buckling**

Buckling of steel frame structures in general, can be categorised into two groups, namely bifurcation instability and limit load instability.

Bifurcation instability occurs when the compressive load increases, and the member or system that originally deflects in the direction of the applied loads suddenly deflects in a different direction. The deflection path that exist before

bifurcation is known as the fundamental or primary path known as the secondary or the post buckling path, which can be divided into types depending on the nature of the path. (Refer to Thin Walled Beams (From Theory to Practice) by K. Zbirohowski-Kościa[83] for an explanation on the two types of bifurcation).

2.3.2 **Transverse Loads on beams**

A beams main function is to support transverse loads. The stability analysis of a beam subjected to transverse loading is different from that of a beam with end moments. In this case, not only the moment varies along the length of the beam and the governing differential equations with variable coefficients, but also, the solution to the critical moment depends on the load's height relative to the cross-section. Figure 2.32 is an example of a simply supported I-beam

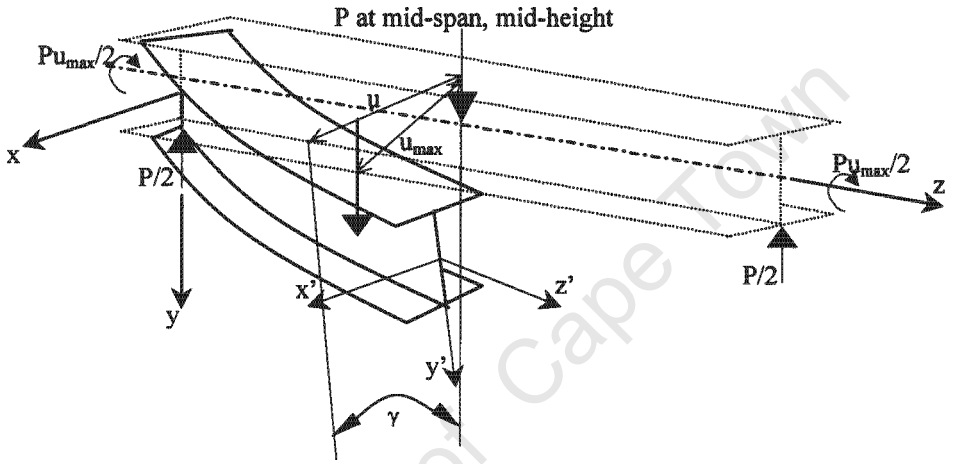

Figure 2.32: Lateral torsional buckling under concentric load at mid-span

subjected to a load at mid-span and mid-height (relative to the cross-section).

When considering the concentric load acting on the shear centre of the I-beam, the external moment for any cross-section in terms of co-ordinates x-y-z is:

$$M_{x(ext)} = \frac{P}{2\left(\frac{L}{2} - z\right)} \qquad (a)$$

$$M_{y(ext)} = 0 \qquad (b)$$

$$M_{z(ext)} = -\frac{P}{2(u_{max} - u)} \qquad (c) \qquad (2.50)$$

Because the internal moment can be easily expressed as in equation 2.44 with respect to x'-y'-z' co-ordinates, then the external moments will become as follows to the x'-y'-z' co-ordinates:

$$M_{x'(ext)} \approx M_{x(ext)} = \frac{P}{2\left(\frac{L}{2} - z\right)} \qquad (a)$$

$$M_{y'(ext)} \approx -\gamma M_{x(ext)} = -\frac{\gamma P}{2\left(\frac{L}{2} - z\right)} \qquad (b)$$

$$M_{z'(ext)} \approx M_{z(ext)} = -\frac{P}{2(u_{max} - u)} \qquad (c) \qquad (2.51)$$

And so, the governing differential equations are:

$$EI_x \frac{d^2v}{dz^2} + \frac{P}{2}\left(\frac{L}{2} - z\right) = 0 \qquad (a)$$

$$EI_y \frac{d^2u}{dz^2} + \gamma \frac{P}{2}\left(\frac{L}{2} - z\right) = 0 \qquad (b)$$

$$GJ\frac{d\gamma}{dz} - EI_w \frac{d^3\gamma}{dz^3} + \frac{P}{2}(u_{max} - u) - \frac{du}{dz}\frac{P}{2}\left(\frac{L}{2} - z\right) = 0 \qquad (c) \qquad (2.52)$$

And the critical moment can be solved from the combination of the second and third equation in a form of:

$$EI_w \frac{d^4\gamma}{dz^4} - GJ\frac{d^2\gamma}{dz^2} - \frac{\gamma}{EI_y}\left[\frac{P}{2}\left(\frac{L}{2} - z\right)\right] = 0 \qquad (2.53)$$

Timoshenko and Gere[17] (1961) have solved this equation by the method of infinite series, which produced the following plot (see figure 2.33)

When the concentrated load is not acting on the shear centre, the external twist moment will vary along the load height as follows:

$$M_{z'(ext)} \approx M_{z(ext)} = -\frac{P}{2}(u_{max} - \gamma_m h/2 - u) \qquad (2.54)$$

where h = the load height from shear centre, positive being below the shear centre

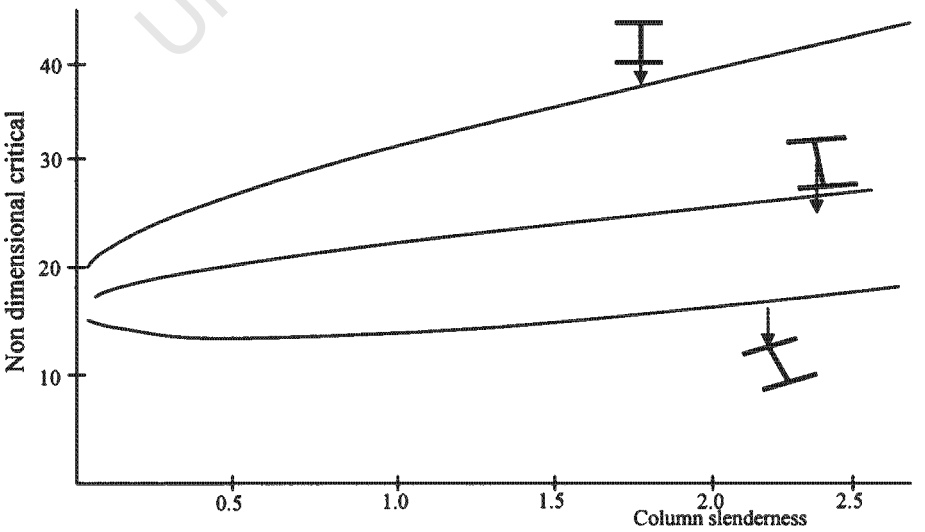

Figure 2.33: Effect of load height

In practice however, it would be very difficult to determine what exact load height is best for stability. So the load is assumed to act on the shear centre, top or bottom flanges.

Since there are infinite combinations of transverse loads and load heights, different design codes of practice adapted different solutions in their design specifications.

2.3.3 **Calculation of rotation and stresses.**

Sectorial properties. For the calculation of rotation and stresses, it is first necessary to determine the sectorial properties, namely, the function ω_s and the sectorial moment of inertia I_ω. These are readily calculated for the core by using the method well documented by V.Z. Vlasov[79].

$$I_\omega = \int_0^s \omega^2 t ds = 2t\left[\frac{d^3e^2}{24} + \frac{d^2e^3}{12} + \frac{d^2(b-e)^3}{12} + \frac{c}{6}\left\{\frac{d}{2}(b-e)\right\}\right]$$

$$\cdot\left[\frac{3d}{2}(b-e)+c(b-e)\right]+\left[\frac{d}{2}(b-e)+c(b-e)\right]$$

$$\cdot\left[\frac{3d}{2}(b-e)+2c(b-e)\ \}\right] \qquad (2.55)$$

2.3.4 **Boundary conditions**

The horizontal loading on the core is replaced by a statically equivalent system of loads parallel to the *x*-axis and acting along the shear center axis and a uniform twisting moment. The simple beam theory is used to analyze the effects of loads through the shear center axis.
The effect of the uniformly distributed twisting moment m_z is accounted for by considering the restraint vector at $z = t$ as [0, 0, 0, m_z] and integrating the last column of the distribution matrix $G_{z\text{-}t}$ of equation 2.55 between the limits 0 and l.
Assuming the core to be completely rigid at the base, the boundary conditions at the ends of the core are

Bottom	:	$\theta_0 = 0$	and	$\theta'_0 = 0$	
Top	:	$B_l = 0$	and	$M_l = 0$	(2.56)

Using these boundary conditions in the general equation 2.56 the expression four the four θ_z, θ'_z, B_z, and M_z are written. The two quantities θ_z and B_z, which are a measure of deflection and stresses, will be:

$$\theta_z = \frac{-m}{GJ\cosh k}\left[\frac{-l^2}{k^2} - \frac{l^2}{k}\sinh k + z\left(l - \frac{z}{2}\right)\cosh k + \frac{l^2}{k^2}\cosh\frac{k}{l}z + \frac{l^2}{k^2}\cosh\frac{k}{l}z + \frac{l^2}{k}\sinh\frac{k}{l}(1-z)\right] \quad (2.57)$$

$$B_z = \frac{-ml^2}{k^2\cosh k}\left[\cosh k - \cosh\frac{k}{l}z + \frac{k\sinh k}{l}(1-z)\right] \quad (2.58)$$

Equations 2.57 and 2.58 are basic equations, which are also applicable in the analysis of a wide variety of complex-shaped shear walls, as well as plate theory.

3 STRUCTURAL FIXITY AND MEMBER STABILITY

3.1 INTRODUCTION

Structures must be capable of sustaining all imposed loads and forces, in order to function. These loads and forces are transferred to the vital "spine" of the building's structural framework. The loads and forces a structure must be designed for are usually stipulated by an applicable code.

All structural material has certain physical properties, which are important to design engineers. These physical properties, which are common to structural steel, make it possible to predict the behaviour of the member in almost all cases.

A material's record of its elastic deformation (elastic range), followed by the plastic deformation (plastic range) and strain hardening is important. The strain from the elastic limit to the onset of the strain hardening (a reserve strength that is not taken into account in classic design) is approximately 15 times the maximum elastic strain. For stability of any member, it is important for the designer to stay within the elastic limit of the steel.

3.2 TYPES OF MEMBERS

Beams utilized as structural floor and roof members in buildings can have different cross-sections (Fig. 3.1), depending upon such factors as economy, aesthetics, and required span.

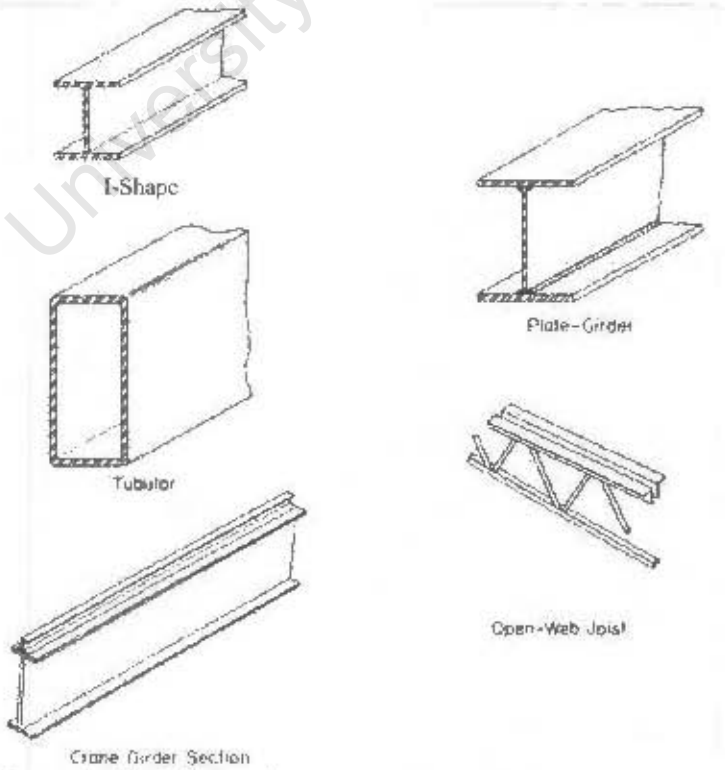

Figure 3.1[9]: Different beam cross-sections

3.3 TYPES OF CONNECTORS IN A STRUCTURE

Structures are assembled by joining elements at element intersections. A building consists of many different single elements. There are basically three ways of connecting these members: the rivet, bolt, and weld.

Field riveting , for the most structures and connections is no longer in use today. Only a few structures are still shop-riveted today. Bolting and welding are the most popular methods of connecting today and are sometimes combined. To use welding or bolting, or a combination of both, is a design decision the engineer must make. As a general rule the option to bolt or weld or to use a combination of both should be left to the decision and choice of the fabricator and/or erector of the steel structure.

3.3.1 Notation of structural fixity

In theory we get the following structural fixity as indicated in the following table which transmit the internal forces indicated where; N denotes axial forces, M denotes bending moments, S denotes shear forces, and T denotes torques.

Table 3.1 Notation of structural fixity

Type name	Schematic	Transmits
Encartre, Clamped, Fully Fixed		M,S,N,T
Pinned,Hinged		S,N,T
Telescopic (Sliding joint)		M,S,T
Rolling Joint, Roller	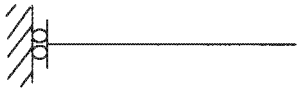	M,N,T
Ball Joint		S,N
Pinned Roller		N,T

3.3.2 **Connection behaviour**

In structural steel design, different types of design assumptions are allowed, depending upon the rigidity of the connection used in the construction. Portal frames are categorized into three different types of designs[64]:

1. Simple frames which use similar shear connections, called AISC Type 2 connections.
2. Fully rigid frames, which use rigid beam-to-column connections, called AISC Type I connections.
3. Semirigid frames, which use partially rigid beam-to-column connections, called the AISC type 3 connections.

The classification is based on the degree of restraint provided by the connection at the beam-to-column joint.

Connections in simple frames are designed to transfer vertical shear only, it is being assumed that there is no bending moments present at the connection. Connections in fully rigid frames are called upon to develop full resistance to both shear and bending moment and are assumed to have sufficient rigidity to hold virtually unchanged the original angles between connecting members. Semi-rigid frames are those whose connection behaviour is intermediate between simple and fully rigid connection.

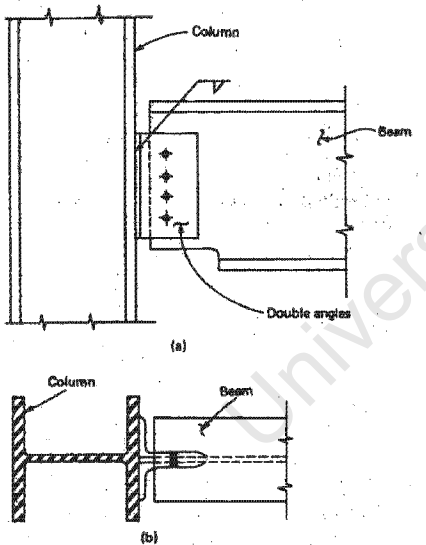

Figure 3.2[64]: Beam-to-column field-bolted shear connection.

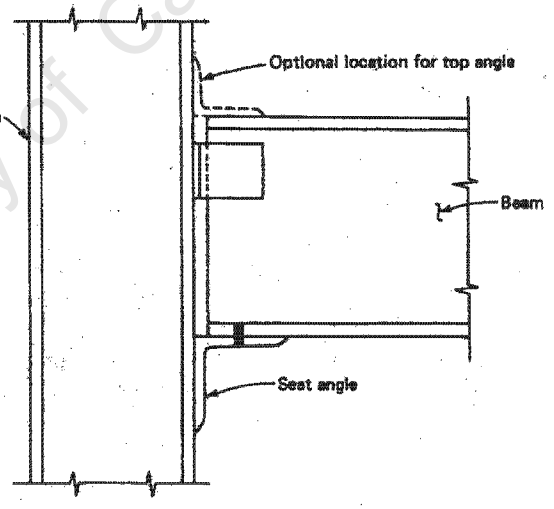

Figure 3.3[64]: Unstiffened seated beam connection

Completely simple and fully rigid behaviour is, of course, ideal conditions, which can only be approached. Practically, it is necessary to accept something less than ideal, since real structural frames perform in the broad range between fully rigid and simple support action frame. For example, consider the typical beam-to-column connection consisting of a double web connection as shown in *figure 3.2*. The conventional framing angles that fasten to the beam web are usually considered to be completely flexible and are assumed to carry shear only. Actually, they offer limited restraint to moment and thus oppose to some extent the rotation at the end of the beam.

Unstiffened seated beam connections as shown in *figure 3.3* are also used for supporting the ends of unrestrained beams in Type 2 construction. The behaviour of the seat angle is shown schematically in *figure 3.4*, the bottom angle acts as cantilever, except that it is restrained by the bottom flange of the beam that is connected to it. The moment-rotation characteristics of a seat angle connection primarily depend on the depth of the beam, stiffness of the top angle, stiffness of the bolts connecting the top angle to the column, and the stiffness of the column flanges to which the top angle is connected. Seat angle connections are typically stiffer than web angle connections but are still considered to be simple flexible connections. By combining the geometry of a web angle and top and bottom angle connections it is possible to develop a connection that has greater moment resistance than either of the previously described connections.

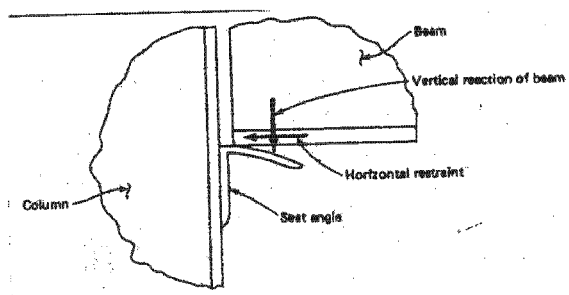

Figure 3.4[28]: Cantilever bending of seat angle

The top and the bottom angles are assumed to carry the moment, and the web angles the shear. Although the load distribution may appear to be arbitrary, such a division of function produces adequately proportioned connections. Structural tees used in place of top and bottom angles of the flexible seat angle connection result in the most rigid connection of the semi-rigid types. The increase in rotational restraint occurs because the top tee is loaded in tension, which acts on the tee without any eccentricity, whereas the top angles are loaded eccentrically, resulting in large deformations.

3.3.3 **Beam line concept**

One of the methods of understanding the behaviour of beam-to-column connection under load is to study a plot of its moment-rotation characteristics, as shown in *figure 3.5*. The vertical axis shows the end moment of the beam acting at the beam-column connection. The resulting rotation at the beam and is plotted along the horizontal axis in radians. The diagram is somewhat similar to a stress-strain diagram. Superimposed upon this plot is the so-called beam line, which expresses the resulting end moment M and rotation θ for a uniformly loaded beam for any end restraint, ranging from full fixity to simply supported condition.

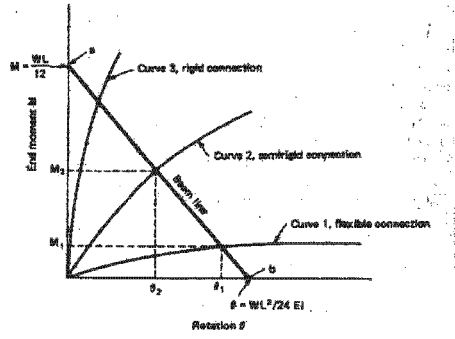

Figure 3.5[70]: Beam line concept

The relation between end moment M and rotation θ can be expressed by the following equation.

$$M = \frac{2EI\theta}{L} - \frac{WL}{12} \qquad (3.1)$$

This is a straight –line relationship and can be plotted by considering the rotation of a simply supported beam and fixed end moment of a completely restrained beam. Point *a* on the beam line is the end moment when the connection is completely restrained. Thus, in equation 3.1, rotation $\theta = 0$, giving

$$M = -\frac{WL}{12} \qquad (3.2)$$

Point b is the rotation end of the beam when the beam has zero restraint at the ends. In other words, the beam behaves as a simply supported beam. Substituting M=0 in Eq. (3.1), we get

$$\theta = -\frac{WL^2}{24EI} \qquad (3.3)$$

The point at which the beam line intersects the connection line gives the resulting end moment and rotation under the given load. The dependence of the beam behavior on the rigidity of the connection can be studied by using this diagram. Curve 1 (in figure 3.5) represents a flexible connection, which is typical of a double-angle web connection. Under a uniform load W, the beam-ends rotate trough an angle θ_1, which is very nearly equal to the rotation θ of a completely unrestrained beam. Corresponding to this rotation, a moment M is generated at the ends, which signifies that even with the so-called flexible connections, some end moment is set up. Normally the bending moment developed is about 5 to 20 percent of the fully fixed moment.

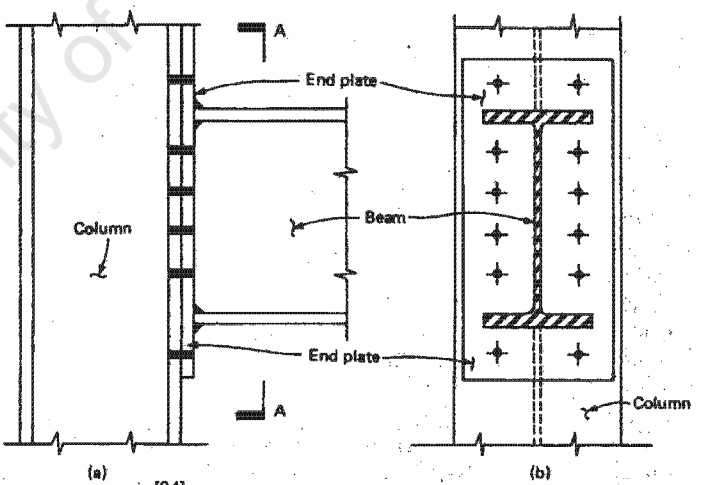

Figure 3.6[64]: Column-to-beam bolted end plate connection

Curve 2 (in figure 3.5) represents a semi-rigid connection, such as that shown in *figure 3.6*, which consist of an end connecting plate so detailed that under working load it elastically yields to provide the necessary rotation of the connection. Although the beam is detailed to undergo a rotation equal to θ_2, significant moment M_2 corresponding to the rotation θ_2 develops at the beam-ends. The restraint offered by this type of connection can vary anywhere from a low 20 percent to a high 90 percent of the full fixity. That is, the end moment could be 20 to 90 percent of the moment generated in a fully fixed beam.

Curve 3 (in figure 3.5) represents the moment-rotation characteristics of a rigid connection so detailed as to allow virtually no rotation at the ends. The beam develops end moments, which are 90 to 95 percent of the fully fixed condition, especially when column flange stiffeners are used to its full potential. AISC provides two approximated solutions[64]. In the first method the connection is designed for the moment caused by the combination of gravity and wind loads using a one-third increase in the allowable stresses. In the second method, the connection is designed for the moment induced by wind loads only, using a one-third increase in the stress allowances. The connection must, however, be designed to yield plastically for any combination of gravity and wind moments. Any additional moment that could occur at the ends beyond the wind moments is relieved because of the yielding of the connection. This type of connection necessitates some elastic but self-limiting deformation of the connection plate without overstressing the fasteners.

3.4 STABILITY ANALYSIS

There are three methods in stability analysis of an elastic structural system, namely, bifurcation approach, energy approach, and dynamic approach. The bifurcation approach is an idealised mathematical approach to determine the critical conditions of a geometrically perfect system. With the aid of an eigenvalue analysis in the bifurcation approach, the state of which two or more different but adjacent equilibrium configurations can be seen. The lowest load that corresponds to this state is the critical load of the system. Because the tangent-stiffness of the system vanishes at the critical load, it's determinant is set equal to zero, which can identify the system's critical conditions. The critical conditions are given by the eigenvalues of the system's stiffness matrix and the displacement configurations are given by the eigenvectors. It is important to note that the eigenvalue approach cannot be applied to a load-deflection (serviceability limit state) problem.

The energy approach can also be used to determine the system's critical condition. The total potential energy of an elastic system can be expressed as a set of functions of generalised displacements and the related external applied loads. The system's total potential energy must be stationary when it is in equilibrium. Thus, setting the first derivative of the total potential energy functions with respect to each generalised displacement equal to zero can identify the equilibrium condition. Hence, with the equilibrium equations, the critical load can then be calculated.

The dynamic approach is the third approach to obtain the critical load. The equations for system free vibration are written as a function of the generalised displacements and the external loads. When the motion ceases to be bounded, the critical load is obtained as the level of external force. If a slight disturbance causes only a slight deviation of the system from the original equilibrium position and if the magnitude of the deviation decreases when the magnitude of the disturbance decreases, it will be in stable equilibrium. However, if the magnitude of the motion increases without bound when subjected to a slight disturbance it will be in unstable equilibrium.

3.5 COLUMN STABILITY

Columns are usually slender structural members that are mostly only subjected to axial compression forces. A perfect straight elastic column subjected to a small concentric load will only undergo axial deformation. Small

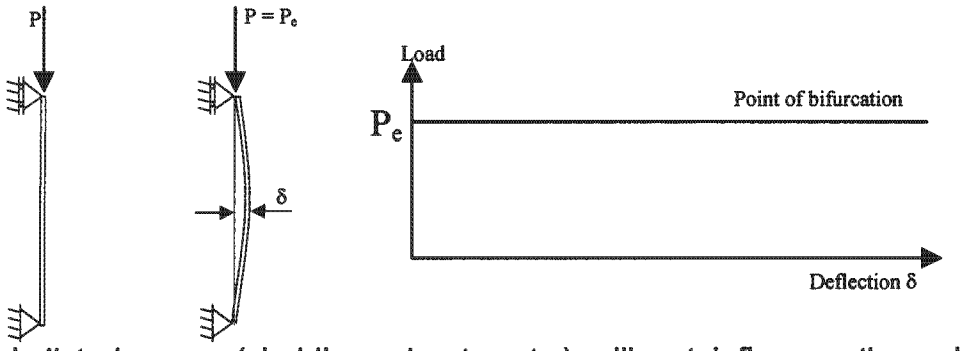

lateral disturbances (cladding, sheets, etc.) will not influence the column's load-deflection relation significantly. However when the load reaches a critical point, a slight lateral disturbing load will turn the member into an unstable equilibrium state. A real column with non-linear material properties usually has initial imperfections and has an eccentric loading (see figure 3.7), which will contribute to increase the complexity into the stability analysis. A column with a symmetric cross-section will deflect laterally about its weaker axis without twisting, for most plane frames and referred to as lateral buckling.

Figure 3.7: Column buckling

3.5.1 Column theory

The column theory is based on the elastic buckling analysis of pinned-ended supports (see figure 3.8)

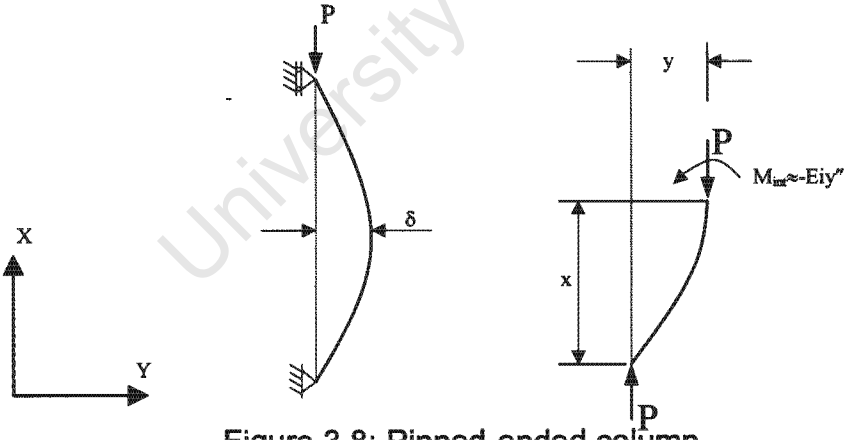

Figure 3.8: Pinned-ended column

The result with this theory is then extended to other end-restraint conditions using an effective length concept. The bifurcation analysis is based on the following assumptions

- The column is perfectly straight.
- The axial load is applied along the centroidal axis of the column.
- Plane sections before deformation remain plane after deformation.
- Deflection of a member is due only to bending.
- The material obeys Hooke's Law.
- The deflection of the member is small, so the curvature can be approximated by the second derivative of the lateral displacement.

The geometry of the column changes from a straight to a slightly deformed shape when the axial load is increasing, which corresponds to a neutral equilibrium configuration. The structural member's capacity in this neutral equilibrium is the critical load.

Take an infinitesimal segment of the deformed column dx (see figure 3.9), which provide an expression for longitudinal strain ε_x as:

$$\frac{\varepsilon_x dx}{y_1} = \frac{dx}{R} \quad or \quad \varepsilon_x = y_1\phi;$$

$$and\ from\ Hooke's\ law, \sigma_x = E\varepsilon_x$$

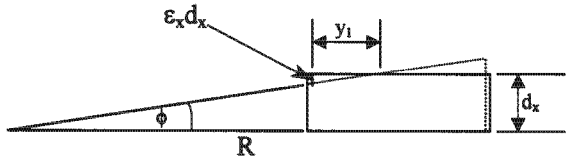

Figure 3.9: Kinematics of a column segment

The initial moment M_{int} from statics can be obtained by the integration of the moment induced by the stress σ_x over the cross-section.

$$M_{int} = \int_A y_1 \sigma_x dA = \frac{E}{R}\int_A y_1^2 dA = EI\phi \qquad (3.4)$$

The curvature ϕ can be approximated by the second derivative of the lateral displacement $\phi = -y''$ when a small deflection is assumed.
Hence, the moment equilibrium at column end is:

$$EIy'' + Py = 0 \qquad (3.5)$$

The solution to this second-order linear differential equation is:

$$y = A\ sinkx + B\ coskx \qquad where\ k^2 = P/EI \qquad (3.6)$$

By using the simply support boundary conditions, the critical load of the column is:

$$P_e = \frac{\pi^2 EI}{L^2} \qquad (3.7)$$

The slenderness ratio is usually used to present the member stability behaviour in the column design curve, which is derived from the relationship between column section plastic strength and the critical load.

3.5.2 **Effective length**

The effective length of an end-restrained column is defined as the length of an equivalent pinned-ended column that will give the same critical load. The effective length can be visualised as the distance between two inflection points of the buckled shape of the end-restrained member. The following demonstrates how the bifurcation load of a column with one end hinged and the other fixed (see figure 3.10) was derived.

The equilibrium equation for the column segment is:

$$EIy'' + Py - \frac{M^F}{L}x = 0 \qquad where\ k^2 = P/EI \qquad (3.8)$$

The general solution is:

$$y = A\sin kx + B\cos kx + \frac{M^F}{L}x \qquad (3.9)$$

The boundary conditions are: $y(0) = 0$; $y(L) = 0$; $y'(L) = 0$

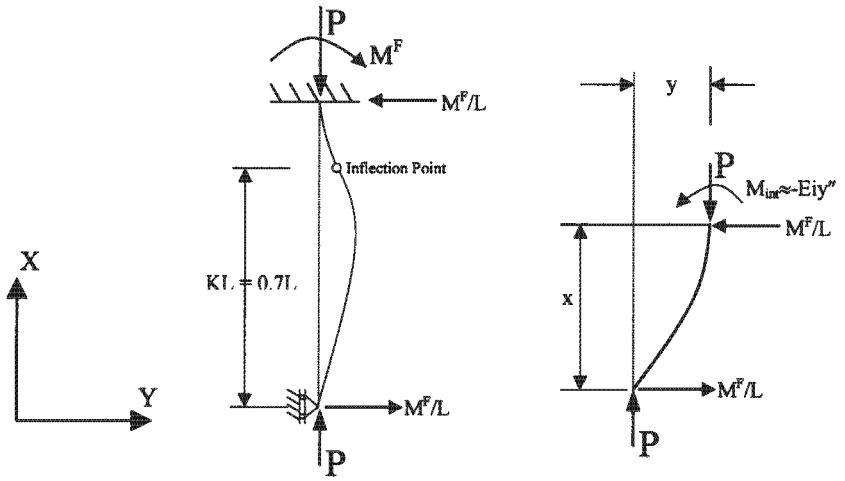

Figure 3.10: Fixed-hinged column

By applying the first two conditions, the deflection becomes

$$y = \frac{M^F}{L}\left(\frac{x}{L} - \frac{\sin kx}{\sin kL}\right) \tag{3.10}$$

And from the third boundary condition it is:

$$TankL = kL \tag{3.11}$$

which gives :

$$P_{cr} = \frac{20.19EI}{L^2} \tag{3.12}$$

If this result is compared with the critical load P_e for the pinned case, the effective length factor is:

$$K = \sqrt{\frac{P_e}{P_{cr}}} = \frac{\pi}{\sqrt{20.19}} = 0.66917 \tag{3.13}$$

3.5.3 **Initial imperfections to columns**

All columns in reality are imperfect. Several kinds of inevitable imperfections must be considered. Imperfections of columns can be grouped into two types: geometrical imperfections and material imperfections. Initial imperfections may have different causes. Dimensional tolerances are one of these causes. Columns may also be subjected to unintended small lateral loads (during manufacturing or storage); or may be initially curved rather than perfectly straight; or the axial load may be slightly eccentric; or disturbing moments and shear forces may be applied at the column ends. Nevertheless, the most basic form is initially the crooked column (see figure 3.11). The initial crookedness amplified the internal moment and lateral deflection in the column.

For an analytical solution, if it is assumed that the out-of-straightness is in the form of a half sine curve describe by $y_0 = \delta_0 \sin\frac{\pi x}{L}$, where δ_0 is the magnitude

of the maximum crookedness. The equilibrium equation for a segment conclude to:

$$EIy'' + P(y_0 + y) = 0 \tag{3.14}$$

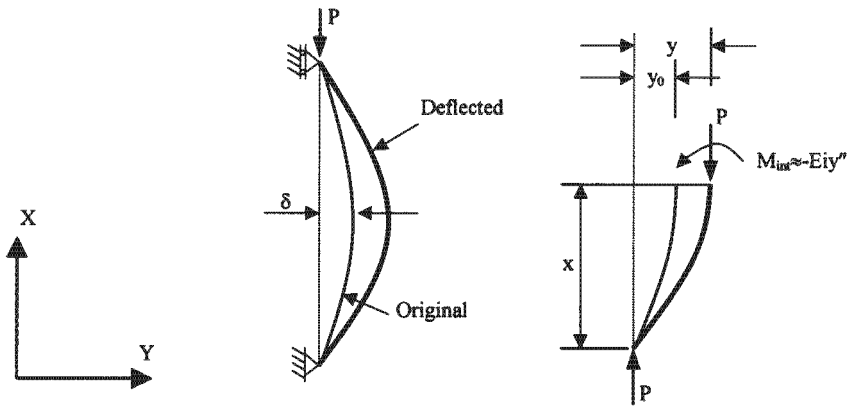

Figure 3.11: Column with initial imperfection

By using the prescribed shape formula, the equilibrium equation will be:

$$y'' + k^2 y = -k^2 \delta_0 \sin\frac{\pi x}{L} \quad where\ k^2 = P/EI \tag{3.15}$$

The general solution is:

$$y = A\sin(kx) + B\cos(kx) + \frac{\delta P / P_e}{1 + P/P_e}\sin\left(\frac{\pi x}{L}\right) \tag{3.16}$$

With the boundary conditions y(0) = y(L) = 0, two results are obtained,

$$P = P_e \ and \ y_{total} = \left(\frac{1}{1 - P/P_e}\right)\delta_0 \sin\left(\frac{\pi x}{L}\right) \tag{3.17}$$

From the first result it is concluded that the initial crookedness has no effect on the elastic buckling load.
By substituting the second results to the segment equilibrium equation manifest that:

$$M_{int} = \left(\frac{1}{1 - P/P_e}\right)P\delta_0 \sin\left(\frac{\pi x}{L}\right) \tag{3.18}$$

The formula will be slightly different for the initial crookedness that is not a half sine curve. The imperfections merely increase deflections but do not lower the maximum load (if the buckling analysis is linearized) for elastic columns. However, the imperfections are found to decrease the maximum load for elastic-plastic columns.

Two important formulas are commonly used in dealing with the maximum stress in a geometrically imperfect compression column. The two formulas are Secant formula and the Perry-Robertson formula, which have a similar format:

$$Secant\ formula \quad \sigma_{max} = \frac{P}{A}\left[1 + \frac{ec}{r^2}\sec\frac{\pi}{2}\sqrt{\frac{P}{P_e}}\right] \tag{3.19a}$$

$$Perry - Robertson \quad \sigma_{max} = \frac{P_{cr}}{A}\left[1 + \frac{\delta_0 c}{r^2}\frac{1}{1 - P/P_e}\right] \tag{3.19b}$$

Substituting the yield stress as the maximum allowable stress into the formula can derive the critical load of initial geometrically imperfect columns. However, their applications are limited to very long and slender columns, so that the stress in the column remains elastic.

3.5.4 **Inelastic columns**

Real structural members are made of inelastic materials to add to all types of geometrical imperfections. Inelastic behaviour is ultimately always the cause for failure of every column or structure. The load reduction for slender members due to inelastic behaviour occurs at very large deflections, thus is irrelevant for design. Inelastic behaviour can significantly reduce the maximum load of non-slender members at relatively small deflections (see figure 3.12), therefore, it must be taken into account in design.

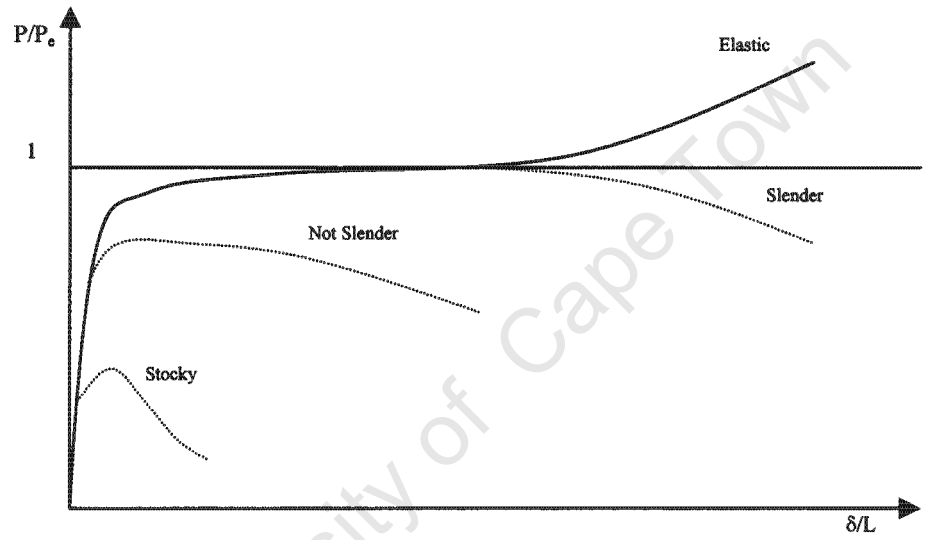

Figure 3.12: Load-deflection curve of inelastic column

The stress in the column can exceed the initial yield point when buckling occurs. The behaviour of the column becomes elastoplastic after yielding with two characteristics: the tangent modulus E_t for continued loading and the unloading modulus E_u.

The first inelastic column theory was produced by Considere (1891) called reduced modulus theory, which was later developed in detail by Engesser (1895)[14]. As buckling occurs, this method assumes that the convex face of the column undergoes extension due to unloading. And due to loading the concave face experiences shortening. The incremental stresses at the convex and concave faces of the column are $-E_u h_1 \phi$ and $E_t h_2 \phi$ (where ϕ is the curvature due to buckling). Since F_1 and F_2 will be equal and opposite and the cross-section is a rectangular section, the neutral axis position h_1 can be derived with the aid of figure 3.13 producing the following equation:

$$h_1 = h\frac{\sqrt{E_t}}{\sqrt{E_u}+\sqrt{E_t}} \tag{3.20}$$

The resultant bending moment of the F_1 and F_2 in the cross section becomes:

$$M = -F_1\left(\frac{2}{3}h_1 + \frac{2}{3}h_2\right) = -F_1\left(\frac{2}{3}h\right) = bh_1\left(E_u h_1 \phi / 2\right)\left(\frac{2}{3}h\right) = \frac{bh^3\phi}{3}\left[\frac{E_u E_t}{\left(\sqrt{E_u} + \sqrt{E_t}\right)^2}\right]$$

$$which\ can\ be\ written\ as: M = E_r I\phi \quad where\ E_r = \left[\frac{1}{2}\left(\frac{1}{\sqrt{E_u}} + \frac{1}{\sqrt{E_t}}\right)\right]^{-2} \tag{3.21}$$

By using the same method as the elastic bifurcation analysis, the first critical load for a simply supported column is:

$$P_{cr} = P_r = \frac{\pi^2 E_r I}{L^2} \tag{3.22}$$

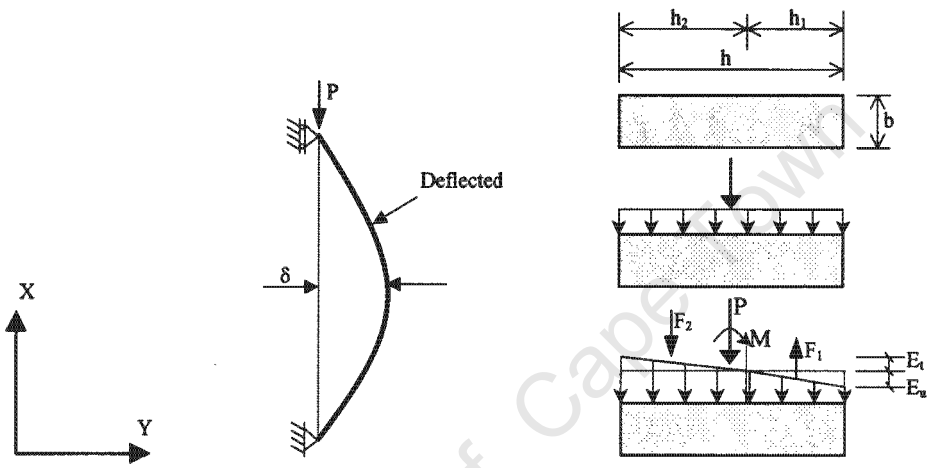

Figure 3.13: Reduced modulus theory

However, after the publication of this theory was revealed, some experimental studies conducted that the columns can fail by buckling at a load that is significantly lower than this critical load. Shanley (1947) showed that, because the buckling deflection occurs simultaneously with further increase of the axial load P, it is possible that there is no unloading[21]. Thus the incremental modulus is the same in the cross-section and equals to the tangent modulus E_t. The elastic critical load of the column then becomes:

$$P_{cr} = P_t = \frac{\pi^2 E_t I}{L^2} \tag{3.23}$$

The experimentally observed critical values of the column loads P_{max} lay between P_r and P_t, and was often much closer to P_t. Thus, P_t is a good estimate of lower bound capacity for column design.

3.6 BEAM INSTABILITY

Beams are regarded as structural members whose primary function is to transfer of loads by means of bending action. In most situations, the structural framing is arranged so that the resulting bending may be regarded as being effectively bending in one plane only.

Generally it would be ideal if the loading acts through the shear centre, which would avoid twisting of the member. In such cases, bending about major axis becomes the principle design consideration and often symmetric I-sections are used for material efficiency. However, due to unavailable lateral stability of the member, the lateral buckling effect often reduces the beam capacity. This type of problem is more complex than the flexural buckling of a column, because the twisting and lateral deformations are coupled.

3.6.1 **Effects of restraints on beams**

Instability analyses of beams become even more complex when the effects of various restraints are considered. Foremost, the application of loads and restraints are inseparable. Also, even for a single segment of beam, there are eight degrees of freedom in terms of constraints (three displacements, three rotations and warping restraint at each segment). This becomes more complicated for a continuous beam where factors such as top or bottom flange supported, bracing rigidities etc. In design of structures, similar constraints are grouped together using the effective length concept, and only the stability of single segment beam is taken into account. Again, no uniformity in design approach is used.

Usually, beam segments are classified into four main groups: cantilever beams, simply supported beams, restrained beams and continuous beams.

3.6.2 **Cantilever beams**

The elastic critical buckling moment of a cantilever with an end moment M_o applied at the free end can be obtained directly for the solution of the simply supported beam by assuming that the beam is consisting of two cantilevers of equal length with fixed ends, which gives equation 3.24 as a result.

$$M_{ocr} = \frac{\pi}{2L}\sqrt{EI_y GJ}\sqrt{\left(1+\frac{\pi^2 EI_w}{(2L)^2 GJ}\right)} \qquad (3.24)$$

Nethercot[54] (1973) has shown that by using the effective length factor K similar to the one used in columns gives a conservative estimate of M_{cr} can be obtained for most applications. The equation for elastic critical loads is:

$$M_{ocr} = \frac{\pi}{KL}\sqrt{EI_y GJ}\sqrt{\left(1+\frac{\pi^2 EI_w}{(KL)^2 GJ}\right)} \qquad (3.25)$$

Cantilever beams with lateral restraints along the length of the members will further complicate the problems. However, by ignoring the restraints, it will result in a conservative design approach.

3.6.3 **Restrained simply supported beams**

A simply supported beam is the most fundamental case of restraint in theory. There are four possible degrees of freedom at each end of the restrained beam. Different combinations of restraints lead to different results of member capacities. Unrestraint segment of the compression flange of a simply-supported beam refers to the distance between lateral bracing to the compression flange. In the design of structures, all segments of beam must be prevented from lateral torsional buckling. The effective length concept is used for restrained beams to calculate the critical M_{ocr} (i.e., with uniform bending moment). The following is one approach by Nethercot[54] and Rockey out of many approaches for three typical restraints conditions in order to consider the moment gradient and load conditions.

The differential equation $EI_w \frac{d^4\gamma}{dz^4} - GJ\frac{d^2\gamma}{dz^2} - \gamma\frac{M_0^2}{EI_y} = 0$ can be solved by different boundary conditions using trial and error methods, when an unbraced segment of beam is subjected to a uniform bending moment. The typical solution can be expressed as:

$$M_{ocr} = \frac{\pi}{K_b L}\sqrt{EI_y GJ}\sqrt{\left(1 + \frac{\pi^2 EI_w}{(K_t L)^2 GJ}\right)} \qquad (3.26)$$

where the effective length factor K_b corresponds to the lateral bending effect and K_t corresponds to the twisting restraint. Values for K_b and K_t are given in table 3.2.

Table 3.2 K values for various boundary conditions with UDL (Vlasov[79], 1959)

Boundary Conditions		K_b	K_t
z=0	z=L		
u=u″=γ=γ″=0	u=u″=γ=γ″=0	1.000	1.000
u=u″=γ=γ″=0	u=u″=γ=γ′=0	0.904	0.693
u=u″=γ=γ″=0	u=u′=γ=γ″=0	0.626	1.000
u=u″=γ=γ″=0	u=u′=γ=γ′=0	0.693	0.693
u=u″=γ=γ′=0	u=u″=γ=γ′=0	0.883	0.492
u=u′=γ=γ″=0	u=u′=γ=γ′=0	0.431	0.693
u=u′=γ=γ′=0	u=u′=γ=γ′=0	0.492	0.492
u=u′=γ=γ″=0	u=u′=γ=γ″=0	0.434	1.000
u=u′=γ=γ″=0	u=u″=γ=γ′=0	0.606	0.492

It is impossible to judge the exact restraint conditions for design purposes. For this reason, the effective length factors are often taken as:
1.0 if both ends are simply supported
0.7 if one end is simply supported and the other end is fixed and
0.5 if both ends are fixed

For the critical moment of unbraced beams subjected to a UDL or a concentrated load in mid-span, Nethercot[53] and Rockey have produced the following equation:

$$M_{cr} = C_{bs}M_{ocr}$$

where C_{bs} is a moment gradient factor but it also account for different end conditions of the beams.
C_{bs} equals to:

$$C_{bs} = \begin{cases} AB & for\ load\ at\ bottom\ flange \\ A & for\ load\ at\ shear\ centre \\ A/B & for\ load\ at\ top\ flange \end{cases}$$

And the effective length factor K used in M_{ocr} equals to:
However, K is often taken as one for design purposes.

$$K = \frac{\pi\sqrt{EI_y GJ}}{\sqrt{2L}(C_{bs}M_{ocr})}\left\{1+\sqrt{\left(1+\frac{4(C_{bs}M_{ocr})^2}{EI_y GJ}\frac{EI_w}{GJ}\right)}\right\}^{0.5} \qquad (3.27))$$

Nethercot[54] and Rockey's solutions for three common restraint cases are given as follows:
Case 1 is a beam with both ends fixed. The plan of the deformed shape is shown in figure 3.14.

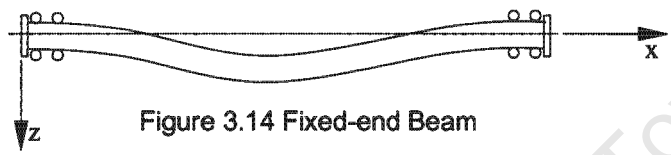

Figure 3.14 Fixed-end Beam

The factors A and B can be obtained from the table 3.3 with

$$W = (\pi / L)\sqrt{EI_W / GJ}$$

Table 3.3 Moment reduction factor for different load cases (Fixed-end)

Loading	A	B
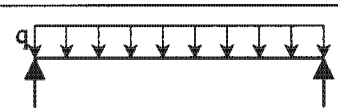	$1.643 + 1.771W - 0.405W^2$	$1 + 0.625W - 0.339W^2$
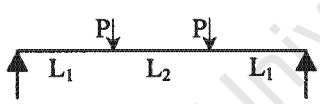	$1.916 + 1.851 - 0.424W^2$	$1 + 0.923W - 0.466W^2$

Case 2 is a beam with warping prevented but lateral bending permitted. The plan of the deformed shape is shown in figure 3.15.

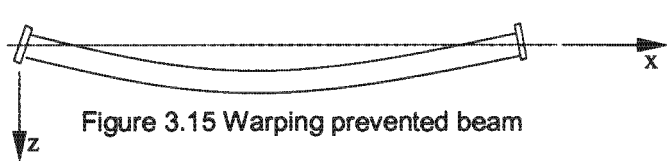

Figure 3.15 Warping prevented beam

The factors A and B can be obtained from the table 3.4 with

$$W = (\pi / L)\sqrt{EI_W / GJ}$$

Table 3.4 Moment reduction factor for different load cases (Warping prevented)

Loading	A	B
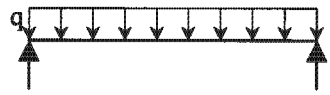	$1.2 + 0.402W + 0.416W^2$	$1 + 0.571W - 0.225W^2$
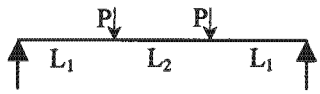	$1.43 + 0.463 + 0.485W^2$	$1 + 0.6913W - 0.317W^2$

Case 3 is a beam with warping permitted but lateral bending prevented. The plan of the deformed shape is shown in figure 3.16.

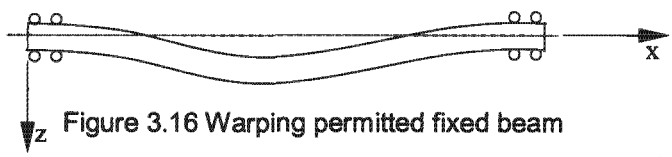

Figure 3.16 Warping permitted fixed beam

The factors A and B can be obtained from the table 3.5 with

$$W = (\pi / L)\sqrt{EI_W / GJ}$$

Table 3.5 Moment reduction factor for different load cases (warping permitted fixed-end)

Loading	A	B
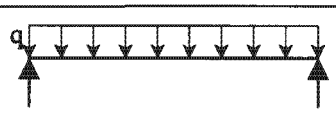	$1.643 + 1.771W - 0.405W^2$	$1 + 0.625W - 0.339W^2$
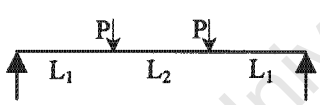	$1.916 + 1.851 - 0.424W^2$	$1 + 0.923W - 0.466W^2$

3.6.4 **Continuous beams**

A continuous beam refers to a beam with lateral restraint(s) between its end supports. These lateral restraints (bracing) change the buckling shape of the beam in favour of the buckling moment capacity of the beams. The simplest case is a simply supported beam with additional lateral restraints at mid-span subjected to a uniform bending moment. The lateral buckling mode will be a complete sine curve with the effective length equals to half the length of the beam, and the corresponding critical moment capacity can be calculated as in figure 3.17.

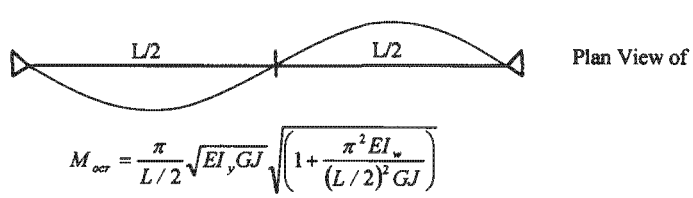

$$M_{ocr} = \frac{\pi}{L/2}\sqrt{EI_y GJ}\sqrt{\left(1 + \frac{\pi^2 EI_w}{(L/2)^2 GJ}\right)}$$

Figure 3.17 Beam with lateral support at mid-span

Partial end restraints will develop between adjacent spans when a continuous beam has more than two lateral restraints. The lateral buckling load depends on the relative stiffness of the segments, the type of bracing or constraint used for intermediate supports, and the type and relative magnitude of the loads on the beam. In reality, most of these parameters are impossible to quantify and thus, lots of engineering judgements are required even with the simplest design approach in determining the segment's end restraint conditions. It is common practise to evaluate the critical load for each segment of the beam separately by assuming the ends of the span to be simply supported. Thus, the lowest value of the critical loads obtained for each individual span will lead to a conservative solution for the continuous beam.

3.6.5 **Stiffness of restraint for steel struts with elastic end supports**

When a strut is restrained at a point along it's length, the effective length is reduced leading to an increase in its load carry capacity. The location and the stiffness of the restraint, the end conditions of the strut and the magnitude of the applied axial load (which has a non-linear effect) to the strut determine the magnitude of the force induced in the restraint. In this section it is assumed that the strut is part of a braced structure where side-sway is prevented and the strut has an out of straightness imperfection. For an ideal strut, the force induced in the restraint can be determined by an eigenvalue-problem procedure[3]. For a real strut however, where imperfection has to be considered, the direct solution to the controlling differential equation will lead to the determination of the restraint force.

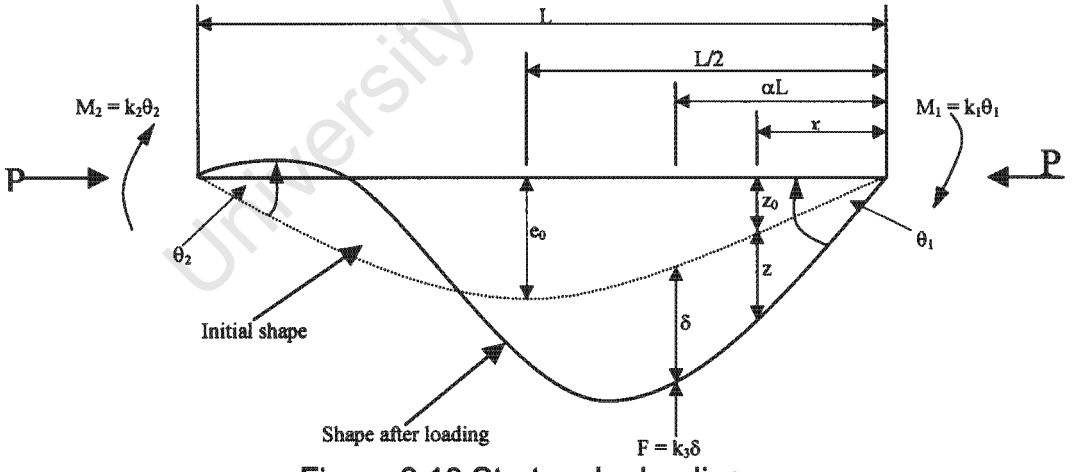

Figure 3.18 Strut under loading

If we consider the strut shown in figure 3.18, which is subjected to an axial load P and is restrained at a point located at a distance αL from its ends. If the stiffness of this restraint is k_3, then the force it exerts on the strut is $F = k_3\delta$. Two restraining moments in addition are acting in the opposite direction to the rotation at the ends of the strut. These moments are $M_1 = k_1\theta_1$ and $M_2 = k_2\theta_2$ respectively, where k_1 and k_2 are the rotational stiffness, and θ_1 and θ_2 are the rotations at the two ends of the strut. The differential equation controlling the behaviour of the strut is:

$$EI\frac{d^2z}{dx^2} = -m_x \qquad (3.28)$$

where m_x is the bending moment at the distance x from the end and is composed of three parts.

The contribution of the axial load, as shown in figure 3.18, is part one, which is given by

$$m_1 = Pz_t = P(z_o + z) \qquad (3.29)$$

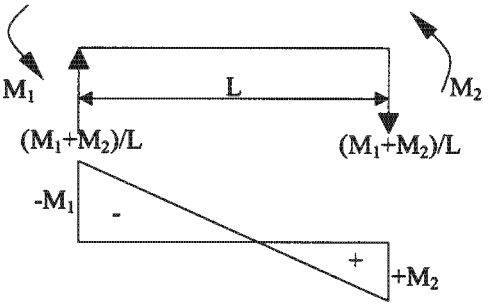

Figure 3.19: Beam subjected to end-moments

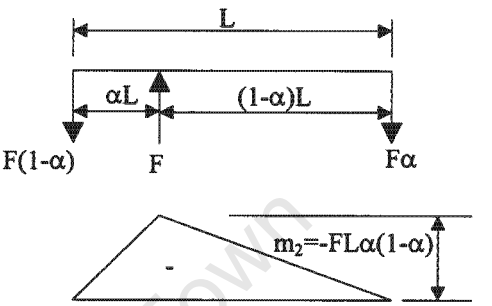

Figure 3.20: Beam subjected to a point load

The second part is due to the moments induced at the elastic supports due to the rational stiffness of the supports, as shown in figure 3.19 and is given by:

$$m_2 = -M_1 + (M_1 + M_2)x/L \qquad (3.30)$$

And the third part is the result of a simple span bending moment due to the restraint force, as shown in figure 3.20 and is given as:

$$m_3 = -F(1-\alpha)x, \text{ for } 0 \le x \le \alpha L \quad (a)$$

$$m_3 = -F\alpha\,(L- x), \text{ for } \alpha L \le x \le L \quad (b) \qquad (3.31)$$

m_3 can be written as a Fourier series, i.e. as a continuous function which will greatly simplify the solution of the differential equation. An infinite (sin) series of equation 3.31 can take the following form:

Al-Shawi[3] took only ten terms of the above series and found that it gave good

$$m_3 = \sum_{n=1}^{\infty} b_n \sin(n\pi x / L)$$

where,

$$b_n = -(2/L)\left[\int_0^{\alpha L} F(L-\alpha)x(\sin(n\pi x/L))dx + \int_{\alpha L}^{L} F(L-x)\alpha(\sin(n\pi x/L))dx\right]$$

thus; $b_n = -2FL(\sin(n\pi x) - \alpha\sin(n\pi))/(n^2\pi^2)$

and $m_3 = -2FL\sum(\sin(n\pi x/l))(\sin(n\pi x) - \alpha\sin(n\pi))(n^2\pi^2) \qquad (3.32)$

accuracy as far as convergence is concerned.

With further evaluation of these formulae, he[3] found that the value of the restraint force F is given by $k_3\delta$ and with the substitution for k_3 and δ by k'_3P_e/L and δe_0 respectively will give:

$$(F/P)\%=100(P_e/P)(e_0/L)\,k'_3\delta' \qquad (3.33)$$

Refer to F.A.N. Al-Shawi's[3] journal in Structures & Buildings 146, issue 2 for results and a design example of a column subjected to an axial load with a restraint at the middle point against buckling.

3.7 BEAM-COLUMN-CONNECTION

All frames are in practice beam-column combinations, which mean that all structural elements are subjected to both bending and axial forces. Beam column theory is the first principles of plastic hinge type advanced analysis method, but unfortunately, it does not include twisting and warping actions in the calculation. It is generally suitable for full laterally restrained frames.
With the beam-column theory in a steel frame, three important problems for individual members get solved. They are:

1. The beam deflection problem where the bending moments induced in the member will cause transverse deflections (primary deflections)
2. The column stability problem where the axial force can cause instability in the member (in the same plane the bending moment or transverse forces)
3. The interaction of axial forces with primary deflections where the axial force will act through the primary deflection to produce additional secondary bending moments and deflections in the member.

4 FINITE ELEMENT ANALYSIS

4.1 INTRODUCTION

A structure such as a building frame can be considered as an assemblage of linear members or elements, each element being undimensional, with its cross-sectional dimensions very small relative to its length. A surface such as a thin slab or shell, on the other hand, can be considered as made up of a network of two-dimensional elements. These elements differ from the beam elements because both their width and length are significant when compared to their thickness. A third category of structures such as a thick container vessel, a dam, or a massive concrete foundation can be thought of as an assemblage of solid three-dimensional elements. All the three dimensions, namely, the length, width, and thickness, need to be considered in the analysis. Before the advent of computers it was necessary, at least from the point of view of structural analysis, to pigeonhole a structure into distinct category. With the use of digital computer analysis it is no longer a requirement to distinguish between these elements in the usual sense. The whole structure can be treated as an assembly of structural elements of different types. It is only necessary for the engineer to discretize the structure into proper categories in order to gain computational economy.

4.2 METHOD OF ANALYSIS

The finite element method essentially consists of

1. Idealization of the structure into an assemblage if discrete elements.
2. Selection of displacement function.
3. Evaluation of stiffness of each element from its geometric and elastic properties.
4. Assembly of the overall stiffness matrix from the individual element stiffness matrices.
5. Modification of the stiffness matrix to take into account the boundary conditions.
6. Solution of resulting equilibrium to obtain nodal displacements.
7. Calculation of stresses.

The general description of the method can be detailed in a step-by-step procedure to describe the sequential process that is followed in setting up and solving a finite element problem. The method is similar to the displacement or the stiffness method familiar to most engineers.

4.2.1 Discretization of the structure

This is a process in which the structure being analyzed is subdivided into a system of finite elements. Depending on the type of structure, the element models can be line elements, two-dimensional plane stress or plane strain elements, flexural plate and shell elements, axisymmetric elements, general three-dimensional solid elements, etc. The element model and its stiffness

characteristics are subjects of immense popularity with researches, who have given us at least 30 types of elements for the general analysis of structures. It is not necessary for practicing engineers to evaluate the stiffness of element models because commercially available general-purpose programs have several such elements in their libraries. The sub-division process is essentially a task that requires engineering judgement. During this process the engineer decides on the number, shape, size and configurations of the elements with the purpose of simulating the structure as closely as possible. The principal objective of such a sub-division is to discretize the structure into sufficiently small elements such that their displacement can adequately reflect the true deflection pattern of the structure, keeping in mind at the same time that too fine a subdivision will lead to extra computational effort.

In a sense, one can consider the finite elements as pieces of the actual structure if one recognizes that the elements are connected to each other not only at the nodes but also at the sides. It is easy to see that if the pieces are held together only at the nodes, the structure is greatly weakened because the elements may separate along the mesh lines. Clearly, the actual structure does not behave this way, so a finite element must deform in certain restricted ways. In formulating this behaviour, it is necessary to ensure that adjacent elements do not behave as if sawcuts were placed between them until only wisps of material at the nodes hold the pieces together.

4.2.2 **Selection of displacement models**

One of the assumptions of the finite element method is introduced at this stage when the analyst chooses displacements functions to represent the actual distribution of the displacements. Usually in structural engineering problems, the displacement function in the form of a polynomial has certain advantages over the types of functions such as trigonometric formulations. Firstly, even though the polynomial selected for structural analysis purposes is of a finite order (i.e., it contains a limited number of terms), it can approximate fairly closely the true displacements for each element. Secondly, it is relatively easy to carry out the mathematical manipulations such as differentiation and integration. Thirdly, by choosing polynomials one is assured that the displacement variation within an element is continuous without any kinks or other discontinuities. Inter-element compatibility is not generally satisfied completely, but solutions sufficiently accurate for purpose of structural design are obtainable even without full displacement compatibility between elements.

4.2.3 **Evaluation of element stiffness matrix**

In the finite element technique, the problem of defining the stiffness properties of any structure reduces basically to the evaluation of the stiffness of a typical element. The structure is assumed to be divided into a system of discrete elements, which are interconnected only at the finite number of nodal points. The behaviour of the complete structure is then found by evaluating the behaviour of the individual finite elements and superposing them appropriately.

The stiffness properties for simple elements such as a linear beam element can be obtained in number of ways by applying the methods of structural mechanics such as unit load method or moment-rotation diagram. However, in finite element analysis a versatile method commonly referred to as the Ritz or Galerkin[85] method is used to establish the stiffness matrix of elements. The method neither has not received much coverage in textbooks on structural mechanics since it is not required for evaluating the stiffness matrix of determinate elements such as beam elements.
The following is merely a summary of the procedure for determining the stiffness matrix [K] of the element.

1. Express the internal displacement v in terms of displacement function M, thus

$$\{v\} = [M]\{\alpha\} \tag{4.1}$$

2. Evaluate displacement at the nodes in terms of generalized coordinates thus

$$\{v\} = [A]\{\alpha\} \tag{4.2}$$

where the matrix-[A] is obtained by substituting coordinates of nodes in the matrix-[M].

3. Express the constant {α} in terms of {v} thus

$$\{\alpha\} = [A^{-1}]\{v\} \tag{4.3}$$

4. Evaluate the strains ε in the element; thus

$$\{\varepsilon\} = [B]\{\alpha\} \tag{4.4}$$

where [B] is obtained by differentiation of [M]

5. Find the stresses

$$\{\sigma\} = [D]\{\varepsilon\} = [D][B]\{\alpha\} \tag{4.5}$$

where [D] is the stress-strain matrix.

6. Compute the stiffness of the element by the principle of virtual displacement as follows. If σ are selected as actual stresses and ε the virtual strains, then the elemental internal work

$$dw_i = \{\varepsilon^{-T}\}[\sigma]dv$$

$$= [\alpha]^{-T}[B]^T[D][B]\alpha dv$$

$$\therefore w = \int_{vol} \partial w_i = \alpha^{-T} \left| \int_{vol} [B][D][B] \partial v \right| \alpha \qquad (4.6)$$

The external work $w_E=[\alpha]^{-T}\{\beta\}$; where $\{\beta\}$ are the forces corresponding to $[\alpha]^{-T}$. If $[\alpha]^{-T}$ is the unit matrix, the procedure is similar to introducing unit displacement one at a time and making all other displacements equal to zero. Equating the internal work to external work gives

$$[\alpha]^{-T}\{\beta\} = [\alpha]^{-T} \left| \int [B]^T [D][B] dv \right| \alpha \qquad (4.7)$$

since $\alpha^{-T} = 1$

$$\{\beta\} = \left| \int_{vol} [B][D][B] dv \right| \alpha \qquad (4.8)$$

and since

$$[K] = \frac{\{B\}}{[\alpha]} \qquad (4.9)$$

we get

$$[K] = \int_{vol} [B]^T [D][B] dv \qquad (4.10)$$

The stiffness [K] in the required coordinates can then be obtained from transformation, thus $[K] =[A^{-1}]^T[K][A^{-1}]$.

The end product the above procedure is a stiffness matrix in which forces and moments at each node are expressed in terms of the geometry and the material properties of the element.

4.2.1 **Assembly and solution of equation**

This is the process of assembling the complete stiffness matrix for the total structure from the individual stiffness matrices and composing the overall global force system from the element nodal forces. In the direct stiffness technique, which is invariable used in structural analysis, the basis for an assembly method is that the displacements at the node common to adjacent elements should be the same for all elements interconnected at that node. The overall equilibrium relations between the total structure stiffness matrix, the total load, and nodal displacement are expressed as a set of simultaneous equations of the form,

$$[K]\{\Delta\} = \{P\} \qquad (4.11)$$

where [K] = the overall stiffness matrix of the complete structure
{Δ} = the column matrix of nodal displacement
{P} = thew column matrix for the total load vector

The procedure is straightforward and is applicable to all types of problems since it is possible to add directly the individual loads and stiffnesses to locations in the overall stiffness matrices.
The mathematical process of deriving the equilibrium equations for the total structure from the equations of the individual elements can be thought of from the physical point of view as the construction of the total structure with individual elements joined together at pre-selected nodes such that all elements common to a particular node have the same displacement.

4.3 INTRODUCTION OF BOUNDARY CONDITIONS

It is necessary to impose boundary conditions to the overall assembled stiffness matrix to remove the singularity of the matrix. The physical significance is that unless supports or kinematic constraints are imposed, the structure is free to experience unlimited rigid body motions. Boundary conditions can be thought of as restraints that arrest the rigid body motions.

4.3.1 Solution of equations

The equilibrium equations are modified for appropriate boundary conditions and then solved for unknown displacements. In linear structural analysis this is a relatively straightforward procedure, which uses techniques of matrix algebra.

4.3.2 Computation of element stresses

By using the computed displacements, the nodal forces and hence the stresses at the nodes are calculated by multiplying the nodal displacements by the element stiffness matrix. Usually an average value of the nodal stresses is taken to provide the stress value for each element.
A detailed finite element analysis offers the best elastic solution for shear walls with complex patterns of openings. However, given the cost and time limitations of typical design projects, it is unlikely the engineer will have the luxury of studying the effect of local stress concentrations. Large elements may be adequate to describe the complex bending and shear behavior of pier-like shear walls, but they cannot come even close to the actual stress distributions near major stepbacks and complex sets openings. Not one modeling technique is adequate to give all the correct answers.
One method of obtaining a reasonable solution is to attempt a two-step procedure. In the first procedure the overall behaviour is duplicated as closely as possible by using the wide-column modelling technique. The second step consists of isolating the area in question and performing a finite element study by using a set of statically balanced forces obtained from the first state. In this manner it is possible to recognize the system's weak spots and detail them appropriately. It is imperative that the analyst review the underlying assumptions made in standard analysis programs. A successful application of computer analysis techniques to practical design problems requires a thorough understanding of each program and its limitations.

5. INSTABILITY OF STRUCTURAL ELEMENTS

5.1 INTRODUCTION

The purpose of this investigation, through finite element modeling of beams and columns, is to establish the effect of end-conditions on the structural members and on critical buckling loads. The K values (from SABS 0162-1[60]: 1993, clause 9.4.1) for the different length of the beams and columns are compared, in order to derive coefficients and formulas that correctly accommodate beam length as a result of their end-conditions.

The current design procedure for steel frame structures includes an elastic analysis to determine loading effects and a member capacity check using semi-empirical specification equations. However, this process is not adequately described in design standards of most countries. This is due to the complexity in modelling structures in three-dimensional space. Members are designed in practice mostly in 2-dimensions and deal only with three different end-conditions, namely fixed, pinned and free.

In this investigation buckling behaviour of variety of end-conditions are investigated using Abaqus[85] and Prokon[86] (FEM) software packages in order to determine the effects of the end-conditions on member capacity and/or structures.

The first step of any finite element simulation is to discretize the actual geometry of the structure using a collection of finite elements. Each finite element represents a discrete portion of the physical structure. Shared nodes are joined to form the finite elements. The collection of the nodes and finite elements are called a mesh. The number of elements used in a particular mesh is referred to as the mesh density. The structural elements analysed are: I-sections, channels, angle irons, and H-sections with different lengths and fixities. All elements have similar mesh density as that shown in *figure 5.1.*

These models will provide more insight into the torsional buckling and instability of steel structural elements subjected to failure loads. The main purpose of this thesis is to investigate the effects of boundary conditions on stability of a structural steel member.

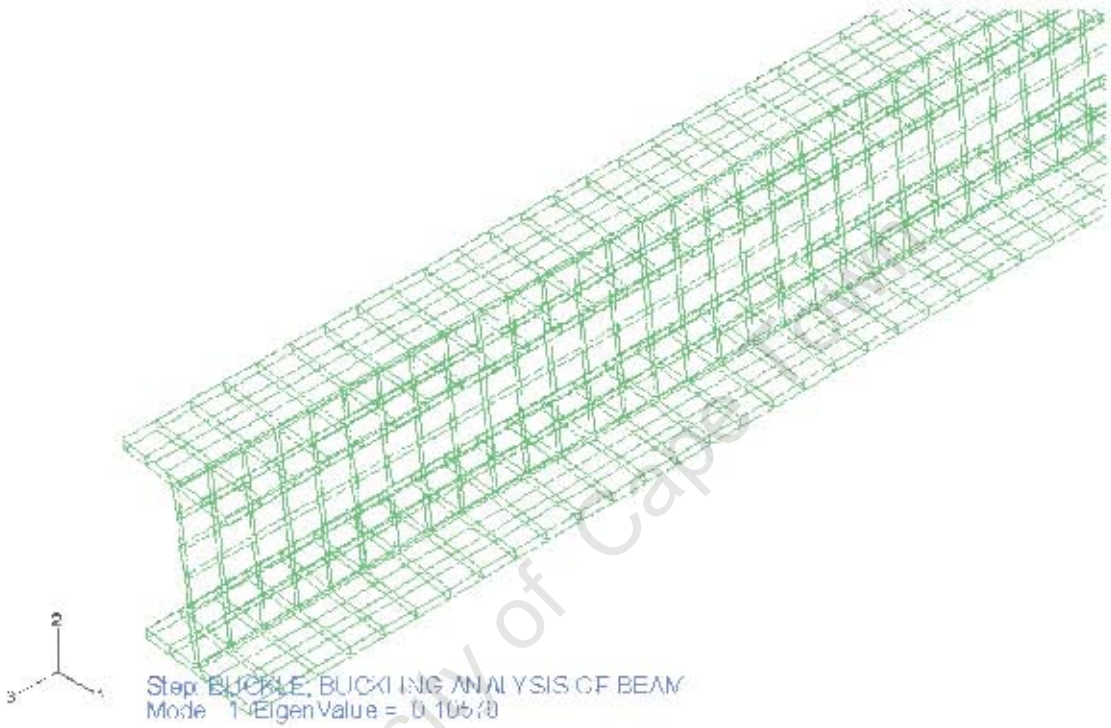

Figure 5.1 Mesh density of an I-beam (using Abaqus[85])

5.2 DESCRIPTION OF THE MODELS USED IN INVESTIGATIONS.

A 150x150x18 angle-iron with lengths 5m, 7.5m, 10m and 15m was subjected to a UDL (uniformly distributed load) for a buckling analysis and stress evaluation. A PFC 200x75 channel and a 1254x146x31 section were also used in the analysis. All the beams were simulated with 6 different types of end conditions given in *table 5.1*.

The pinned-end was simulated with 2 bolts in one line, longitudinal to the member and the semi-fixed with 4 bolts (2x2). The end conditions in *table 5.1* do not include all possible end conditions, but represent most of the connections used in practice.

Table 5.1 Notation for various boundary conditions for analyses

Boundary Conditions		
Abbr.	z=0	z=L
CANT.	fixed	free
F-F	fixed	fixed
F-SF	fixed	semi-fixed
SF-SF	semi-fixed	semi-fixed
F-P	fixed	pinned
P-P	pinned	pinned

The other section investigated was a 305x305x118 H-section as a column with lengths of 3m, 4m, 5m and 6m, respectively.

5.3 MATERIAL PROPERTIES.

The material properties used for the analyses were:

- Density of steel: 7850 kg/m^3
- Poison's ratio: 0.30
- E modulus: 205E6 kPa
- G modulus of rigidity: 77E3 MPa for steel

These properties are assumed to remain constant. Material properties like thermal expansion and thermal conductivity that usually vary were not considered for this investigation.

5.4 THE ANALYSIS OF THE 150x150x18 ANGLE-IRON.

The end-conditions simulated in the analysis are given in *table 5.2*.

Table 5.2 End-conditions of a 150x150x18 angle-iron beam

CANT.	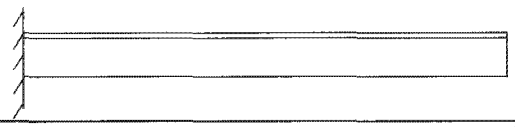
F-F	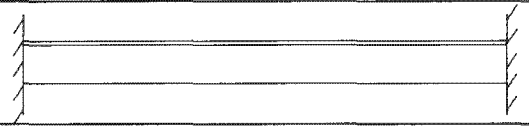
F-SF	
SF-SF	
F-P	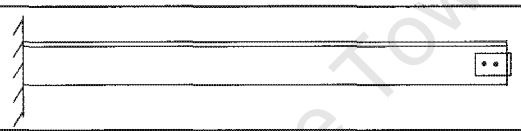
P-P	

A buckling analysis was done for the angle-iron subjected to a UDL loaded on top (destabilizing load) of the element. A deflection criteria is set for each beam and when it is exceeded, the load applied is called the critical buckling load. For each end-condition, a critical load is recorded, which was analysed by comparing the stiffness for each type of end-condition. The analyses were done, using both Prokon[86] and Abaqus[85] to verify the results. The results differ by a marginal 6%. The results shown in chapter 5 are from Prokon[86] only, for consistency in analyses and discussions. (For results from Abaqus[60], refer to Appendices 4 and 5). The results from the two programs differed by less than 6 percent.

The buckling loads for the 150x150x18 angle-iron are given in *table 5.3* for different end-conditions and lengths and compared in *graph 5.1*. It can be interpreted from the graph that the end-conditions (type of fixity) and length of a member greatly influence the buckling load for that member and structure as a whole.

Table 5.3 Load bearing capacity of 150x150x18 angle-iron (kN/m)

End Conditions	Buckling load of 150x150x18 angle-iron			
	5m long	7.5m long	10m long	15m long
F-F	327.86	27.62	3.73	0.309
F-SF	240.15	20.61	2.74	0.348
SF-SF	162.53	17.37	2.67	0.189
F-P	44.21	4.56	0.85	0.083
P-P	16.38	1.44	0.30	0.030
CANT.	7.56	0.51	0.07	0.009

Graph 5.1 Buckling load for a 150x150x18 angle iron.

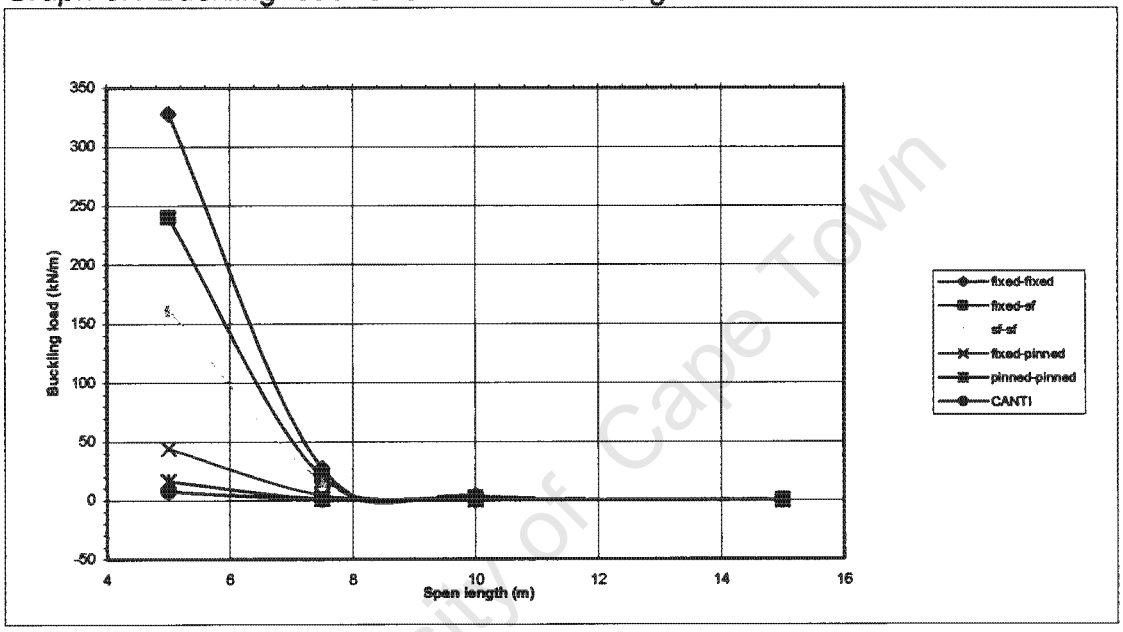

As the length increases or for a less stiff joint, the beam becomes relatively weaker in resistance to torsion and to bending about the minor axis, and becomes unstable under load. The instability manifests itself as a sidewise bending accompanied by twist and is called lateral buckling or lateral-torsional-buckling.

Most design codes provide a simplified classification op boundary conditions. Engineers have used design codes, where boundary conditions can easily be defined as free, pinned or fixed, for many years. This work, shows that many of the member connections cannot simply be classified into these three categories, but that the classification of end-conditions into these three groups is an oversimplification. *Graph 5.1* suggests that there are many end-conditions that exhibit characteristics that lie between pinned- and fixed

The type of beam-to-column connection, which is directly related to the degree of warping restraint of the beam, which is simplified in the SABS 0162-1[60], is given in *table 5.4* for simply supported beams.

The factor K given in this table is dependent on the degree of lateral rotational restraint offered at the supports. It is recommended that the values in *table 5.4* be increased by 20% when the beam-ends are not restrained against torsion. Usually, restraint against torsion is provided by web-plates; web or flange cleats; beams built into walls; and or a better section at the end of the beam. In this analysis, it is evident that there are not only three types of end-conditions that should be considered.

In an attempt to verify or broaden the knowledge on the effective length factor K used in *formulae 5.1* and *5.2*, the buckling load results from Prokon have been used to calculate K with the aid of *formulae 5.1* and *5.2*. The critical

$$M_{cr} = \frac{\omega_2 \pi}{KL}\sqrt{EI_y GJ}\left(B_1 + \sqrt{1 + B_2 + B_1^2}\right) \qquad (5.1)$$

(see Appendix 1 for descriptions)

elastic load of an unbraced monosymmetric section member is given by:

For the cantilever beam, the critical elastic load is given by:

$$M_{cr} = \frac{\pi}{KL}\sqrt{EI_y GJ}\left(1 + \frac{\pi^2 EC_w}{(KL)^2 GJ}\right) \qquad (5.2)$$

(see Appendix 1 for descriptions)

(Table OA was used for the simply supported beams and table OB for the cantilever beams, both from SABS 0162-1[60])

(Refer to Appendix 1) *Equations 5.1 & 5.2* gives the value of the load M_{cr} where lateral-torsional buckling begins but gives no information about postbuckling behaviour. As in the case of the Euler column, the deflection is indeterminate. When the results from Prokon are compared to that, using the rational method of analysis suggested in the commentary on SABS 0162-1 (see Appendix 1), the results of the F-F end-conditions is fairly consistent. The dramatic decrease in buckling load, using Prokon can be due to the fact that

the slenderness of the beam influences the capacity of the beam more than what the formula anticipates. The two tables in Appendix 1, arguably indicates that the P-P end-condition using the rational method, corresponds more likely with the SF-SF end-condition beam using Prokon. The cantilever beams also compare well, except were the 150x150x18 angle-iron become impractically long. By using the critical buckling load results from Prokon (*table 5.3*) and *equations 5.1 & 5.2*, the K values for the beams were calculated (see *table 5.5*). The results from Prokon[86] with *equation 5.1* (for simply supported beams) and *equation 5.2* for cantilever beams, were used to calculate the K values in *table 5.5*.

Table 5.5 Effective length factor K for 150x150x18 angle-iron beam

End Conditions	5m long	7.5m long	10m long	15m long
FF	13.65	47.83	149.34	534.59
F-SF	14.53	50.00	158.63	369.99
SF-SF	17.55	48.54	133.05	557.85
F-P	56.33	161.76	364.72	1118.94
P-P	77.20	260.05	521.30	1568.04
CANT.	41.85	183.71	548.82	1304.11

The K values in *table 5.5* do not do any justice to the two equations used in these calculations. As the beam's length increases, the K values become ridiculously large. The K values for the 5m beams seem to fit the norm of beams with this type of end-conditions. In laboratories at most universities and research centers, the length of beams almost never exceeds 4m. It can be concluded from the results that the formula is valid for up to a certain length of member. Comparing stiffness of the beams, the relationship of the end-conditions seems fairly consistent in relation to each other.

With valuable assessment of the two tables in Appendix 1, SF-SF end-condition is allocated to a K value of 1 and the other end-conditions, compared to it for the different lengths in *table 5.6*. With the analysis, it was observed that the length factor K according to SABS 0162-1[60]: 1993 (stiffness factor related to end-condition) does not accommodate for the length

accurately in *equations 5.1* and *5.2*. It is evident that no trend can be established for the K values of the beams with different fixities and beam lengths using these formulae.

Table 5.6 Effective length factor K for simply supported 150x150x18 angle-iron beams taken to a unit number

End Conditions	5m long	7.5m long	10m long	15m long	Average
F-F	0.78	0.99	1.12	0.96	0.96
F-SF	0.83	1.03	1.19	0.66	0.93
SF-SF	1.00	1.00	1.00	1.00	1.00
F-P	3.21	3.33	2.74	2.01	2.82
P-P	4.40	5.36	3.92	2.81	4.12
CANT.	2.38	3.78	4.12	2.34	3.16

When the results of the beams with SF-SF end-condition from Prokon are taken as P-P end-condition in accordance with the SABS 0162-1, then the average of F-F corresponds well with that in table 5.4. The equations are derived for pure bending and are limited in scope. It is restricted further by the assumed freedom to warp and to rotate about the minor axis at the supports. For these reasons, further investigations including finite element modelling to determine these effects are necessary.

Graph 5.2 Buckling load for a 150x150x18 angle iron (different fixities).

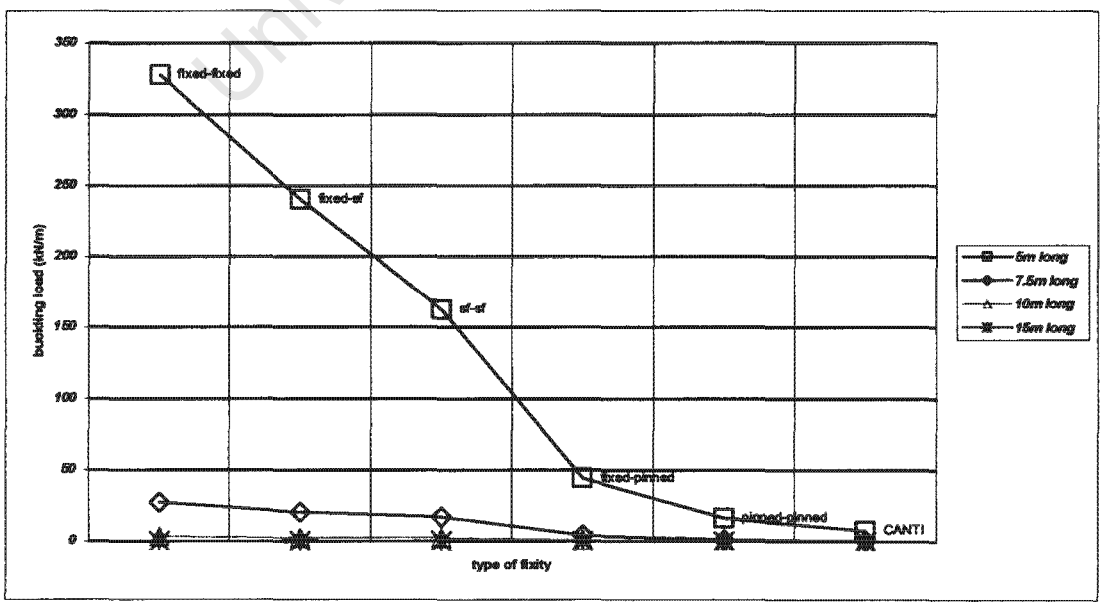

From *graph 5.2*, it can be seen that the buckling load of the member decrease as the stiffness at the joint varies from high to low (from fixed to semi-fixed to pinned to free). As the length of the beam increases, the buckling load decreases.

From the *tables 5.5* and *5.6* it is perceived that with a given factor for the length of the beam in *formula 5.1* and 5.2, K values can be established for an angle-iron. It is also evident that the *formula 5.1* and *5.2* from the commentary on the SABS code[60] must be used with caution. From *graph 5.2*, it can be seen that for the beams with the same length, the beam with pinned-pinned fixity can resist only 5% of the buckling load with fixed-fixed ends, before it starts to buckle. From this we can see that there is a wide range of fixities to be taken into account in order to implement the most economical designs in our design codes and methods.

5.5 THE ANALYSIS OF THE PFC 200X75.

The end conditions simulated in the analysis for the PFC 200x75 are the same as that for the 150x150x18 angle-iron.

A buckling analysis was done for the PFC subjected to a UDL loaded on the element. The buckling loads are given in *table 5.7* and vivified in *graph 5.3*. It is evident in the dramatic change in the buckling loads that the end-fixity conditions have a great influence on the buckling load of the parallel flange channel. The K values are calculated using the rational method suggested in commentary on SABS 0162-1[60]: 1993 and compared to the results from Prokon[86] and Abaqus[85].

Table 5.7 Load bearing capacity of PFC 200x75 (kN/m)

End Conditions	Buckling load of PFC 200x75			
	5m long	7.5m long	10m long	15m long
FF	124.16	13.21	2.51	0.05
F-SF	75.24	7.49	1.44	0.03
SF-SF	43.54	4.10	0.81	0.02
F-P	42.30	4.34	0.83	0.02
P-P	12.92	1.31	0.26	0.005
CANT.	7.85	1.70	0.68	0.01

The buckling loads for different end-conditions and lengths are compared in *graph 5.3* and found that the end-conditions (type of fixity) and length of a member influence the buckling load of the member greatly and structure as a whole. From the graph, it is evident that for the different end-fixities, the buckling load changes in the same pattern with change of beam length.

Graph 5.3 Buckling load for a PFC 200x75.

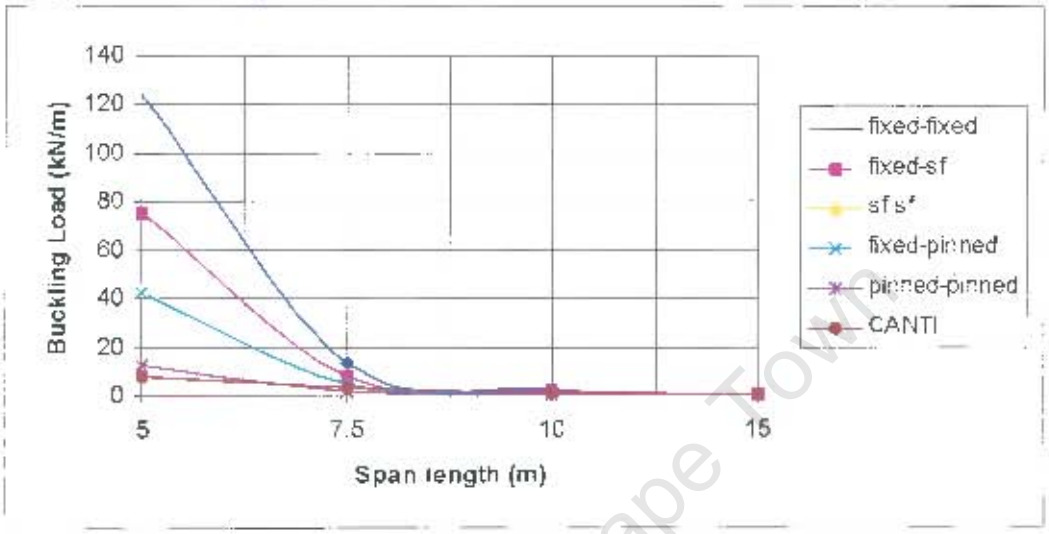

From *graph 5.3* it can be seen that as the end conditions (type of fixity) becomes less stiff, the buckling loads become much less for the same length of beam. If the designer does not take these factors such as end-stiffness into account, it might result in inaccurate results. The trend of the graph is exactly the same as for that of the 150x150x18 angle-iron. The beam with the fixed-fixed end-conditions have the most stiff end-condition, that can resist almost three times that of a beam with SF-SF end-conditions and almost ten times that of a beam with pinned end-conditions.

The cantilever beam for the same length, larger than say for example 6m reflects that it has a bigger buckling load capacity than that of a beam with pinned end-conditions. The fact that the end is built-in might contribute to this difference. Despite the fact that the upper flange of a cantilever beam is always in tension, it is this flange that deforms more due to the buckling load, which reduce the lateral stability of the member further. It is for this reason that a cantilever needs special consideration – Nethercot[53] (1983) developed a method (*equation 5.2*) to calculate the resistance of a cantilever beam.

Initially, the cantilever beam deflect in the vertical plane due to bending, but as the moment increases, it reaches a critical value M_{cr}, where it buckles sideways, twists and collapses (lateral torsional buckling).

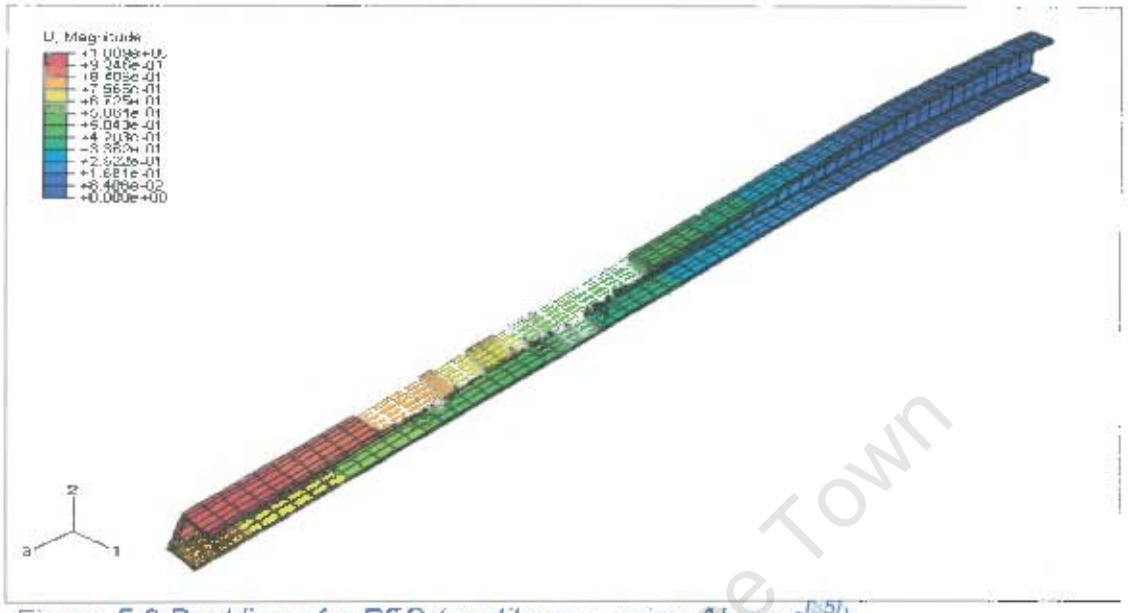

Figure 5.2 Buckling of a PFC (cantilever - using Abaqus[85])

Figure 5.2 is a computer simulation of an exaggerated deformed shape of a cantilever parallel flange channel failing under a buckling load using the program Abaqus[85]. The different colours indicate the different stresses in the element when buckling occurred.

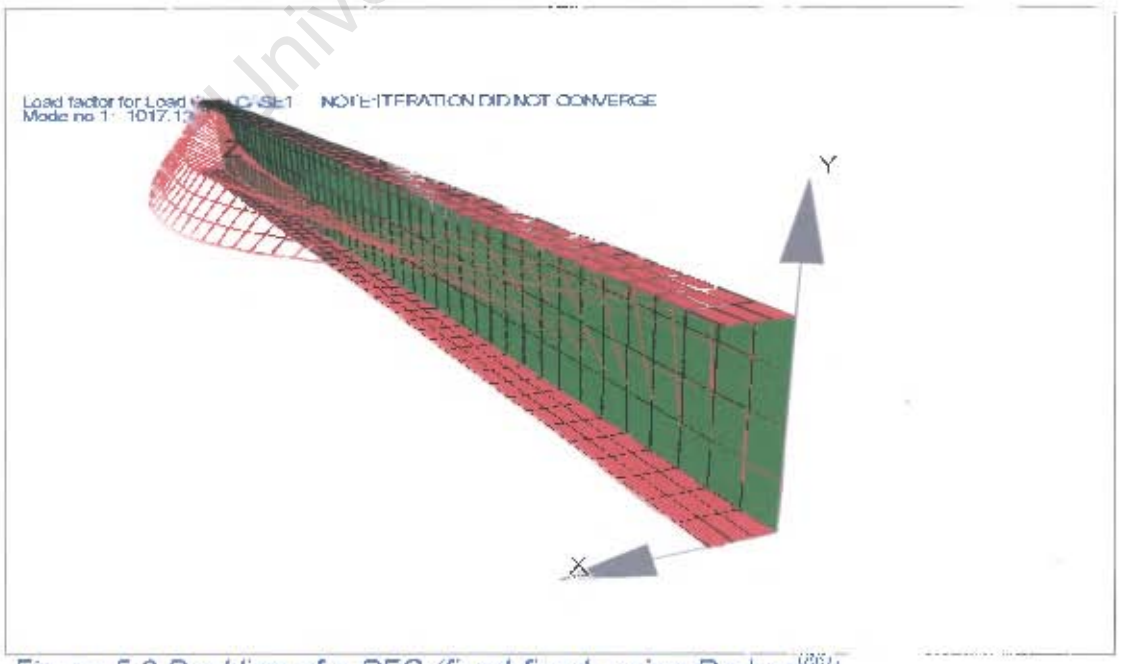

Figure 5.3 Buckling of a PFC (fixed-fixed- using Prokon[86])

Figure 5.3 is a computer simulation from Prokon[86] of an exaggerated deformed shape of a parallel flange channel, fully fixed at both ends, failing under a buckling load using the program Prokon. The line diagram is the deformed shape of the PFC due to the buckling load applied.

The buckling loads for a specific length of beam were plotted versus different fixities as shown in *graph 5.4*.

Graph 5.4 Buckling load for a PFC 200x75 (different fixities)

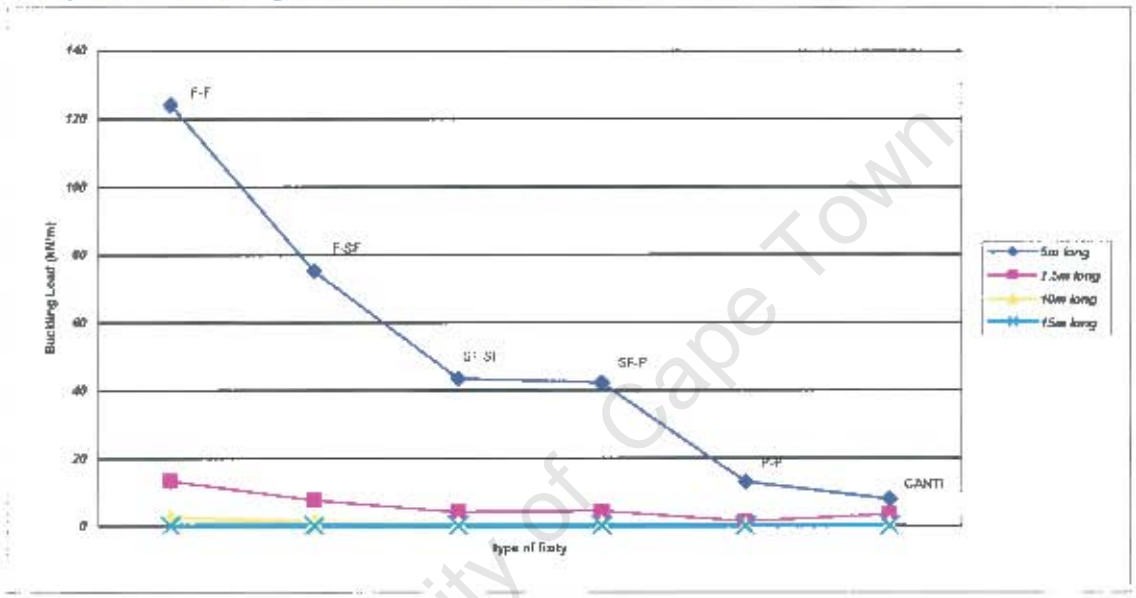

From *graph 5.4*, it can be seen that the buckling load of the member decreases as the stiffness at the joint becomes less (from fixed to semi-fixed to pinned to free). The beam length is indirectly proportional to the buckling load; with an increase in length there is a decrease in the buckling load. As the length increases or the end-condition becomes less stiff, the beam becomes relatively weaker in resistance to torsion and to bending about the minor axis, and becomes unstable under loading. The instability manifests itself as a sidewise bending accompanied by twist and is known as lateral buckling or lateral-torsional buckling.

From the graph, it is noticed that when the length of the beam increases by 50%, the critical buckling load reduces by approximately 90%, and if the length doubles, it reduces by a huge 98%, for all end-conditions except for the cantilever beams, which reduces respectively to approximately 43% and 9%.

Focusing on end-conditions, a beam with F-F end-conditions, a beam with F-SF end-conditions resist merely 60% of the original load, and with SF-SF end-condition 30% of the load compare to the 10% of the beam with P-P end-conditions.

There is a need to adequately address end-fixity conditions persuaded in *graph 5.4*. There are such a great variety of joints (fixities), which result in a wide range of buckling loads for the same length of beam. In this work, only a section of these end-fixities were modelled. The end-fixities can be divided into numerous categories according to; number of bolts, amount of welding, endplate design.

The analysis results of the PFC 200x75 beam can be used to verify or broaden the knowledge on the effective length factor K from SABS 0162-1[60]: 1993 with the same method used for the 150x150x18 angle-iron. The codes take the limit states (the critical buckling load) at which the structure becomes unfit into consideration. The K values in *table 5.8* were calculated for the simply supported beams using results from Prokon and the limit state formulas suggested in the commentary on the SABS 0162-1 (see Appendix 2). From *graph 5.4* and *table 5.8*, it is obvious that no trend can be established for the K values of the beams with different fixities for the PFC.

Table 5.8 Effective length factor K for PFC beams

End Conditions	5m long	7.5m long	10m long	15m long
FF	35.35	75.27	154.07	2364.70
F-SF	42.64	100.34	207.27	3017.45
SF-SF	55.87	145.81	298.30	4255.09
F-P	51.44	121.85	257.16	3733.88
P-P	77.96	199.67	417.92	6725.36
CANT.	15.39	16.92	16.70	228.20

For the 5m and 7.5m long beams, the cantilever does not give the expected K value if compared to either the SF-SF end condition or P-P end-condition. The 5m long beams do not show much of a variation in K values due to end-fixities

whereas all the other beams with lengths 7.5m, 10m and 15m do. The high values for K might be an indication that the formulae used are very conservative.

In the computer analysis, six types of end-conditions combinations were considered in order to demonstrate the great diversity in end-conditions, and what affect these have on the design of the structural element. In practice, the worst-case scenario is taken with safety factors and this might not be economical. If the SF-SF end-condition is allocated with a K value of 1 and the other end-conditions are compared to it for the different lengths, then *table 5.9* is produced.

Table 5.9 Effective length factor K for PFC simply supported beams using results from Prokon and equation 5.1 taken to a unit number

End Conditions	5m long	7.5m long	10m long	15m long	Average
FF	0.63	0.52	0.52	0.56	0.56
F-SF	0.76	0.69	0.69	0.71	0.71
SF-SF	1.00	1.00	1.00	1.00	1.00
F-P	0.92	0.84	0.86	0.88	0.87
P-P	1.40	1.37	1.40	1.58	1.44
CANT.	0.28	0.12	0.06	0.05	0.13

From the *table 5.9* and *graph 5.1* it can be seen that there is a certain trend for the different lengths and fixities of the PFC beam subjected to a UDL on the beam. From *graph 5.1* and *table 5.9* it is evident that the length of a member is indirectly proportional to the buckling load; as the length increases, the buckling load decreases. Furthermore, the stiffer the end-condition the higher the buckling loads of the PFC. When the beam length changes from a 5m length to a 7.5m length, the critical load decreases by approximately 90%, and when the end-condition changes from fixed-fixed to semifixed-semifixed, the critical load decrease by approximately 90%. From this it is observed that there is a wide range of structural capacities for the same beam and that many of the laboratory experiments and computer analysis still need to be done in order to make steel design more accurate.

5.6 THE ANALYSIS OF THE I254X146X31 I-BEAM.

The end conditions simulated in the analysis for the I254x146x31 I-beam are the similar to that for the 150x150x18 angle-iron.

A buckling analysis was done for the I-beam subjected to a UDL. The buckling loads are given in *table 5.10* and *graph 5.5*. It is evident that the end fixity conditions have a great influence on the buckling load of the parallel flange I-section. Unlike the angle-iron and the channel, an I-section is symmetrical about both axes. For the angle-iron and the channel, it was logical that the beam twists to the weaker side of the section causing it to buckle under a load, whereas in the case of an I-section, it must have a deficiency like permissible variation given in The South African Steel Construction Handbook[68] in dimension or weakness in element. The allowable dimensional deviations also need to be taken into account. The K values are calculated using the SABS 0162-1[60]: 1993. In the computer analysis, six types of end-conditions combinations were considered in order to observe the great diversity in end-conditions, and what affect this can have on the design of the structural element.

Table 5.10 Load bearing capacity of I254x146x31 (kN/m)

End Conditions	Buckling load of I 254x146x31			
	5m long	7.5m long	10m long	15m long
FF	363.67	32.97	5.88	0.51
F-SF	114.69	11.41	2.15	0.20
SF-SF	36.85	3.81	0.75	0.07
F-P	51.88	6.19	1.29	0.11
P-P	10.45	1.61	0.37	0.04
CANT.	9.08	1.40	0.32	0.03

From *table 5.10* and *graph 5.5* it can be seen that there is a trend for the different lengths and fixities of the I254x146x31 I-beam loaded with an UDL on top of the beam. From the graph and the table it is evident that as the length increases, the buckling load decreases. Also the stiffer the end-condition the higher the buckling load of the I-beam.

When the beam length changes from a 5m to 7.5m the critical load decrease by approximately 90%, and when the end-condition changes from fixed-fixed to semifixed-semifixed, the critical load decreases by approximately 90%.

From this it is observed that there is a wide range of structural capacities for the same beam with its different end-conditions.

Graph 5.5 Buckling load for an I254x146x31

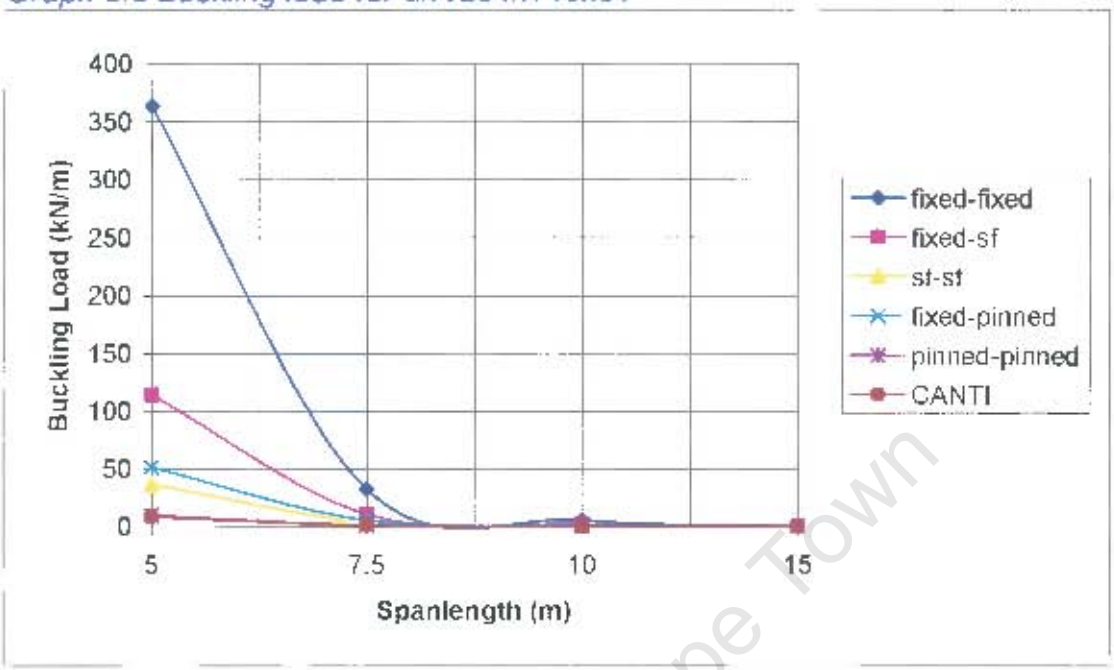

The South African Steel Construction Handbook[68] allows for several dimensional deviations (tolerances), which might trigger a failure mechanism with a smaller buckling load than anticipated. The buckling load for a specific length of beam has beam plotted with different fixities as in *graph 5.6*.

Graph 5.6 Buckling load for an I254x146x31 (different fixities)

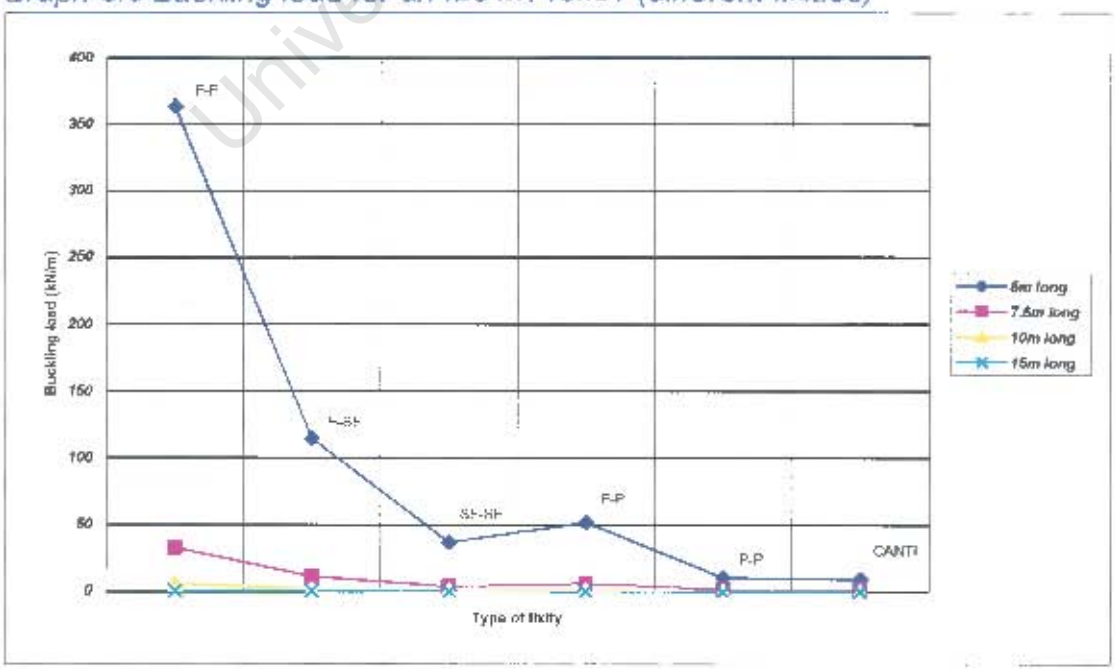

From *graph 5.6*, it can be seen that the buckling load of the member decreases, as the stiffness at the joint becomes less (from fixed to semi-fixed to pinned to free). As the length of the beam decreases, the buckling load increases. As the length increase or for a less stiff joint, the beam becomes relatively weaker in resistance to torsion and to bending about the minor axis, and becomes unstable under load. The instability manifests itself as a sidewise bending accompanied by twist and is called lateral buckling or lateral-torsional buckling. If the graphs (*5.3 & 5.4*) of the PFC and the graphs (*5.5 & 5.6*) of the I-beam are compared, it follows a similar trend for both the change in length and different end-fixities.

The buckling load results from Prokon[86] and Abaqus[85] have been used to calculate K in accordance with SABS 0162-1[60] (refer to Appendix 3). The effective length factors are listed in *table 5.11*. No definite trend can be established for the K values of the I-beams with different fixities. Comparing to the first two beams, the I-beam meets more the expected values in design practice.

Table 5.11 Effective length factor K for I-section simply supported beams using results from Prokon and equation 5.3

End Conditions	5m long	7.5m long	10m long	15m long
FF	0.20	0.57	1.28	4.21
F-SF	0.50	1.30	2.73	8.51
SF-SF	1.50	2.10	4.23	9.89
F-P	0.79	1.72	3.27	10.71
P-P	2.00	3.35	5.82	16.85
CANT.	0.87	1.08	1.64	5.28

In SABS 0162-1[60]: 1993, clause 9.4.1, the effective length factor K is implemented (results from laboratories and analysis) to account for the type of fixity, but only three types of "ideal" fixities have been used ignoring the wide range of fixities. In an attempt to verify or broaden the knowledge on the effective length factor K used in formula 5.3(a), the buckling load results have been used to calculate K with formula 5.3(a). When the buckling load of a

beam is designed according to SABS 0162-1[60]: (1993) – clause 13.6, the critical elastic load of an unbraced member is given by:

$$M_{cr} = \frac{\omega_2 \pi}{KL}\sqrt{EI_y GJ + \left(\pi E/L\right)^2 I_y C_w} \qquad \text{(SABS 0162-1[60])} \qquad (5.3.a)$$

compared to

$$M_{cr} = \frac{\omega_2 \pi}{KL}\sqrt{EI_y GJ + \left(\pi E/KL\right)^2 I_y C_w} \qquad \text{(AISC Manuals)} \qquad (5.3.b)$$

where: KL is the effective length of unbraced portion of a beam
$\omega_2 = 1.75 + 1.05\kappa + 0.3\kappa^2 \leq 2.5$ (for unbraced lengths subject to end moments), or
$\omega_2 = 1.0$ (when bending moment at any point within the unbraced length is greater than the larger end moment or when there is no effective lateral support for the compression flange at one of the ends of the unsupported length)
C_w is the warping torsional constant
κ is the ratio of the smaller to larger ultimate moment at opposite ends of the unbraced length (positive for double curvature and negative for single curvature)

It is evident that no trend can be established for the K values of the beams with different fixities and beam lengths. There are a couple of reasons why this is the phenomenon. One being the fact that equation 5.3(a) was rewritten from the equation 5.3(b) from AISC manuals. The K value to the length inside the square root was omitted when implemented in the SABS 0162-1[60].

However, if the SF-SF end-condition is taken as the fixity with a K value of 1 and the other end-conditions are compared to it for the different lengths, then *table 5.12* is produced.

Table 5.12 Effective length factor K for I-section simply supported beams using results from Prokon and equation 5.1 taken to a unit number

End Conditions	5m long	7.5m long	10m long	15m long	Average
FF	0.13	0.27	0.30	0.43	0.28
F-SF	0.33	0.62	0.65	0.86	0.61
SF-SF	1.00	1.00	1.00	1.00	1.00
F-P	0.53	0.82	0.77	1.08	0.80
P-P	1.33	1.60	1.38	1.70	1.50
CANT.	0.58	0.51	0.39	0.53	0.50

From *table 5.12* it can be observed that with a given factor or part formula for the length of the beam in *equation 5.3(a)*, K values can be established for I-sections.

Figure 5.4 is an example of the type of computer simulation in aid to help ease our analysis and ultimately designs methods.

Figure 5.4 is an example of a cantilever I-beam buckling using, Abaqus to get the eigenvalue and ultimately the buckling load.

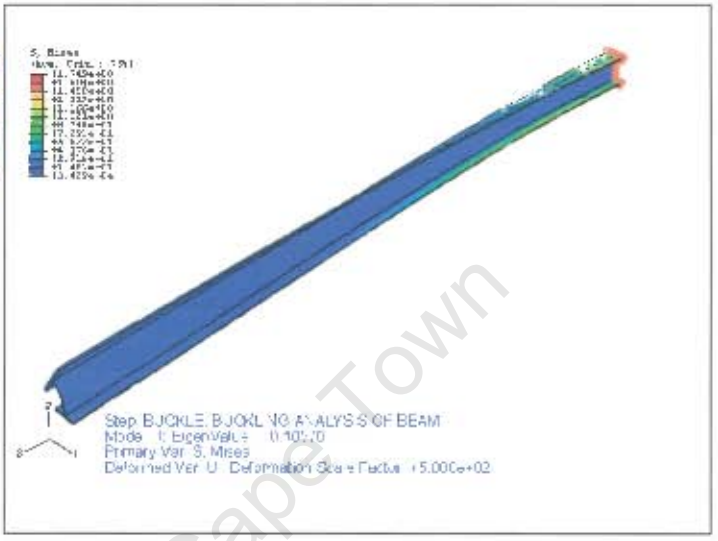

It is also evident that the formula in the SABS code must be used with caution. From all of the above discussions, it can be concluded that there are still work to be done on torsional buckling of steel elements.

With further investigation and mathematical knowledge, the equation 5.3 can be properly examined leading to a reformulation or factor that can account for the length and fixity properly.

5.7 THE ANALYSIS OF THE 305X305X118 H-SECTION.

A buckling analysis was done for the H-section subjected to a point load on the top of the structural element (column) for different end-conditions. *Figure 5.5* shows the result of a buckling analysis of a cantilever column with an axial load. The line diagram depicts the deflected shape of the column. The column was analysed in lengths of 3m, 4m, 5m and 6m respectively.

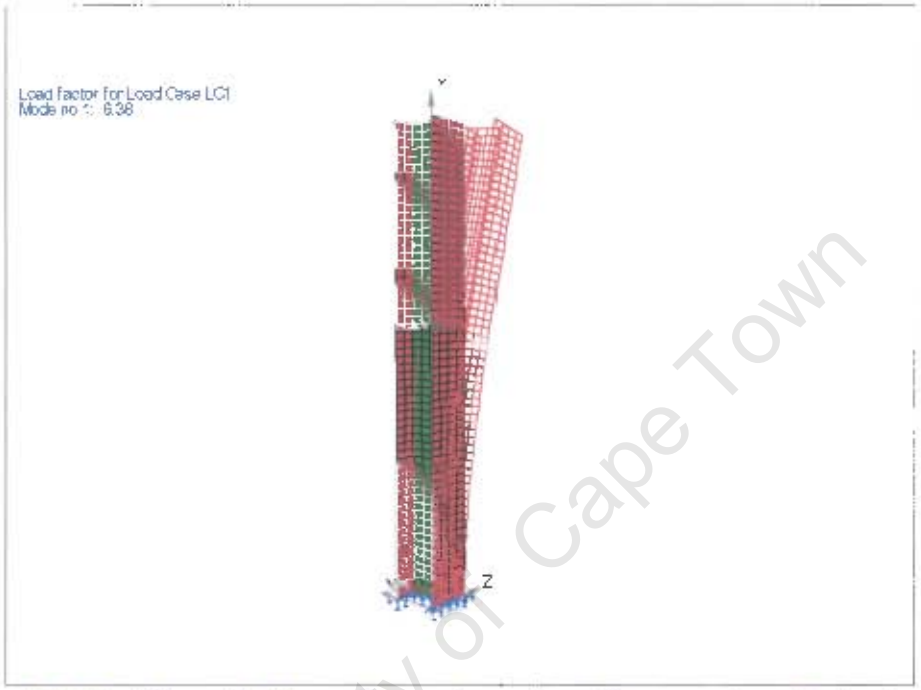

Figure 5.5 Buckling of a H-section column (cantilever- using Prokon)

The buckling analysis of the 305x305x118 H-section column produced *table 5.13*. From the table, a graph (*graph 5.7*) was produced by plotting length of the member versus the buckling load for a specific end-condition.

Table 5.13 Load bearing capacity of a 305x305x118 H-section column (kN)

End Conditions	Buckling load of 305x305x118 H-section			
	3m long	4m long	5m long	6m long
FF	130143	45110	19253	9503
F-SF	58331	30381	16393	8671
SF-SF	25194	13728	7280	3796
F-P	15054	6396	3458	2132
P-P	1222	832	611	468
CANT.	8294	2639	1084.2	520

Graph 5.7 Buckling load for a 305x305x118 H-section column

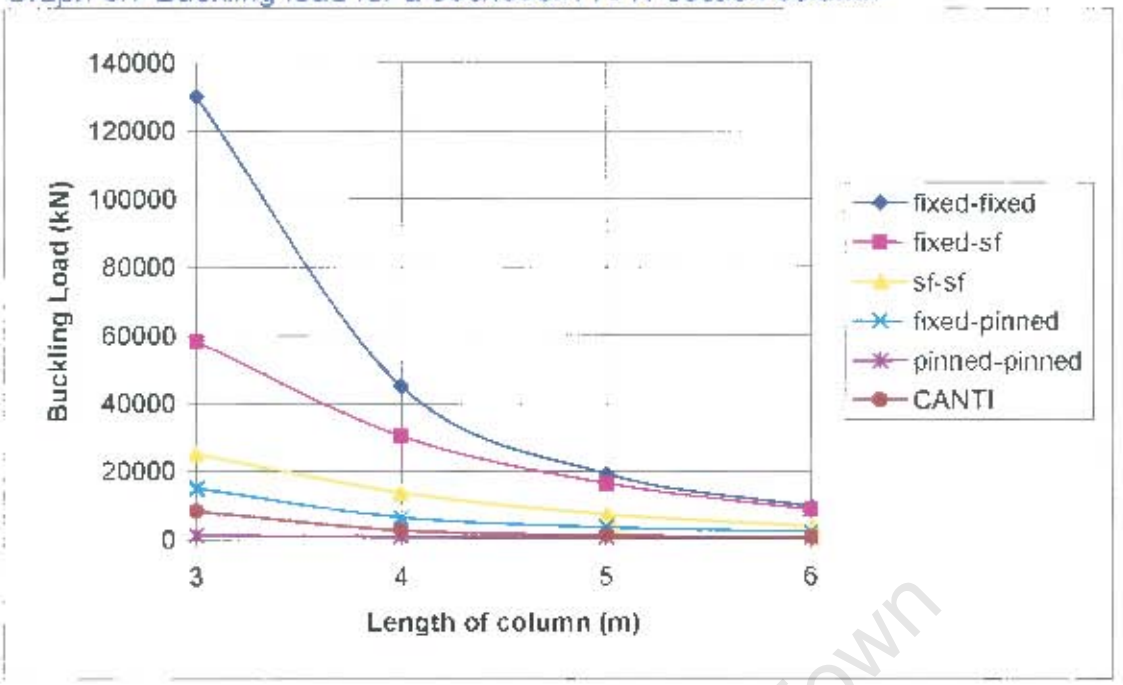

From the *graph 5.7*, it is evident that there is a definite trend between the end-conditions and change in length of the column. Leonhard Euler formulated a formula (see *Eq. 5.4*), which claims that the critical bucking load of a perfect column is indirectly proportional to the member's length squared. To prove Euler's theory, the buckling loads were multiplied by the length squared of the member and plotted (see *graph 5.8*) for the different end-conditions.

$$P_{cr} = \frac{\pi^2 E_t I}{(KL)^2} \qquad (5.4)$$

Graph 5.8 Buckling load x l^2 for a 305x305x118 H-section column

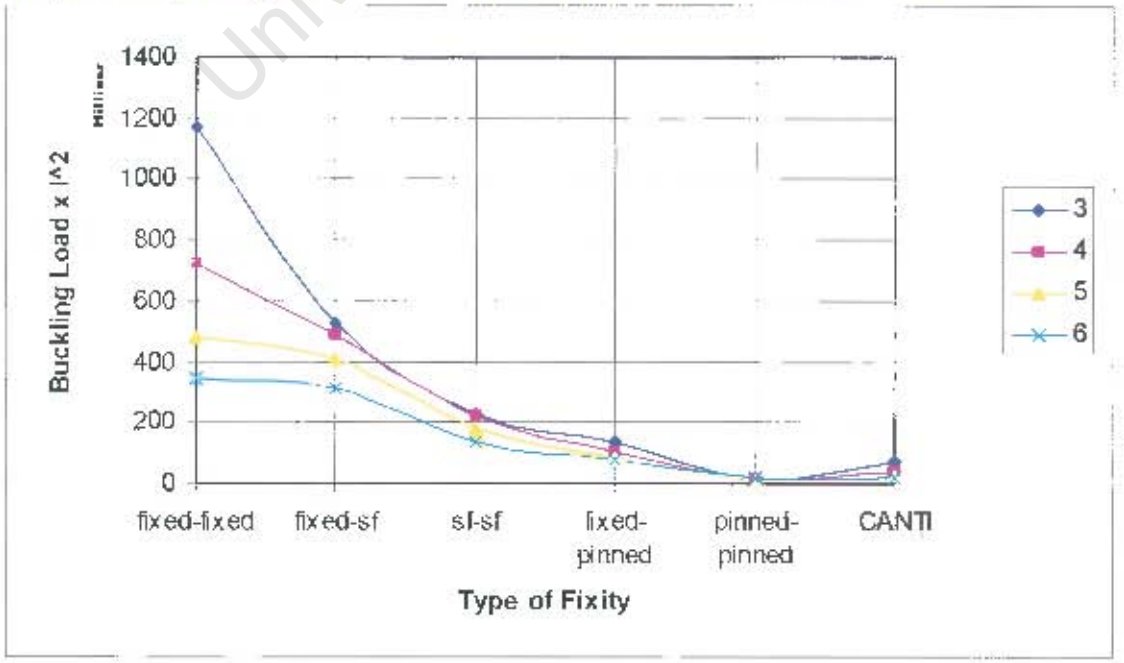

As expected, for all the lengths with pinned-pinned end-conditions, the buckled load multiplied by the length squared is almost similar. Although, for the other conditions, the figures do not correspond that well, but are very close. With the formula and methods used in the SABS 0162, it is impossible to use the answers (buckling loads) to calculate the K values and compare the end-conditions in terms of stiffness for design purposes. However, *equation 5.4*, derived from Euler's formula was used to calculate the K values in order to achieve valuable conclusions. The K values were calculated with the use of the *equation 5.4* and results from the analysis with the aid of the FEM of Prokon[86] and Abaqus[85] and are listed in *table 5.14*.

Table 5.14 Effective length factor K for 305x305x118 H-section column using results from Prokon and equation 5.4

	3m long	4m long	5m long	6m long
FF	6.14	13.90	26.60	45.43
F-SF	9.17	16.94	28.82	47.56
SF-SF	13.95	25.20	43.25	71.88
F-P	18.05	36.92	62.76	95.91
P-P	63.34	102.36	149.30	204.71
CANT	24.31	57.47	112.08	194.21

Graph 5.9 K Unit Multiplier for a 305x305x118 H-section column

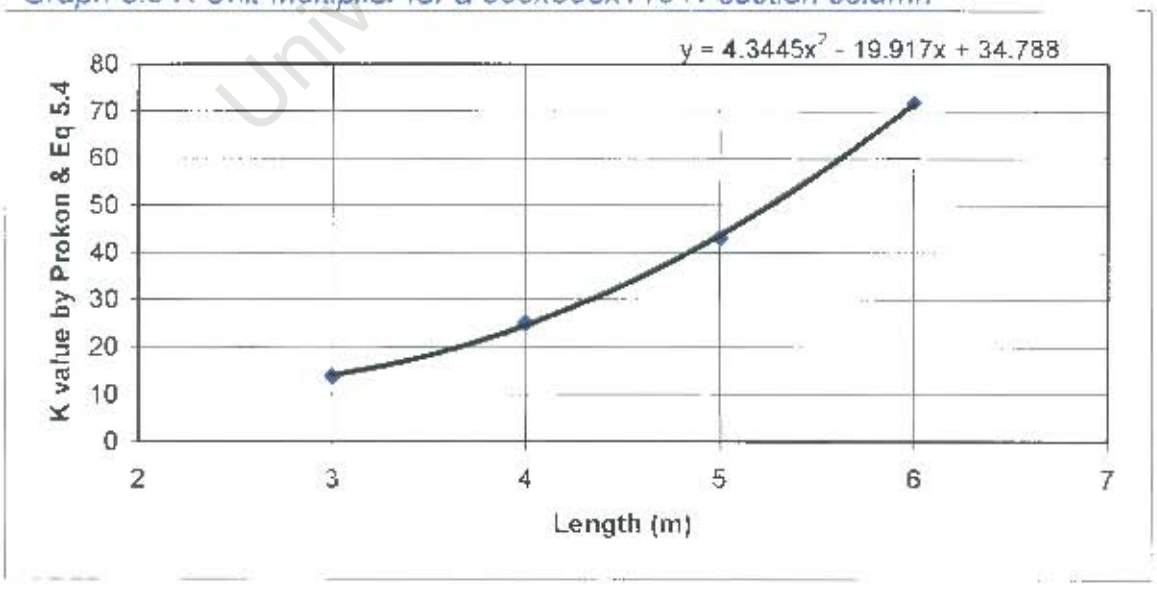

The values of the SF-SF end conditions corresponding to the length were used to calculate a formula in order to convert the K-values to unity for these end-conditions. The values were plotted against the length as in *graph 5.9*, which was used to translate the K-values to unity for the SF-SF end-conditions and the corresponding K values for the other end conditions. The equation from *graph 5.9* was incorporated in *equation 5.5*, which produced the following equation:

$$P_{cr} = \frac{\pi^2 E_s I}{\left(\frac{KL}{\left(4.3445L^2 - 19.917L + 34.788\right)}\right)^2} \qquad (5.5)$$

Equation 5.5 and the buckling load values from Prokon were used, which produced the K-values in *table 5.15*.

Table 5.15 Effective length factor K for 305x305x118 H-section columns using results from Prokon and equation 5.4 taken to a unit number

	3m long	4m long	5m long	6m long	Average
FF	0.43	0.56	0.61	0.63	0.56
F-SF	0.65	0.69	0.66	0.66	0.66
SF-SF	0.99	1.02	0.99	1.00	1.00
F-P	1.28	1.50	1.43	1.34	1.39
P-P	4.48	4.16	3.41	2.86	3.72
CANT	1.72	2.33	2.56	2.71	2.33

With *Equation 5.5* and the values from Prokon or Abaqus a proper, consistent value for K can be obtained. Thus the column buckling formula can be rewritten as in *equation 5.5* and the K values for the end-conditions used as in the average column in *table 5.15*. With the same method, the K values for any other end-condition can be calculated and used in the formula.

6. Analysis of Thesis

6.1 FINDINGS AND CONCLUSION

Legislation attempts to set minimum standards of safety to comply with, and is written for the enforcement authorities to check that designs being produced are intrinsically and fundamentally safe. It can be observed that the SABS 0162-1[60]:1993 code does not provide accurate guidelines on how to deal with torsional buckling and instability of steel structures.

An attempt should be made to get the true formulae and design methods for any member with any end-condition in structures. A structure should be designed as an entity and not by parts, since other members influence the stability of members positively, thus increasing the buckling resistance depending on the joint fixity.

It has been shown that the critical buckling load of steel beams and columns is influenced by the stiffness of the structure/member (which includes end-conditions) that restrains member/structure against twist or torsion. This influence is important for small load eccentricities and stability of a structure as a whole. In the Prokon[86] and Abaqus[85] analyses it was found that the beam with fixed ends have a critical buckling load more than ten times that of pinned ends, which does not correspond with most codes of practice. However, in all the beams, the semi-fixed end-conditions were taken to unity in order to derive a K value and ultimately a formula for each end-condition used. It was also noticed that the formula in the SABS 0162-1[60]:1993, clause 13.6 does not allow properly for change in length of beam. However, there was a trend for each end condition with relationship to the length of the member.

In the analysis of the columns, it was found that all end-conditions followed a trend in terms of critical buckling loads and column length. Euler's buckling load was used to calculate the K values for the end-conditions used, which resulted in an altered Euler's Buckling load formula, which takes the change in length of a beam properly into account and take K value for a semifixed end-conditions as unity.

For both the beams and columns under lateral-torsional buckling, the SABS 0162-1[60]: 1993 code appears inadequate.

6.2 RECOMMENDATIONS

The following recommendations are made as a result of this investigation:

More investigations and research should be done on the behaviour of steel structures.

Further investigation need to be taken in order to formulate a concrete equation, which will make designs user friendly and economical.

Computer programs should be validated and incorporate in the design process, thus result in timeously designs by alleviating the designer from doing complicated iterations.

Further modeling should be done on Prokon[86] and Abaqus[85] to simulate 3-d structures and for not only elastic modulus but for the other properties influenced by temperature etc.

8. BIBLIOGRAPHY

1. Abu-Sena, AB, Chapman, JC & Davison, PC. Interaction between critical torsional flexural and lip buckling in channel sections. Journal of Constructional Steel Research. Research 57 (2001), pp 925-944.

2. Allen, HG and Bulson PS. Background to Buckling. First Edition. (McGraw-Hill, Maidenhead, 1980).

3. Al-Shawi, FAN. Stiffness of restraint for steel struts with elastic end supports. Journals of Structures & Buildings 146. Issue 2 (2001), pp 153-159.

4. Baba, S and Kajita, T. Plastic analysis of torsion of a prismatic beam. Int J Numer Meth Eng (1982), pp 927-944.

5. Bai, Y. Collapse of thick tubes under combined tension and bending. Journal of Constructional Steel Research 32 (1995), pp 233-257.

6. Barsoum, RS and Gallagher, RH. Finite element analysis of torsional and torsional-flexural stability problems. International Journal for Numerical Methods In Engineering (1970), pp 335-352.

7. Bedair, OK and AN. Sherbourne. The elastic stability of partially-restrained plates under compression and In-plate bending. Journal of Constructional Steel Research. Volume 35 No.3 (1995), pp 339-360.

8. Borri, C and Hufendiek, HW. Geometrically nonlinear behaviour of space beam structures. Journal of Structural Mechanics (1985), pp1-26.

9. Britvec, SJ. The Stability of Elastic Systems. (New York, Pergamon Press, 1973).

10. Brush, Don, O and Bo, O. Almroth who cover cylindrical shell subjected to torsion.

11. BS 5950: Part 1: 1990 – Steelwork Design. (BSI, London, 1990).

12. Chajes, Alexander. Principles of Structural Stability. (Civil- and Mechanical Engineering Series). First Edition. (Prentice-Hall, 1974).

13. Chen, W. Theory of beam columns. Volume 1: In plane behaviour and Design.

14. Chen, WF and Lui, EM. Structural Stability: Theory and implementation. (CRC Press, London, 1987).

15. Cheung, YK. Finite strip method in structural analysis. Pergamon Press, New York. (1976).

16. Chilver, AH. The behaviour of thin-walled Structural members in compression. (Engineering, 1951).

17. Chou, SM, Chai, GB & Ling, L. Finite elements technique for design of stub columns. Journal - Thin walled Structures 37 (2000), pp 97-112.

18. Chou, SW, Seah, LK, and Rhodes, J. Accuracy of some Code of Practice in predicting the load capacity of cold-formed columns. Journal of Constructional Steel Research (1996) 37.

19. Coull, A & Stafford, E. Tall Buildings. (Oxford, Pergamon, 1967).

20. Cowan, Henry J. Reinforced and Prestressed Concrete in torsion.(London, Arnold, 1965).

21. Constructional Steel Research and Development Organisation - Crosby, Lockwood, Staples. Steel Designers Manual 4th Edition. (Granada Publishing Limited, 1975).

22. Creaghan SG and Palazotto AN. Nonlinear large displacement and moderate rotational characteristic of composite beams incorporating transverse shear strain. Comput Struct (1994).

23. Daali, ML and Korol RM. Prediction of local Buckling and rotation capacity at maximum moment. Journal of Constructional Steel Research. Volume 32 No. 1 (1995), pp 1-13.

24. Dabrowski, Ryzard. Curved Thin-walled Girders, Theory and analysis. (London, 1971).

25. Davies, JM. Second-order elastic-plastic analysis of plane frames. Journal of Constructional Steel Research. Research 58 (2002), pp 1315-1330.

26. Della Corte et al. Seismic analysis of MR steel frameson refined hysteretic models of connections. Journal of Constructional Steel Research. Research 58 (2002), pp 1331-1345.

27. Fenner, RT. Engineering Elasticity: Application of numerical and analytical techniques. (New York, Halsted Press, 1986).

28. Foley, CM and Vinnakota S. Towards design office moment-rotation curves for end plates beam-to-column connections. Journal of Constructional Steel Research. Volume 35 No.2 (1995), pp 217-253.

29. Goldberg, JE, Bogdanoff, JL and Glauz, WD. Lateral and torsional buckling of thin walled beams. Proceedings, IABSE Volume 24 (1964).

30. Gotluru, BP, Schafer, BW & Peköz, T. Torsion in thin walled cold-formed steel beams. Journal - Thin walled Structures 37 (2000), pp 127-145.

31. Griffel, W. Beam Formulas. (Frederick Ungar Publishing Co., New York, 1970).

32. Guo, YL. Theoretical study of ultimate load of locally buckled stud columns loaded eccentrically. Journal of Constructional Steel Research. Volume 38 No.3 (1996), pp 239-255.

33. Hancock, GJ. Distortional buckling of steel storage rack columns. Journal of Structural Engineering (ASCE – 1985).

34. Johnson, BG. SSRC Guide to Stability design Criteria for structures. Third Edition (1976).

35. Johanson, B, Maquoi, R & Sedlacek, G. New design rules for plated structures in Eurocode 3. Journal of Constructional Steel Research. Research 57 (2001), pp 279-311.

36. Karren, KW. Effects of cold-forming on light-gage steel members. (Ph.D. Thesis (1965) at Cornell University. Ithaca, New York).

37. Katori, H. Consideration of the problem of shearing and torsion of thin walled beams with arbitrary cross-section. Journal - Thin walled Structures 39 (2001), pp 671-684.

38. Kemp, AR. A mixed flexibility approach for simplifying elastic and inelastic structural analysis of frames. Journal of Constructional Steel Research 55 (2002), pp 1297-1313.

39. Ketter, LR, Lee, GSP and Prawel Jr., SP. Structural analysis and design. (New York, McGraw-Hill, 1979).

40. Kim, S, Kim, Y & Choi, S. Nonlinear analysis of 3D Steel frames. Journal - Thin walled Structures 39 (2001), pp 445-461.

41. Kleinlogel, A. Rigid Frame Formulas. (Frederick Ungar Publishing Co., New York, 1958).

42. Krenk, S. & Damkilde, L. Warping of joints in I-beam assemblages. Journals of Engineering Mechanics. Volume 117, No. 11, (1991).

43. Kwak, H, Kim, D & Lee, H. Effect of warping in geometric nonlinear analysis of spatial beams. Journal of Constructional Steel Research. Research 57 (2001), pp 729-751.

44. Liew JYR. et al. Behaviour and design of horizontally curved steel beams. Journal of Constructional Steel Research. Volume 32 No. 1 (1995), pp 37-67.

45. Linberg, HE and Florence AL. Dynamic pulse buckling. (Dordrecht, M. Nijhoff, 1987).

46. MacGinley, TC & Ang, TC. Structural Steelwork, Calculating and Detailing. (Newnes-Butterworths, 1973).

47. Masarira, A. The effect of joints on the stability behaviour of steel frame beams. Journal of Constructional Steel Research. Research 55 (2002), pp 1375-1390.

48. Masika, RJ and Dunai L. Behaviour of bolted end plates portal frame joints. Journal of Constructional Steel Research. Volume 32 No.2 (1995), pp 207-225.

49. Mazor, D & Rand, O. The influence of the in-plane warping on the behaviour of thin walled beams. Journal - Thin walled Structures 37 (2000), pp 363-390.

50. McCormac, JC. Structural Steel design. Third Edition. (New York, Harper & Row, 1981).

51. Murray, NW. Introduction to the Theory of Thin-Walled Structures. (Oxford University Press, 1983).

52. Mofid, M, Asl, M & McCabe, SL. On the analytical model of beam to column semi-rigid connections, using plate theory. Journal - Thin walled Structures 39 (2001), pp 307-325.

53. Nethercot, DA. Frame structures: global performance, static and stability behaviour, General Report. Journal of Constructional Steel Research. Research 58 (2000), pp 109-124.

54. Nethercot, DA. The importance of combining experimental and numerical study in advancing structural engineering understanding. Journal of Constructional Steel Research. Research 58 (2002), pp 1283-1296.

55. Nethercot, DA et al. Required rotations and moment redistribution for composite frames and continuous beams. Journal of Constructional Steel Research. Volume 35 No.2 (1995) pp 121-163.

56. Newmark, Nathan M. Selected papers by Nathan M. Newmark, Civil Engineering Classics

57. Paik, JK & Thayamballi, AK. Buckling strength of steel plating with elastically restrained edges. Journal - Thin walled Structures 37 (2000), pp 27-55.

58. Reid, CN. Deformation geometry for material scientists. (Oxford, Pergamon Press, 1973).

59. Rosen A, Rand O. Numerical model of the non-linear behaviour of curved rods. Comput Struct (1986), pp 785-799.

60. SABS 0162-1: 1993 – The Structural use of steel: Part 1: Limit States design of hot-rolled steelwork. The Council of the SA Bureau of Standards.

61. Samuel H Marcus. Basics of structural steel design. (Reston Pub. Co., 1977).

62. Schafer, BW. A correction to AISI specification B2.3 and B4.2 in order to partially alleviate the unconservative prediction of members with edge stiffened elements. (1998).

63. Shanmugan, NE and Arockiasamy, M. Local buckling of stiffening plates in offshore structures. Journal of Constructional Steel Research. Volume 38 No. 1 (1996), pp 41-59.

64. Shermer, CL. Design in Structural Steel. (New York, Ronald Press, 1972).

65. Simitses, George J. An introduction to the Stability of structures. (Prentice-Hall, 1976).

66. Slater, G. Buckling (April 2001). http://www.twi.co.uk/j32k/protected/band_3/ksgs001

67. Suryaotmono, B & Ho, D. The moment-gradient factor in lateral torsional buckling on wide flange steel sections. Journal of Constructional Steel Research. Research (2001).

68. (The) South African Institute of Steel Construction. South African Steel Construction Handbook (Limit Sates Design). Revised Third Edition 1999

69. (The) South African Institute of Steel Construction. Structural Steelwork connections. Limit States Design 1st Edition (1992).

70. Tall, L. Structural Steel Design. Second Edition. (New York, Ronald Press, 1974).

71. Taranath, Bungale S. Structural analysis and design of tall buildings.

72. Terrington, JS. Combined bending and torsion of beams and girders. British Constructional Steelwork Association Ltd.: Publication No 31, First part, 1968.

73. Terrington, JS. Combined bending and torsion of beams and girders. (British Constructional Steelwork Association Ltd.: Publication No 31, Second part, 1970).

74. Timoshenko, SP and Gere, JM. Theory of elastic stability. Second edition. (McGraw-Hill, New York, 1971).

75. Timoshenko, SP and Goodier, JN. Theory of elasticity. Second edition and Third edition. (McGraw-Hill, New York, 1975).

76. Tomka, P. Lateral stability of coupled simply supported beams. Journal of Constructional Steel Research 57 (2001), pp 517-523.

77. Trahair, NS. The Behaviour and Design of Steel Structures. (Chapman and Hall, London, 1977).

78. Van den Broek, JA. Elastic Energy Theory. (1931).

79. Vlasov VZ. Thin walled Elastic beams. Isreal program for Scientific (Translations, Jerusalem, 1961).

80. Yong, BA. Collapse of thick tubes under combined tension and bending. Journal of Constructional Steel Research. Volume 32 No.2.

81. Yuan, Z. Research Proposal: Steel member stability design. 8 March 2000.

82. Zha, Y. and Moan, T. Ultimate strength of stiffened aluminium panels with predominantly torsional failure modes. Thin-Walled Structures 39 (2001), pp 631-648.

83. Zbirohowski-Koscia, K. THIN WALLED BEAMS: From theory to practice. (Crosby Lockwood & Son Ltd., London, 1967).

84. EC3 – Eurocode 3 (1993). Design of steel structures. Part 1.1. General rules and rules for buildings. ENV 1993-1-1: 1992, European Committee for Standardisation CEN, Brussels.

85. Abaqus. Finite Element Program. Version 6.0, 2002.

86. Prokon. Finite Element Program. Win32 Version, 2002.

87. Steelwork Design – Guide to BS5950: Part 1: 1990 and worked examples by the steel Construction Institute. Volume 1 (BSI, London, 1997).

88. Steelwork Design – Guide to BS5950: Part 1: 1990 and worked examples by the steel Construction Institute. Volume 2 (BSI, London, 1999).

Appendix 1

Calculation of Buckling Load of a 150x150x18 angle-iron beam

The critical elastic moment of the unbraced angle-iron (monosymmetric section) acting as a beam, according to the commentary on SABS 0162-1: 1993 – clause 13.6(c) is calculated with the following equation:

$$M_{cr} = \frac{\omega_2 \pi}{KL}\sqrt{EI_y GJ}\left(B_1 + \sqrt{1 + B_2 + B_1^2}\right) \qquad (5.1)$$

where :

$$B_1 = \frac{\pi \beta_x}{2KL}\sqrt{\frac{EI_y}{GJ}}$$

(β_x is a parameter which is a function of the degree of mono - symmetry of the section)

given as : $\beta_x \approx 0.9h'\left[\frac{2I_{yc}}{I_y} - 1\right]\left[1 - \left(\frac{I_y}{I_x}\right)^2\right]$; for equal leg angle - iron $\beta_x \approx 0$, since $I_y = I_x$

thus, $B_1 = 0$

and, $B_2 = \frac{\pi^2 EC_w}{(KL)^2 GJ}$

where:

KL is the effective length of unbraced portion of a beam
$\omega_2 = 1.75 + 1.05\kappa + 0.3\kappa^2 \leq 2.5$ (for unbraced lengths subject to end moments), or
$\omega_2 = 1.0$ (when bending moment at any point within the unbraced length is greater than the larger end moment or when there is no effective lateral support for the compression flange at one of the ends of the unsupported length)
C_w is the warping torsional constant
κ is the ratio of the smaller to larger ultimate moment at opposite ends of the unbraced length (positive for double curvature and negative for single curvature)

The following parameters were used:

- Density of steel = 7850 kg/m^3
- I_y - moment of inertia = 4.35x10^6 mm^4
- E - modulus = 205E3 MPa
- G - modulus of rigidity = 77E3 MPa for steel
- C_w - warping torsional constant = 841x10^6 mm^6
- J - St. Venant's Constant = 576x10^3

The critical loadings was calculated to be that as in the following table below compare to what was analysed with the aid of Prokon.

Load bearing capacity of 150x150x18 angle-iron (kN/m) according to commentary on SABS 0162-1:1993

End Conditions	Buckling load of 150x150x18 angle-iron			
	5m long	7.5m long	10m long	15m long
F-F	163.96	48.55	20.5	6.07
P-P	32.93	9.75	4.11	1.22
CANT	7.06	2.09	0.88	0.26

Load bearing capacity of 150x150x18 angle-iron (kN/m) with Prokon

End Conditions	Buckling load of 150x150x18 angle-iron			
	5m long	7.5m long	10m long	15m long
F-F	327.855	27.615	3.7305	0.309
SF-SF	162.525	17.37	2.673	0.189
P-P	16.38	1.44	0.303	0.03
CANT	7.56	0.51	0.072	0.009

From the above tables, it can be seen that the two tables does not correspond.

The figures in the second table with the formula above, along with the general moment-loading formulae for each end conditions were used to calculate the K-values as listed in table 5.5.

In SABS 0162-1[60], the effective length factor K is implemented (results from laboratories and analysis) to account for the fixities, but only three types of "ideal" fixities are considered ignoring the wide variety of fixities.

Appendix 2

Calculation of Buckling Load of a PFC 200x75 beam

The critical elastic moment of the unbraced PFC (monosymmetric section) acting as a beam, according to the commentary on SABS 0162-1: 1993 – clause 13.6(c) is calculated with the following equation:

$$M_{cr} = \frac{\omega_2 \pi}{KL}\sqrt{EI_y GJ}\left(B_1 + \sqrt{1 + B_2 + B_1^2}\right) \qquad (5.1)$$

where :

$$B_1 = \frac{\pi \beta_x}{2KL}\sqrt{\frac{EI_y}{GJ}}$$

(β_x is a parameter which is a function of the degree of mono - symmetry of the section)

given as : $\beta_x \approx 0.9h'\left[\frac{2I_{yc}}{I_y} - 1\right]\left[1 - \left(\frac{I_y}{I_x}\right)^2\right]$

and, $B_2 = \frac{\pi^2 EC_w}{(KL)^2 GJ}$

where:

KL is the effective length of unbraced portion of a beam

$\omega_2 = 1.75 + 1.05\kappa + 0.3\kappa^2 \leq 2.5$ (for unbraced lengths subject to end moments), or

$\omega_2 = 1.0$ (when bending moment at any point within the unbraced length is greater than the larger end moment or when there is no effective lateral support for the compression flange at one of the ends of the unsupported length)

C_w is the warping torsional constant

κ is the ratio of the smaller to larger ultimate moment at opposite ends of the unbraced length (positive for double curvature and negative for single curvature)

The following parameters were used:

- Density of steel = 7850 kg/m^3
- I_y - moment of inertia = 1.67x10^6 mm^4
- E - modulus = 205E6 kPa
- G - modulus of rigidity = 77E3 MPa for steel
- C_w - warping torsional constant = 10.6x10^9 mm^6
- J - St. Venant's Constant = 104x10^3
- β_x - Degree of monosymmetry = 87.55

The critical loadings was calculated to be that as in the following table below compare to what was analysed with the aid of Prokon.

Load bearing capacity of PFC 200x75 (kN/m) with SABS 0162-1:1993

End Conditions	Buckling load of PFC 200x75			
	5m long	7.5m long	10m long	15m long
F-F	56.02	15.08	6.08	1.72
P-P	10.35	2.87	1.18	0.34
CANT	1.96	0.56	0.23	0.07

Load bearing capacity of PFC 200x75 (kN/m) with Prokon

End Conditions	Buckling load of PFC 200x75			
	5m long	7.5m long	10m long	15m long
F-F	124.16	13.21	2.51	0.05
SF-SF	43.54	4.10	0.81	0.02
P-P	12.92	1.31	0.26	0.005
CANT	7.85	3.40	0.68	0.01

From the above tables, it can be seen that the two tables does not correspond.

The figures in the second table with the formula above, along with the general moment-loading formulae for each end conditions were used to calculate the K-values as listed in table 5.8.

Appendix 3

Calculation of Buckling Load of a I 254x146x31 I-beam

The critical elastic moment of the unbraced I-section acting as a beam, according to the SABS 0162-1: 1993 – clause 13.6 is calculated with the following equation:

$$M_{cr} = \frac{\omega_2 \pi}{KL}\sqrt{EI_y GJ + \left(\pi E/L\right)^2 I_y C_w}$$

where:

KL is the effective length of unbraced portion of a beam

$\omega_2 = 1.75 + 1.05\kappa + 0.3\kappa^2 \leq 2.5$ (for unbraced lengths subject to end moments)

$\omega_2 = 1.0$ (when bending moment at any point within the unbraced length is greater than the larger end moment or when there is no effective lateral support for the compression flange at one of the ends of the unsupported length)

C_w is the warping torsional constant

κ is the ratio of the smaller to larger ultimate moment at opposite ends of the unbraced length (positive for double curvature and negative for single curvature)

The following parameters were used:

- Density of steel = 7850 kg/m^3
- I_y moment of inertia = 4.48x10^6 mm^4
- E modulus = 205E6 kPa
- G modulus of rigidity = 77E3 MPa for steel
- C_w warping torsional constant = 66x10^9 mm^6
- J - St. Venant's Constant = 88.2x10^3

The critical loadings was calculated to be that as in the following table below compare to what was analysed with the aid of Prokon.

Load bearing capacity of I254x146x31 (kN/m) with SABS 0162-1:1993

End Conditions	Buckling load of I 254x146x31			
	5m long	7.5m long	10m long	15m long
F-F	86.46	22.30	8.88	2.51
P-P	17.38	4.48	1.78	0.50
CANT	3.90	0.97	0.384	0.11

Load bearing capacity of I254x146x31 (kN/m) with Prokon

End Conditions	Buckling load of I 254x146x31			
	5m long	7.5m long	10m long	15m long
F-F	363.67	32.97	5.88	0.51
SF-SF	36.85	3.81	0.75	0.07
P-P	10.45	1.61	0.37	0.04
CANT	9.08	1.40	0.32	0.03

From the above tables it can be seen that the two tables arguably corresponds.

The figures in the second table with the formula above, along with the general moment-loading formulae for each end conditions were used to calculate the K-values as listed in table 6.11.

Appendix 4

Some visual results from Abaqus

The program, Abaqus was used to verify the some of the results from the program, Prokon. A few of the visual results follows:

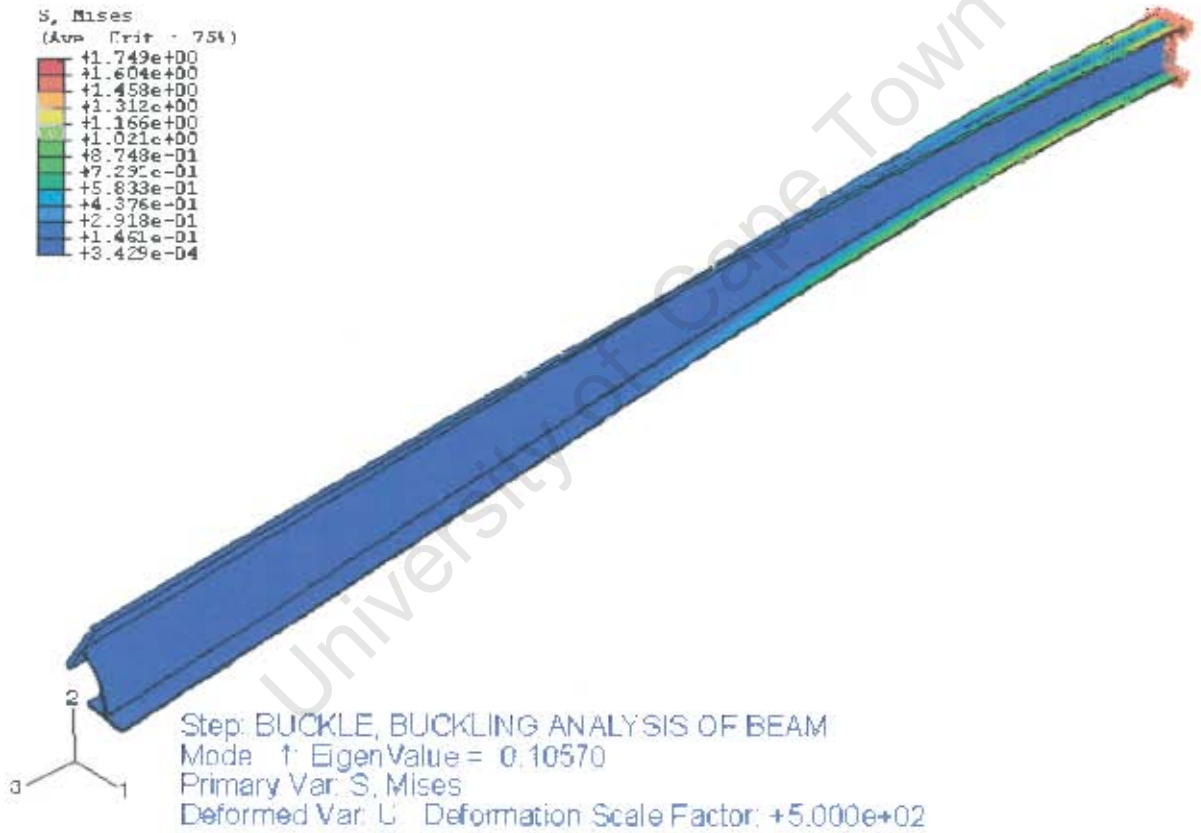

BUCKLING OF AN I-BEAM: CANTILEVER

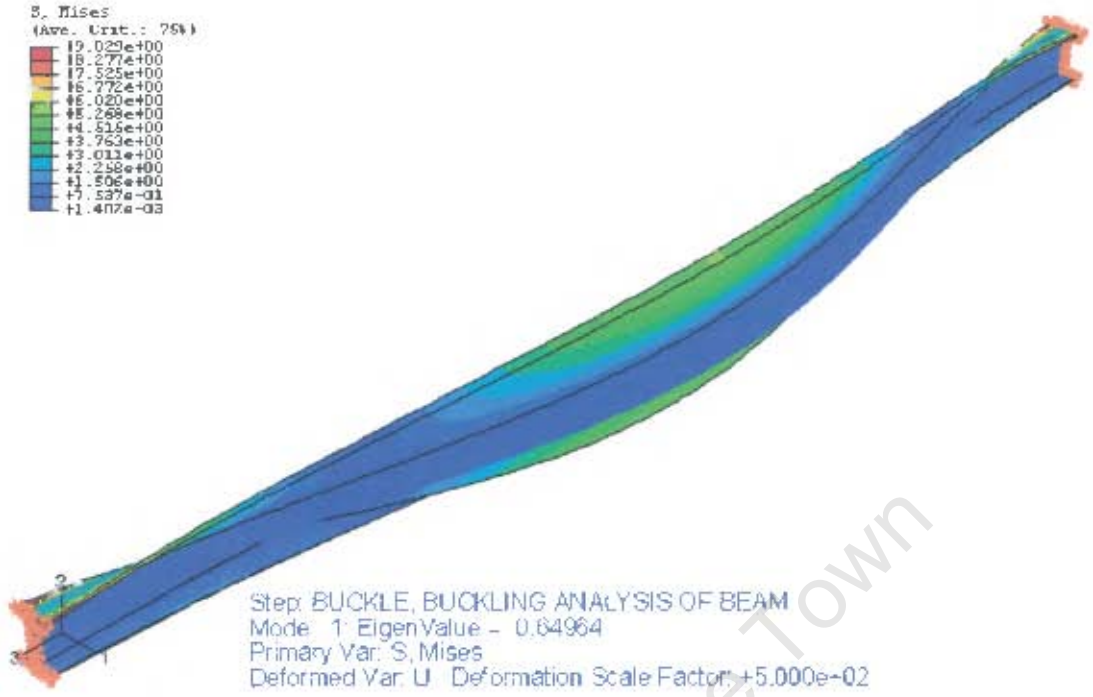

BUCKLING OF AN I-BEAM: FIXED ENDS

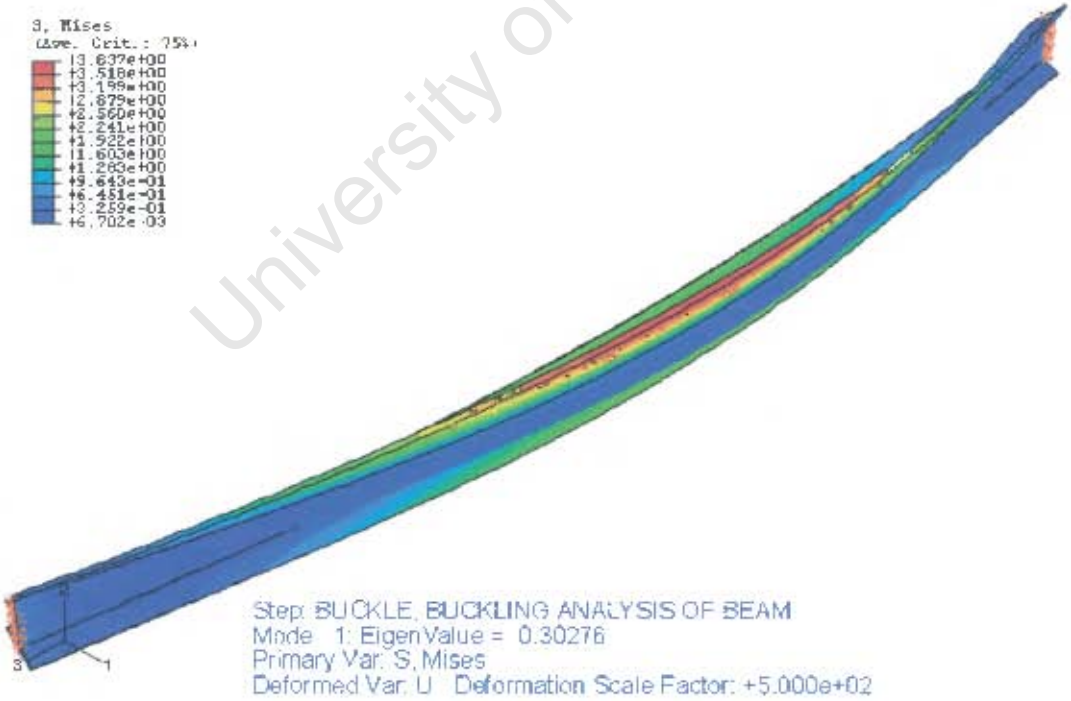

BUCKLING OF AN I-BEAM: PINNED-PINNED

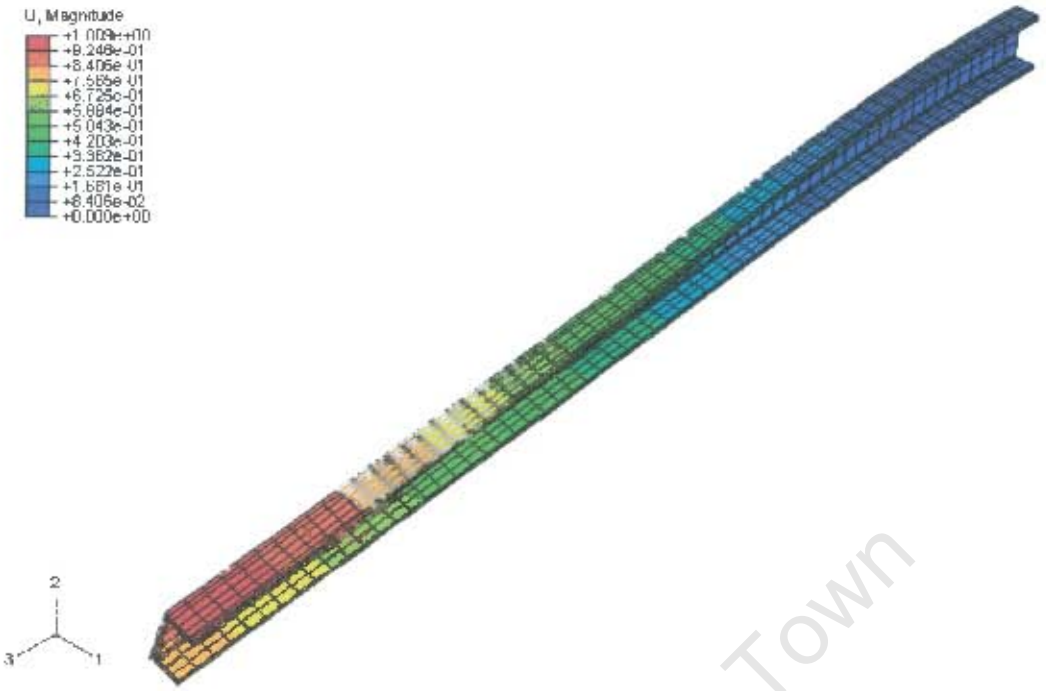

BUCKLING OF A CHANNEL: CANTILEVER

The eigenvalue for each particular beam and column were multiplied by the loading in order to get the buckling load of the particular member.

Appendix 5

Data from Abaqus

The following table the results of an I254x146x31 I-beam subjected to a UDL.

Load bearing capacity of I 254x146x31 (kN/m) using FEM program, Abaqus

End Conditions	Buckling load of I 254x146x31			
	5m long	7.5m long	10m long	15m long
FF	327.304	29.669	5.291	0.456
F-SF	116.983	11.643	2.197	0.200
SF-SF	35.594	3.680	0.722	0.071
F-P	55.247	6.593	1.371	0.118
P-P	9.863	1.518	0.347	0.034
CANT	9.794	1.507	0.345	0.030

Compared to the results from Prokon, the results differ by less 6%.

The following table the results of 305x305x118 H-section column subjected to a Point Load.

Load bearing capacity of a 305x305x118 H-section column (kN) using FEM program, Abaqus

End Conditions	Buckling load of 305x305x118 H-section			
	3m long	4m long	5m long	6m long
FF	121944	42268	18040	8904
F-SF	59498	30989	16721	8844
SF-SF	26605	14497	7688	4009
F-P	14678	6236	3372	2079
P-P	1210	824	605	463
CANT	7564	2407	989	474

Compared to the results from Prokon, the results differ by less 7%.

With this, the results were verified and the results of Prokon were used in this thesis.

Appendix 6

Some visual results from Prokon

A few of the visual results from the program Prokon to follow:

The first two figure are of a 150x150x18 angle iron subjected two a UDL.

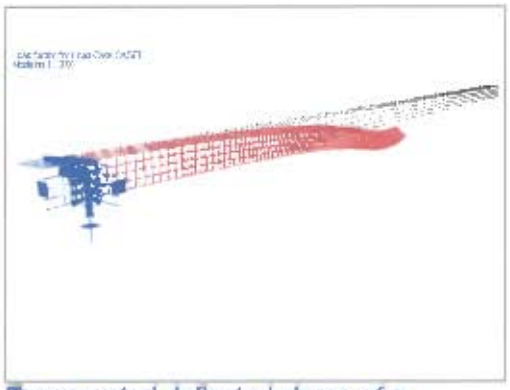

Exaggerated deflected shape of a 150x150x18 angle iron

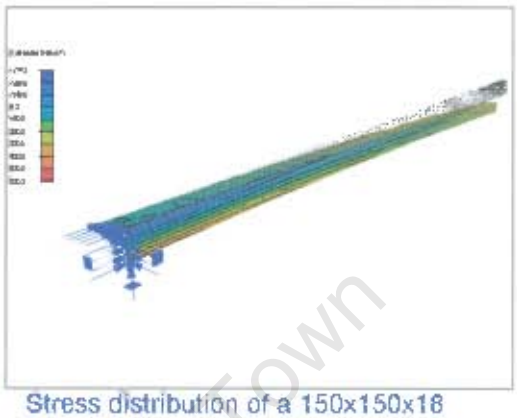

Stress distribution of a 150x150x18 angle iron

The following is the output from Prokon from the buckling analysis:

========== OUTPUT: BUCKLING ANALYSIS ==========

********** LOAD CASE CASE1 **********

========== BUCKLING LOAD FACTOR FOR EACH MODE SHAPE ==========

Mode shape	Load factor
1	0.0070
2	0.0252

========== NORMALIZED BUCKLING MODE SHAPES ==========

========== STATISTICAL DATA ==========

Own weight of structure = 0.00

No. of real numbers in Stiffness/mass matrix = 521847 (4174776 bytes)
Time used to analyse = 0: 0:10.990 seconds
Total number of : Nodes = 1359
Beam Elements = 0
Shell Elements = 1200
Supports = 9
Section properties = 0
Load cases = 1
Load combinations = 0
Mode shapes = 2
No of subspace iterations = 4

========== END OF OUTPUT==========

The following is the results of a 5m PFC 200x75 subjected to a UDL with both ends fixed.

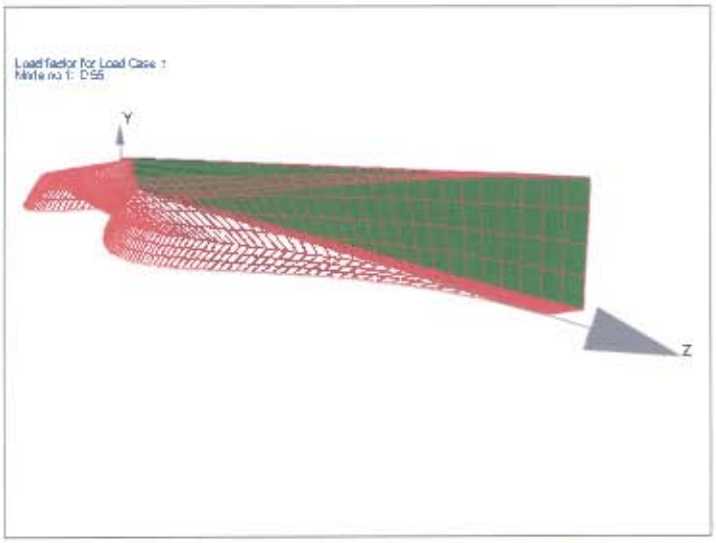

Exaggerated buckling displacement of a PFC 200x75, 5m long with Fixed ends

OUTPUT: BUCKLING ANALYSIS

********** LOAD CASE 1 **********

BUCKLING LOAD FACTOR FOR EACH MODE SHAPE

Mode shape	Load factor
1	0.5518
2	5.6766
3	6.1163

NORMALIZED BUCKLING MODE SHAPES

Node	Shape No.	X-disp.	Y-disp.	Z-disp.	X-rot.	Y-rot.	Z-rot.
1	1	0.00	0.00	0.00	0.0000	0.0000	0.0000
	2	0.00	0.00	0.00	0.0000	0.0000	0.0000
	3	0.00	0.00	0.00	0.0000	0.0000	0.0000
2	1	0.00	0.00	0.00	0.0000	0.0000	0.0000
	2	0.00	0.00	0.00	0.0000	0.0000	0.0000
	3	0.00	0.00	0.00	0.0000	0.0000	0.0000
3	1	0.00	0.00	0.00	0.0000	0.0000	0.0000
	2	0.00	0.00	0.00	0.0000	0.0000	0.0000
	3	0.00	0.00	0.00	0.0000	0.0000	0.0000
4	1	0.00	0.00	0.00	0.0000	0.0000	0.0000
	2	0.00	0.00	0.00	0.0000	0.0000	0.0000
	3	0.00	0.00	0.00	0.0000	0.0000	0.0000
5	1	0.00	0.00	0.00	0.0000	0.0000	0.0000
	2	0.00	0.00	0.00	0.0000	0.0000	0.0000
	3	0.00	0.00	0.00	0.0000	0.0000	0.0000
6	1	0.00	0.00	0.00	0.0000	0.0000	0.0000
	2	0.00	0.00	0.00	0.0000	0.0000	0.0000
	3	0.00	0.00	0.00	0.0000	0.0000	0.0000
7	1	0.00	0.00	0.00	0.0000	0.0000	0.0000
	2	0.00	0.00	0.00	0.0000	0.0000	0.0000
	3	0.00	0.00	0.00	0.0000	0.0000	0.0000
500	1	0.64	0.08	-0.00	-0.0000	0.0001	-0.0023
	2	-0.66	0.15	-0.00	-0.0002	0.0007	-0.0021
	3	0.70	-0.32	-0.00	0.0000	0.0002	0.0052
501	1	0.75	0.08	-0.00	-0.0000	0.0001	-0.0023

	2	-0.55	0.15	-0.01	-0.0002	0.0010	-0.0021
	3	0.43	-0.32	-0.00	0.0000	0.0002	0.0052
502	1	0.86	0.08	-0.00	-0.0000	0.0002	-0.0023
	2	-0.45	0.15	-0.02	-0.0002	0.0012	-0.0021
	3	0.17	-0.32	-0.00	0.0000	0.0003	0.0052
503	1	0.98	0.08	-0.00	-0.0000	0.0002	-0.0023
	2	-0.34	0.15	-0.03	-0.0002	0.0014	-0.0021
	3	-0.09	-0.32	-0.00	0.0000	0.0003	0.0053
504	1	0.98	0.14	0.00	-0.0000	0.0002	-0.0023
	2	-0.34	0.20	0.01	-0.0003	0.0014	-0.0022
	3	-0.09	-0.45	0.00	0.0000	0.0003	0.0053
505	1	0.98	0.20	0.01	-0.0000	0.0002	-0.0023
	2	-0.34	0.25	0.04	-0.0004	0.0014	-0.0022
	3	-0.09	-0.58	0.01	-0.0000	0.0003	0.0053
506	1	0.98	0.25	0.01	-0.0000	0.0002	-0.0023
	2	-0.34	0.31	0.08	-0.0005	0.0015	-0.0022
	3	-0.09	-0.71	0.02	-0.0000	0.0003	0.0053

========== STATISTICAL DATA ==========

Own weight of structure = 1.31

No. of real numbers in Stiffness/mass matrix = 512355 (5123550 bytes)
Time used to analyse = 0: 0:20.189 seconds
Total number of: Nodes = 1111
Beam Elements = 0
Shell Elements = 1000
Supports = 22
Section properties = 0
Load cases = 1
Load combinations = 0
Mode shapes = 3
No of subspace iterations = 3

========== END OF OUTPUT ==========

Output above is for the displacement of each node (only a few listed).

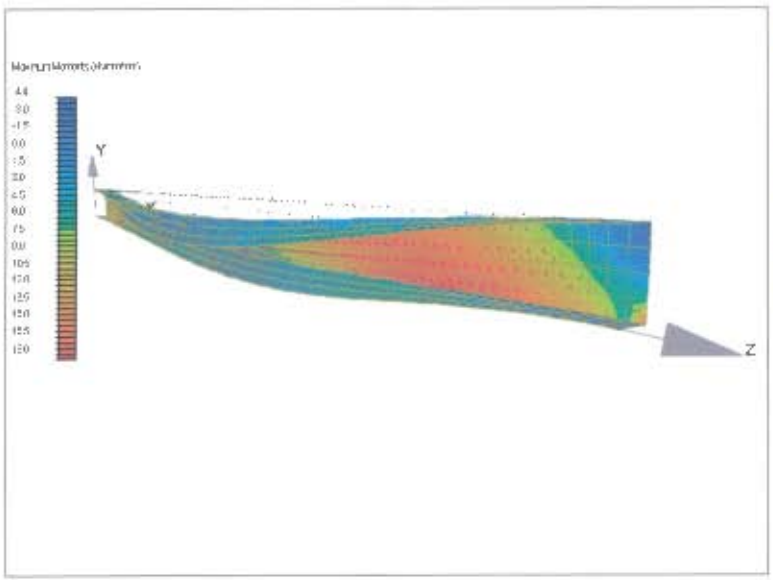

Bending Stresses for: Maximum Moments (kNm/m) for a PFC 200x75, 5m long subjected to a buckling UDL load.

The figure above is the result of a linear analysis of the buckling load applied to a PFC 200x75 beam fixed at both ends.

The following is some of the output giving the stresses in the PFC at the different nodes

========== SHELL ELEMENT STRESSES IN LOCAL ELEMENT AXES at ULS ==========

========== OUTPUT: LINEAR ANALYSIS ==========

IN-PLANE STRESSES /mm width

Elem	Leas	Node	Sx	Sy	Sxy	Smax	Smin	Angle	Von Mises(T)	Von Mises (B)
			kN/mm²	kN/mm²	kN/mm²	kN/mm²	kN/mm²	°	kN/mm²	kN/mm²
1	1	mid	-175E-3	-1.06	-74.8E-3	-169E-3	-1.06	85.18	1.31	663E-3
		1	-537E-3	-1.96	-131E-3	-525E-3	-1.98	-84.82	2.22	1.33
		2	-70.3E-3	-314E-3	7.68E-3	-70.1E-3	-314E-3	-91.80	681E-3	113E-3
		13	45.7E-3	-235E-3	-89.0E-3	71.6E-3	-261E-3	-73.79	531E-3	97.4E-3
		12	-139E-3	-1.71	-87.1E-3	-134E-3	-1.71	-86.84	1.95	1.35
2	1	mid	-75.3E-3	-890E-3	-68.3E-3	-69.6E-3	-896E-3	85.24	1.16	572E-3
		12	-139E-3	-1.71	-87.1E-3	-134E-3	-1.71	-86.84	1.95	1.35
		13	45.7E-3	-235E-3	-89.0E-3	71.6E-3	-261E-3	-73.79	531E-3	97.4E-3
		24	-6.27E-3	-157E-3	-95.4E-3	39.9E-3	-204E-3	-64.20	569E-3	120E-3
		23	-202E-3	-1.46	-1.64E-3	-202E-3	-1.46	-89.93	1.71	1.04
3	1	mid	-103E-3	-721E-3	-37.5E-3	-100E-3	-724E-3	86.55	1.05	351E-3
		23	-202E-3	-1.46	-1.64E-3	-202E-3	-1.46	-89.93	1.71	1.04
		24	-6.27E-3	-157E-3	-95.4E-3	39.9E-3	-204E-3	-64.20	569E-3	120E-3
		35	-10.7E-3	-69.3E-3	-110E-3	73.5E-3	-153E-3	-52.48	622E-3	221E-3
		34	-192E-3	-1.20	56.8E-3	-189E-3	-1.21	-93.21	1.53	752E-3
4	1	mid	-92.5E-3	-559E-3	-24.5E-3	-91.2E-3	-561E-3	87.00	963E-3	229E-3
		34	-192E-3	-1.20	56.8E-3	-189E-3	-1.21	-93.21	1.53	752E-3
		35	-10.7E-3	-69.3E-3	-110E-3	73.5E-3	-153E-3	-52.48	622E-3	221E-3
		46	-6.26E-3	8.93E-3	-102E-3	104E-3	-101E-3	-42.87	675E-3	330E-3

		45	-161E-3	-975E-3	56.9E-3	-157E-3	-979E-3	-93.98	1.39	515E-3
5	1	mid	-76.8E-3	-417E-3	-22.1E-3	-75.4E-3	-418E-3	86.29	902E-3	284E-3
		45	-161E-3	-975E-3	56.9E-3	-157E-3	-979E-3	-93.98	1.39	515E-3
		46	-6.26E-3	8.93E-3	-102E-3	104E-3	-101E-3	-42.87	675E-3	330E-3
		57	-4.43E-3	74.7E-3	-87.7E-3	131E-3	-61.1E-3	-32.86	743E-3	427E-3
		56	-136E-3	-776E-3	44.5E-3	-133E-3	-779E-3	-93.95	1.27	371E-3
6	1	mid	-65.1E-3	-294E-3	-20.9E-3	-63.2E-3	-296E-3	84.82	858E-3	425E-3
		56	-136E-3	-776E-3	44.5E-3	-133E-3	-779E-3	-93.95	1.27	371E-3
		57	-4.43E-3	74.7E-3	-87.7E-3	131E-3	-61.1E-3	-32.86	743E-3	427E-3
		68	-3.76E-3	128E-3	-76.0E-3	163E-3	-36.4E-3	-24.51	825E-3	497E-3
		67	-116E-3	-603E-3	35.6E-3	-114E-3	-605E-3	-94.17	1.17	365E-3

========== STATISTICAL DATA ==========

Own weight of structure = 1.31 kN

No. of real numbers in Stiffness matrix = 512355 (5123550 bytes)
Time used to analyse = 0: 0:4.497 seconds
Total number of : Nodes = 1111
Beam Elements = 0
Shell Elements = 1000
Supports = 22
Section properties = 0
Load cases = 1
Load combinations = 0

========== END OF OUTPUT ==========

The results (visual and numerical) of the other analyses (I-beam and column) were also available through Prokon.